Physical characterization of the electroporation process on *Escherichia coli* C600 and *Bacillus subtilis* 168

Dissertation

zur Erlangung des akademischen Grades
Dr. rer. nat.
der Fakultät Physik der Technischen Universität Dortmund

vorgelegt von
Diplom-Physikerin

Birgit Christiane Brambach

Dortmund

14. August 2013

technische universität
dortmund

Leibniz-Institut für Analytische
Wissenschaften - ISAS - e.V.

Erstgutachter: PD Dr. Joachim Franzke

Zweitgutachter: Prof. Dr. Thomas Weis

Abstract

To examine the physical characteristics of the electroporation process, *E.coli* C600 with pDsRed-Express and *Bacillus subtilis* 168 with pBluescript KS II+ were treated with electric fields.

The transformation and survival of *E.coli* C600 have been evaluated in dependence on the electric field strength and current density by changing the conductivity of the bacteria suspension. In this context, the impact of making bacteria electro-competent and the addition of several volumes of 10 mM salt solution on the transformation efficiencies was examined. For these experiments a voltage generator was used, which produces single pulses with an exponential decay (decay time $\tau = 3\,\text{ms}$).

In dependence on the electric field strength, the transformation efficiency shows no effect on changing the conductivity. Regarding the transformation efficiency in dependence of the current density, a clear shift of the transformation maximum is observed. For higher conductivities higher current densities are needed to reach the transformation maximum. This can be observed for all added salt solutions.

Based on the measured conductivity of the bacteria suspension before and during the electroporation process a graph was developed, which can be used to predict the electric field. This electric field then has to be applied for maximal transformation efficiencies of *E.coli* C600 with pDsRed-Express plasmid DNA, when using the voltage generator with an exponential decay and a decay time of $\tau = 3\,\text{ms}$. This means, a transformation mixture of unknown composition (except for the kind of cells and nucleic acid) can be measured for its conductivity in the first place and then treated with the voltage determined by usage of the developed graph to reach optimal transformation efficiencies.

Comparable experiments showed, that a similar calibration graph could be developed for *Bacillus subtilis* 168 with pBluescript KS II+.

By using a square wave generator, it is explicitly shown, that the electroporation of *E.coli* depends only indirectly on the current density. The key parameter is the amount of charges applied to the bacteria.

During the measurements with the square wave generator an extraordinary behavior of the current pulses can be observed which leads to the assumption, that during the electroporation process there is not only a direct current but also a dielectric coupled current in form of a displacement current within the cuvette.

Contents

1 Introduction **1**

2 Bacteria, electric potentials and charge transport **5**

2.1 Bacteria 5

2.1.1 Proteins 7

2.1.2 Cell membrane 8

2.1.3 Gram positive and Gram negative bacteria 9

2.1.4 Taxis 10

2.1.5 *Escherichia coli* 12

2.1.6 *Bacillus subtilis* 14

2.2 Conductivity 15

2.2.1 Electrolyte-conductivity in dependence on concentrations 18

2.2.2 Debye-Hückel-Onsager theory of diluted electrolyte solutions . . 18

2.3 Potentials and structures of phase interfaces 20

2.3.1 Membrane potentials 20

2.3.2 Potentials of electrodes 21

The zeta-potential ζ 22

Double-layer capacity 23

Surface over-potential and the current density 25

2.4 Transport processes in electrolytic solutions 25

2.4.1 Infinitely diluted solutions 25

2.4.2 Concentrated solutions 27

2.4.3 Transport properties 28

2.4.4 Fluid mechanics 28

2.5 Transport in membranes 30

2.6 Adsorption of ions, dipoles, and neutral molecules on metal surfaces . . 32

3 Methods for DNA transfer into cells **35**

3.1 The $CaCl_2$-method 35

3.2 The electroporation process 36

4 Experimental arrangement and preparation of the samples 47

4.1 Preparation of the bacteria samples 47
4.1.1 Preparation of electro-competent *E.coli* C600 48
4.1.2 Preparation of electro-competent *Bacillus subtilis* 168 48
4.2 Experimental arrangement 49

5 Electroporation in dependence on the electric field, current density and the charge 53

5.1 Electroporation of *E.coli* C600 in comparison to other cells 54
5.2 Conductivity and the influence of electroporation cuvettes 55
5.3 Threshold value of electric field to electroporate *E.coli* C600 56
5.4 Electroporation in dependence on electric field strength and current density 59
5.5 Experiments with bacteria suspensions of different conductivities 60
5.5.1 Electroporation of *E.coli* C600 with addition of NaCl-solution . . 60
Transformation in dependence on the electric field strength . . . 60
Transformation in dependence on current density 63
5.5.2 Electroporation of *E.coli* C600 washed in different ways 65
5.5.3 Electroporation of *E.coli* C600 with addition of several salt solutions 70
5.5.4 Transformation of *Bacillus subtilis* 168 in dependence on current density 77
5.6 Charge dependent electroporation 78
5.7 Electroporation of *E.coli* C600 in dependence on the applied frequency . 79
5.8 Conductivity and changes on the electrode surface 83
5.9 Influence of current flow direction on transformation rate 88
5.10 Transformation in dependence on charge 89

Summary 96

Appendix 97

Bibliography 99

Danksagung 106

Chapter 1

Introduction

The transformation of naturally competent bacteria* was described for the first time by GRIFFITH in the year 1928 long before DNA was known as genetic material [CMF88].
In 1958, it was firstly reported about reversible "electrical breakdown" of membranes by STÄMPFLI, who examined membranes of single nodes of Ranvier of isolated frog nerves [St8]. Furthermore, NEUMANN and ROSENHECK in 1972 and ZIMMERMANN *et al.* in 1973 observed that there are physical and biological changes such as an increase of membrane permeability in cells, which are exposed to electric pulses [Ros98, CMF88].
By treating biological cells with an electric impulse, a permeability of the cell membrane occurs. When the resulting electric field strength inside the cell is larger than a special threshold value, pores are formed in the cell membrane. If these pores are large enough, DNA-sequences can be introduced into the cell [TS11, TT81, SD88]. When the electric field is decreased to zero these pores close again. So the permeability of the membrane is reversible [LNR77, SD88] except in the case, when the applied electric field is too high. Then the cell membrane is damaged [N^+82, SH67, HS67, SD88]. When a critical potential difference inside the cell membrane is exceeded, a breakdown of the membrane results, which leads to lysis [SH68] †. The mechanism of permeabilizing cell membranes by electric pulses is called "electroporation".
Since NEUMANN *et al.* in 1982, electroporation is applied to introduce molecules and macromolecules manually into cell cytoplasm through the electrically formed pores of the cell membrane [Ros98]. By electroporation it is possible to clone and express homologous and heterologous genes in microorganisms and to introduce these genes into novel hosts [CMF88, MC88].
Except for pharmacological studies with biological cells, the principle of electroporation offers new opportunities in future gene replacement therapy for certain human diseases [OM93, Pot88]. The genetically modified cells, which have altered functions, have emerged as promising materials in cell-based therapies such as cancer immunother-

* bacteria, which are able to take up DNA by themselves, and thus acquire new genetic traits
† lysis is the process of cell collapsing due to the damage of the cell membrane

apy, stem cell therapy, and skeletal tissue regeneration [G$^+$10, BG04, KTSD05, GPG07]. Many cell types can contribute to anti-tumor immunity. By modifying cells genetically, a production of leukocytes with increased anti-tumor activity can result [KTSD05]. Another possibility is a combination of an anticancer drug (e. g. bleomycin) and local electric pulses which are delivered to the tumor site. This method is called electrochemotherapy. Bleomycin is almost unable to enter intact non-permeabilized cells. When bleomycin enters into tumor cells through electropores, it can reach the cytosol directly and remain trapped there [B$^+$94]. Electroporation also plays a role in stem cell therapy. Bone marrow-derived mesenchymal stem cells (MSC) are multi-potent adult stem cells of mesodemal origin, localized within the bone marrow compartment and are ideal resources for regenerative medicine. By modifying MSC, they can serve as cell carriers for local or systemic therapy [KCP08].

Due to the potential theory about mechanisms which determine the passive electrical properties of biological systems by SCHWAN in 1957 [Sch57], it is found, that the formation of pores by electroporation is in direct relation to the cell diameter. Hence, it is possible to apply defined electric field pulses to form irreversible pores into cell membranes selectively. So larger cells can be killed due to lysis without altering the viability of smaller cells including hematopoietic stem cells (HSCs). As HSCs are generally 6 µm to 8 µm in diameter, whereas myeloma cells and other tumor cells are generally more than 10 µm in diameter, it is possible to erase tumor cells by electroporation [C$^+$05].

Besides genetic manipulation and chemotherapy of cancerous cells, electroporation finds an application in monoclonal antibody production [T$^+$04] and cloning of human DNA fragments [S$^+$92a]. In 1992, SHIZUYA *et al.* found a bacterial artificial chromosome system based on *E.coli* and its single-copy plasmid F-factor[‡] which is capable of maintaining human genomic DNA fragments of more than 300-kilobase-pairs [S$^+$92a].

Still, the mechanism of electroporation is not understood. Theoretical considerations propose that there is a movement of ions inside the cell membrane due to the applied external electric field. Thus, there will be a potential difference in the cell along this field [N$^+$82, TT81, SH68, SD88]. The maxima of the potential difference is directed towards the applied electric field [SH68]. The external electric field causes a new orientation of charged particles which leads to a dipole interaction. This interaction seems to be the reason for the formation of stable pores [TT81].

Up to now, transformation of biological cells via electroporation only was examined in dependence on the applied electric field.

In the medical application, high transformation efficiencies are desired. In this dissertation a method to simplify the search for maximal transformation rates is presented. Therefore, several electrical parameters of the experimental setup are used to find a parametrization for the transformation rate.

In this thesis, transformation efficiencies of *E.coli* C600 and *Bacillus subtilis* 168 were mea-

[‡] The fertility factor (F-plasmid) encodes genes for the genetic exchange of bacteria. For further information see section 2.1.5.

sured as a function of the current density by changing the conductivity of the cell suspension, which should be electroporated, and as a function of the applied amount of charges.
Chapter 2 gives an introduction into the biological and physical background of this thesis. Moreover, the $CaCl_2$-method and the electroporation process are presented as methods to transfer DNA fragments into biological cells in chapter 3, whereat the focus is on the electroporation process. The experimental arrangement which was used for the measurements, is described in detail in chapter 4.
In chapter 5 the results of the measurements are presented.
Parts of the presented results and the experimental setup were already published or submitted. The published parts can be found in BRAMBACH *et al.*, "Current density and conductivity dependent electroporation of *Escherichia coli* C600", Progress in Biophysics and Molecular Biology, Vol. 111, pp. 46-54 (2013) [BMFK13].

Chapter 2

Bacteria, electric potentials and charge transport

This chapter deals with the necessary biological and physical prerequisites. Beside the characteristics of bacteria, the physico-chemical nature of electrolytes will be explained. In the first part, the biological background is provided. Here, the structure and the characteristics of bacteria in general and especially of *Eschericha coli* are presented.
The second part concerns to the physical aspects according to the conductivity of electrolytes.

2.1 Bacteria

Bacteria are attributed to prokaryotes [Pie89, MMP03] which differ from eukaryotes in many aspects. Compared to eukaryotes, prokaryotes do not have different organelles like a cell nucleus, which is encased in a nuclear membrane, or mitochondria. In eukaryotes the chromosomes can be found inside the nucleus. In prokaryotes, on the other hand, the chromosomes exist in a free state but are connected to the cell membrane by a protein complex [MMP03].

Figure 2-1: Inner structure of a prokaryote cell (left) and an eukaryote cell (right) [MMP03].

In prokaryotes the DNA is arranged in a large double-stranded molecule (bacterial chromosome). Most prokaryotes have just one chromosome as a circular DNA, which includes only one single copy of each gene. The chromosome of an *E.coli* consists of 4.6 million base pairs with a minimum of 4300 genes. In eukaryotes the DNA is located inside the cell nucleus on linear molecules and normally there can be found at least two copies of each gene [MMP03].
Bacteria occasionally have additional genetic information, the so called plasmids, which are circular DNA molecules. These plasmids are not essential, but with their help bacteria can have selective advantage in special environmental conditions. Plasmids code additional genetic information for the degradation of rare energy resources or for the resistance to fatal effects of antibiotics [Pie89, MMP03].
Like most natural systems, bacteria have a negatively charged surface [LCP99]. Inside a bacterial cell there can be found lipids, sugars, fats, amino acids, and nucleotides. The amino acids are the components of proteins. The characteristics of the proteins are determined by the genes, which consist of molecules, which are linked together in a catenarian way, forming macromolecules, the so-called nucleotides. On average, each single gene is composed of one thousand nucleotides. Each gene contains specific genetic information for the synthesis of a protein or functional RNA. When needed, the genetic information will be transcribed in an RNA copy. The short living RNA molecules contain all information for the synthesis of specific proteins by the ribosomes [Pie89].
The largest molecule in a bacteria cell is the bacterial chromosome, a circular closed double stranded DNA. The total length of the DNA molecule equals a thousandfold of the cell diameter. The chromosome is coiled very tight. It consists of 3 million pairs of nucleotides, which are linked together linearly. Each nucleotide is composed of three different constituents: sugar desoxyribose, phosphoric acid, and nucleic base [Pie89].
There are four different DNA bases: adenine, thymine, guanine, and cytosine.
Single nucleotides are connected forming the spine of a DNA single strand. From the spine, consisting of sugar and phosphoric molecules, different DNA bases protrude in a specific order. In all cases two complementary single strand spines are connected to each other by hydrogen bonds between the bases. They form a spiral, whereas the orientation of the single strands is antiparallel to each other. Only pairs of adenine and thymine or guanine and cytosine can be found [Pie89].
The bacterial chromosome must not only identify the genetic information but also duplicate itself. In that way the bacterial chromosome can be transferred to new bacteria cells during the segmentation [Pie89].
Many bacteria are able to move in two or three dimensions. While some move on surfaces without flagella by gliding motility, others rely on flagella to move on surfaces exhibiting swarming motility. Movement in three dimensions is called swimming [Man92]. Each flagellum, which has a thickness of about 20 nm, consists of a flexuous protein structure [MMP03]. In *E.coli* and *S.typhimurium* the products of many of the 37 genes are known to be involved in the formation of intact flagella [Man92]. Bacteria move through liquids by rotation of the flagella [MMP03]. They are remarkably rapid

swimmers. For example, *E.coli* can swim with a speed of 20-40 $\frac{\mu m}{s}$ at physiological temperatures, meaning that an *E.coli* cell can move a distance of 10-20 of its body lengths per second. The flagella filament is quite massive and turns at speeds of up to several hundred Hertz [Man92].

2.1.1 Proteins

Nearly every biochemical reaction in a cell is catalyzed by a specific protein (enzyme). Proteins also assist in transport, movement, regulation, and many other activities. Therefore, a huge amount of different proteins is demanded. Nearly two thousand kinds of proteins are known. In a biological cell, there are many copies of every type of proteins [Pie89]. In a single *E.coli* cell, there can be found 1900 different types of proteins and 2.4 million single protein molecules [MMP03].
A protein is very complex. Even the simplest proteins consist of 1000-2000 atoms. The atoms are arranged in a tertiary structure, which determines the function of the particular protein [Pie89].
Initially a protein is synthesized as a one dimensional structure of amino acids. Normally, a protein consists of 100-1000 amino acids, whereat there are 20 different types of amino acids. Due to a special order of the amino acids, there is a self organized folding of the protein [Pie89]. The protein folds itself automatically or with the help of chaperones appropriate to the sequence of components (amino acids) within minutes [Pie89, Cot08]. The function of a protein depends on a specific sequence of the amino acid chain. Due to the folding, each protein gains a characteristic structure corresponding to its function [Pie89].
The atoms of a protein are bound to each other in a covalent way, by van der Waals bonds and hydrogen bonds but the most important stabilization factor of a protein is given by hydrophobic effects. The role of hydrogen bonds differs for each kind of protein [Cot08].
By heating proteins, which are dissolved in water, the bonds loosen due to the temperature and finally burst. The three dimensional structure is destroyed. As a result of the changed spatial surface structures the proteins lose their function [Pie89]. In fact, the melting temperatures of proteins are close to the human body temperature. For example, barnase melts at a temperature of about 312 K (39 °C) and ribonuclease at about 306 K (33 °C). At these temperatures the denaturation* degree of the respective proteins is about 50 % [Cot08].

* process in which proteins or nucleic acids lose the structure, which is present in their native state, by application of some external stress or compound

2.1.2 Cell membrane

A biological cell is encased by the cytoplasm membrane, which is a thin structure with a thickness of about 8 nm and separates the cell content from the environment [MMP03]. A membrane transports ions in or out of a cell, interacts with other cells (primarily by sugar molecules which can be found on the outer cell surface), and transforms energy, for example by creating ATP-molecules [Cot08].

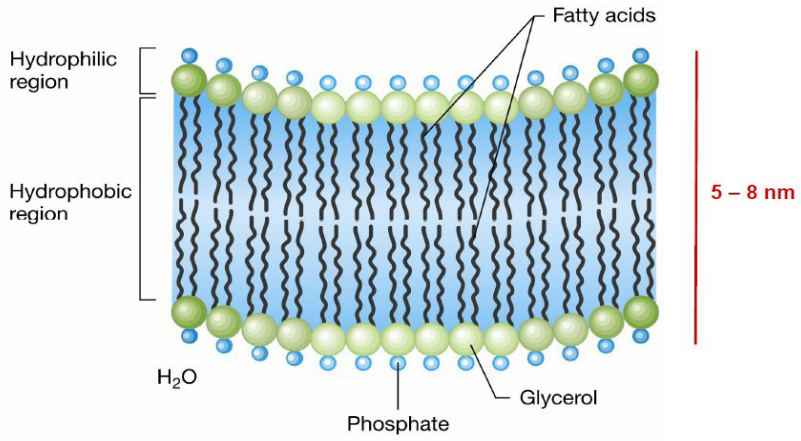

Figure 2-2: Scheme of a phospholipid double layer [MMP03].

Biological membranes consist of a phospholipid double layer [Pie89, MMP03]. Phospholipids are composed of hydrophobic (fatty acids), and hydrophilic parts in the form of glycerin [MMP03]. Thus, phospholipids have a water-repellent "tail" but a water-searching "head". Within the phospholipid double-layer the "tails" are facing each other [Pie89, MMP03].
The structure of the cytoplasm membrane is stabilized by hydrogen bonds, hydrophobic interactions and van der Waals interactions [MMP03]. The membranes of a bacterium protect the interior of the cell from osmotic and mechanical forces [BA65]. When the membrane gets destroyed, the interior of the cell leaks and the cell dies [MMP03]. The cell membrane is a highly complex system, which regulates the concentrations of substances inside the cell [Pie89, MMP03]. Nutrients and metabolites are transported and enzymes and toxins are released from the cell by the membrane [BA65]. Specific proteins in the cytoplasm membrane recognize the substances by their size, profile, and electric charge. According to requirements for the survival of a bacterium, substances are pumped in or out of the cell [Pie89].
The proteins in the cell membrane do not only regulate the concentrations of substances inside the cell, but also cause the movement of bacteria in liquids. They sense gradients of physical and chemical agents and send a signal to the flagella to move towards or away from these agents. This directed movement of bacteria is called "taxis" (see section 2.1.4) [MMP03].

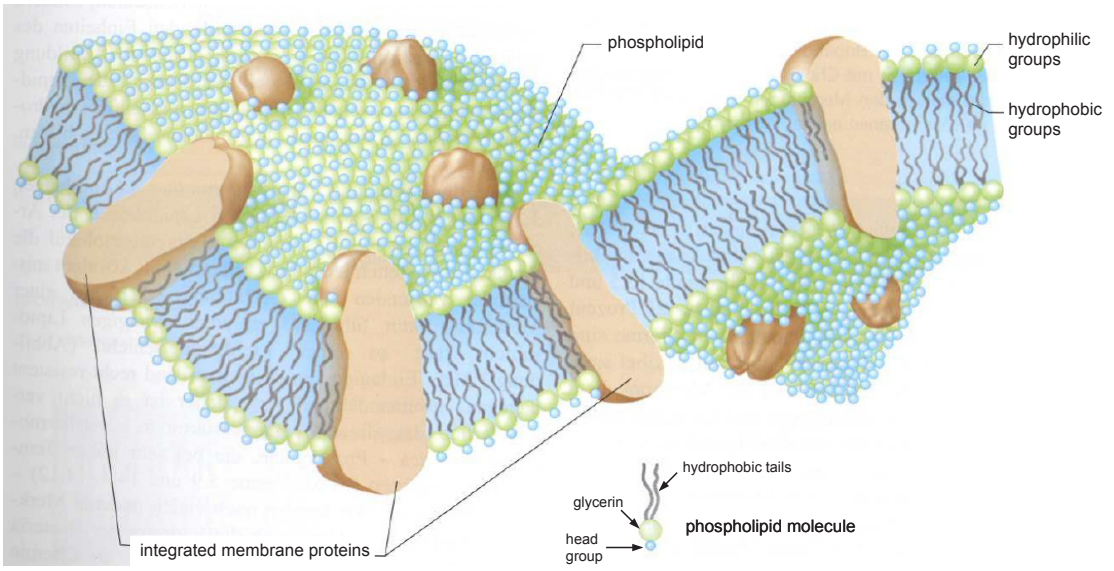

Figure 2-3: Structure of a cytoplasm membrane with integrated membrane proteins [MMP03].

2.1.3 Gram positive and Gram negative bacteria

Bacteria can be divided into two large groups: Gram positive and Gram negative bacteria. The original differentiation between these two groups is based on a special stain method (Gram stain). For Gram stain, a primary stain of crystal violet is applied to a heat-fixed smear of a bacteria culture. Afterwards iodine is added, which binds to the crystal violet and traps it in the cell. When washing[†] the bacteria with alcohol or acetone, Gram positive cells remain in a purple or blue stain, while Gram negative cells lose their color. The discrepancy in stain behavior is caused by the difference in the structure of their cell walls. Gram negative cell walls have a complex multi-layer structure. Cell walls of Gram positive cells on the other hand are mostly much thicker than those of Gram negative cells, although they consist of only one type of molecules [MMP03].

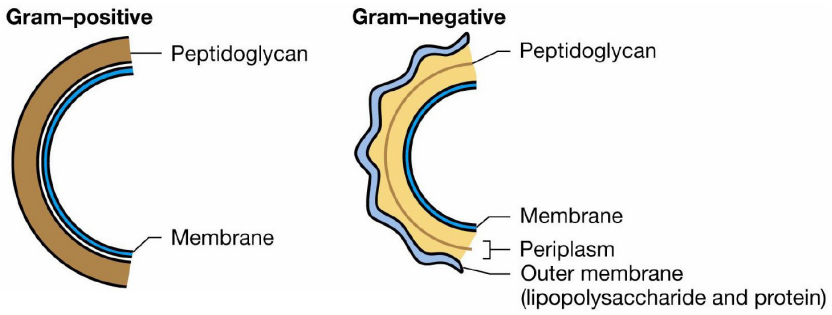

Figure 2-4: Scheme of a Gram positive (left) and a Gram negative (right) cell wall [MMP03].

[†] The washing of bacteria with distilled water is explained in section 4.1.

Regarding the surfaces of Gram positive and Gram negative bacteria, significant differences can be found. Both, Gram positive and Gram negative, have a stiff layer, the peptidoglycan, which is very similar in its composition for both types of cell walls.
Up to 90 % of a Gram positive bacteria cell wall consists of peptidoglycan. While most bacteria are encased by only one layer of peptidoglycan, Gram positive bacteria have up to 25 layers of peptidoglycan. In Gram negative bacteria, peptidoglycan represents only about 10 % of the cell wall [MMP03].
Aside from peptidoglycan, the cell wall of Gram negative bacteria has a layer of lipopolysaccharide (LPS). This additional layer does not only consist of phospholipid but also of polysaccharides and proteins. The lipide and polysaccharide form specific LPS structures. This LPS layer is also known as the outer membrane of the cell [BR70, MMP03]. The outer membrane of Gram negative bacteria often has a toxic effect on humans and animals, leading to the production of heavy immuno-response, which strengthens the immune system under normal conditions. But if the immune system is not healthy enough, the toxic nature of the outer membrane is responsible for several infection symptoms caused by Gram negative bacteria. In contrast to the cytoplasm membrane, which forms the inner membrane of Gram negative bacteria, the outer membrane is relatively permeable to small molecules due to proteins (porins), serving as passages for the entrance and exit of hydrophilic substances of small molecular mass [MMP03].
In *Escherichia coli*, which are Gram negative bacteria, the distance between the outer surface of the cytoplasm membrane and the inner surface of the LPS-including outer membrane is about 12-15 nm [MMP03].

2.1.4 Taxis

For the movement of bacteria, the viscosity of the surrounding area is of importance. The gliding-length for bacteria is proportional to the Reynolds number [Cot08]. The Reynolds number *Re* equals the inertial forces divided by the viscous forces:

$$Re = \frac{\ell v \rho}{\eta}\,, \tag{2.1}$$

where ℓ is the typical length of a bacterium, v is its mean velocity, ρ is the density of the fluid and η is the dynamic viscosity of the fluid. Within a second a bacteria can cover a distance which equals the tenfold of its body length [Cot08].
Usually, the movement of bacteria is a reaction of orientation. This reaction of free-moving beings is called "taxis". It describes the direction of movement in an environmental gradient. The movement can be towards a source of stimulus (pos. taxis) or away from it (neg. taxis) [Pos94].
There are different types of taxis. The probably best understood kind of taxis is **chemotaxis**. Chemotaxis is an ability to sense and respond to chemicals. These chemicals may be nutrients or toxic substances. T. W. ENGELMANN, a microscopist, was a pioneer in

this area of research. He described chemotaxis for the first time in 1881. It was found that organisms such as *E.coli* can show positive or negative chemotaxis by T. W. ENGELMANN and later in 1883 by W. PFEFFER. This behavior of organisms means that they are attracted by some substances and repelled by others [Pos94]. In response to attractants wild-type *E.coli* move towards these attractants and in response to repellents they tumble and move away [SLA93].
Once again, it was ENGELMANN who first described **aerotaxis**. Oxygen molecules are generally sensed in different ways. Though oxygen is needed for respiration, too much oxygen has a damaging effect on *E.coli* and *Salmonella*, a close relative of *E.coli*. So oxygen can become a repellant at high concentration. In this case, oxygen is sensed by a different, unknown mechanism [Pos94].
Another kind of taxis is **phototaxis**. Bacteria can be photosynthetic. In general, they can be found in illuminated places. Like plants some of these bacteria can use light to synthesize carbohydrate out of carbondioxide. In this way they provide their own major nutrient. Photosynthetic bacteria are colored red or purple as often as green. As in leaves of plants the color is just a matter of the balance of pigments. The photosynthesis of these bacteria depends on the green pigment (chlorophyll). Cyanobacteria form oxygen during photosynthesis but many bacteria have a more primitive photosynthetic equipment. They do not produce oxygen. Indeed, there is no photosynthesis at all in this kind of bacteria if oxygen is present, but only in presence of organic food the bacteria can grow with air in the dark. So they show aerotaxis which is suppressed in light. Photosynthetic bacteria rather escape from the dark instead of swim towards light. So phototaxis seems to be a negative taxis, as in chemotaxis [Pos94].
Some bacteria sense the Earth's magnetic field and align themselves with the field. This phenomenon is called **magnetotaxis**. The bacteria in the northern hemisphere move northwards, while the bacteria in the southern hemisphere move southwards. This movement is due to tiny, very uniform crystals of magnetic iron oxide inside the magnetotactic bacteria [Pos94].
Bacteria also react on changes of their environmental temperature. The behavioral response to temperature changes is called **thermotaxis**. In the case of *E.coli*, increasing temperature results in running and decreasing the temperature causes tumbling [SLA93].
In 1889, M. VERWORN described another bacterial sense, the so-called **galvanotaxis**. Galvanotaxis is the movement of bacteria in response to an electric field. While in the case of *E.coli* the movement is towards the anode [Pos94], [RMG94], there is a strain of *Salmonella* which seeks the cathode [Pos94]. Actually, it was observed that at low applied electric fields ($< 0.2\,\mathrm{V/cm}$) *E.coli* of the strain K-12 were moving unidirectionally towards the anode and the cathode, whereat there is a significant difference between the mean moving speeds towards the two electrodes. At pH 7 the measured speed of the cells towards the cathode was $27.3 \pm 9.3\,\mu\mathrm{m/s}$ and towards the anode $11.5 \pm 3.5\,\mu\mathrm{m/s}$. When removing the electric field, they had the same average swimming speeds of $19.0 \pm 6.3\,\mu\mathrm{m/s}$ towards both directions. With increasing voltages, all cells were swept

by the electro-osmotic flow exclusively towards the cathode [LCP99].
Experiments with different *E.coli* and *Salmonella* strains with altered surface structure showed that there is a correlation between the direction of galvanotaxis and the surface structure of the cell. While motile rough bacteria (without O polysaccharide, e. g. *E.coli* K-12 and *S. typhimurium* mutants of classes *galE* and *rfa*) swam towards the anode, motile smooth bacteria (with O polysaccharide, e. g. wild-type *S. thyphimurium* LT2) swam towards the cathode. But smooth bacteria like K1 in *E.coli* and Vi in *Salmonella typhi*, which have acidic polysaccharide capsules swam towards the anode [SSA96].

2.1.5 *Escherichia coli*

The intestinal bacteria *E.coli* (originally: "bacteria coli communale") was found for the first time in 1887 by the pediatrist THEODOR ESCHERICH (1857-1911) [Pie89].
In total, about 10^{14} bacteria live in the gastrointestinal canal of a human being. In one gram of excrement about $2 \cdot 10^8$ of *E.coli* are excreted. Nevertheless, strict anaerobic bacteria dominate in the intestine of a grown-up human being [Pie89]. *Escherichia coli* typically colonizes the gastrointestinal tract of a newborn human within a few hours [Pie89, vHM05]. Usually, the coexistence of *E.coli* with its human host is of mutual benefit. Due to the fecal origin of *E.coli*, it is used as an indicator of the sanitary quality of water and of the food-processing environment [vHM05].
Firstly *E.coli*, which is the molecular best understood creature, was found to be a harmless parasite. But some types of *E.coli* can cause a broad spectrum of infectious diseases (meningitis, urinary tract infections, pneumonia, toxemia) [Pie89, vHM05]. A harmless type of *E.coli* is the strain K-12. It was isolated of the excrement of a patient diseased on diphtheria. The strain K-12 is the progenitor of the standard object of the molecular biology. It is still used all over the world in the academic education (scientific fundamental research, biotechnological products with manipulated strains of *E.coli*). Of no other biological species so many genes are identified and characterized [Pie89].
With dimensions of 1 µm in diameter and a length of 2 µm an *E.coli* cell is significantly longer than wide and high [Pie89, Han83, Man92]. It has a weight of $1 \cdot 10^{-12}$ g and a cell volume of $1 \cdot 10^{-9}$ µl [Pie89].
The oval formed cell has two membranes and therefore belongs to the Gram negative bacteria [Pos94, MMP03]. While the inner membrane, which encases the cytoplasm, is rather fragile, the outer one is tougher. The outer membrane serves as an protective coat. Between the two membranes is a narrow space in which reside some important parts of the microbe's metabolic machinery. Molecules like sugars, amino acids, salts and similar ones can penetrate the outer cover and enter the space, while big molecules such as starch or proteins cannot enter. If a molecule, which is one of *E.coli* attractants, gets in, it is detected by a special protein awaiting it. The protein is embedded in the inner membrane and is large enough to reach right through it. The protein can serve as a transporter and channel. Receptors are distributed all over the inner membrane.

They feed their information into the cytoplasmic cascade system. Some receptors are very specific. They sense only one kind of molecule. Others sense whole classes of molecules. With the help of proteins the *E.coli* cell is able to realize that an attractant, which it perceived a moment earlier, is no longer so plentiful. If something nice is wafting towards an *E.coli* in the surrounding fluid, the microbe will manipulate its flagellar motors to meet it seekingly. Contrary, if there is something nasty abroad, the *E.coli* will reverse abruptly, tumble and make a change of course towards a new direction. So the *E.coli* ultimately achieves a jagged path away from the noxious substance [Pos94]. More than two million proteins can be found in one single *E.coli* whereat there are nearly two thousand different kinds of proteins [Pie89]. The information needed for sensing and motility in *E.coli* is carried by over forty genes, at least ten of them concerned with chemotaxis. *E.coli* show no special sensory area or site on its inner surface. So there is nothing corresponding to a nose or a tongue. This is the reason why *E.coli* swim in a random manner. When an *E.coli* finds itself swimming away from where an attractant is plentiful, it pauses and changes direction. But an *E.coli* cannot reverse. Instead it does a right-angle shift. For this its path to an attractant is jagged. However *E.coli* is led to the source of an attractant very effectively [Pos94].
E.coli is one out of a large group of bacteria which breathe oxygen but can do without it if necessary. *E.coli* prefers to have oxygen and it is able to sense it (aerotaxis) [Pos94]. But *E.coli* does not only have aerotaxis but also galvanotaxis. If a current, weak enough to avoid heating, is passed by electrodes, inserted into a culture of *E.coli*, the bacteria swim towards the positive pole (anode) [Pos94].
Like all bacteria, *E.coli* proliferate by bisection. With optimal conditions (37 °C) an *E.coli* cell splits all 20-30 minutes. In one second one thousand DNA letters can be copied. The cells are splitting until the capacity of nutriment and room is run out. At that instant of time about one billion of bacteria can be found living on one square-millimeter of Luria-Bertani (LB)-Agar [Pie89].
Normally, bacteria are asexual organisms. But in *E.coli* strain K-12 parasexual mechanisms were found by J. LEDERBERG. Due to the parasexual activity, *E.coli* have the ability to exchange genetic material among each other. For that reason *E.coli* bacteria got the standard object of the microbe genetic and molecular biology. With the help of *E.coli* questions to the regulation of gene activity, their structure and the expression of genetic information, as well as the occurrence of mutations could be answered. Without exchange activities due to parasexuality, no such genetic analyses could be done [Pie89].
The parasexuality, also known as conjugation, of *E.coli* is permitted by an extrachromosomal factor. The so-called fertility factor belongs to the group of plasmids. It carries gene encoding proteins that build up the so-called sex pili. During conjugation, where the cells have to be in direct contact, there is an exchange of genetic material, which leads to a change in characteristics. Once sequences of genetic material are introduced into the bacteria cell, a part of the genetic material of the cell is changed in its characteristics. The genetic exchange is carried out by the ring-shaped fertility factor (F-plasmid).

The F-plasmid is up to autonomic duplication. Proteins accomplish the synthesis of plasmid copies. In that way, each new bacteria cell can get copies of the plasmid during the cell splitting. Furthermore, the plasmids carry genetic information, which is not indispensable to life but can bring an advantage for the cell under certain conditions [Pie89].
Bacteria with an F-plasmid feature a modified cell surface. Contrary to F^- bacteria, which have no F-plasmid, F^+ bacteria develop appendages (sex pili). These appendages facilitate a contact to nearby cells. As soon as a pair of cells has been found, a duplication of the F-plasmid is initiated. The copy of the F-plasmid is transferred into the other cell by the bridge between the cells. In this case, there is an one-way transfer from a F^+ to a F^- cell. Though sexuality is verified for the strain K-12, *E.coli* B is sexual sterile. Medial, only one of twenty *E.coli* strains, randomly isolated from nature, shows conjugation. Apart from the gene transfer between different individuals of bacteria, which have a F-plasmid, *E.coli* can transfer genes by transduction. In the process, a part of bacterial DNA is packed in a bacteriophage and injected into the next bacteria cell [Pie89]. Another possibility of gene transfer is transformation. Thereby DNA fragments are transferred into intact cells. In this content AVERY, MACLEOD and MCCARTHY showed unambiguously that genetic information is transported by DNA and not by proteins in 1944 [Pie89].

2.1.6 *Bacillus subtilis*

The Gram positive bacterium *Bacillus subtilis* is also known as the hay bacillus or grass bacillus [MMP03]. Originally, in 1835, the bacterium was named *Vibrio subtilis* by CHRISTIAN GOTTFRIED EHRENBERG [Ehr35]. In 1872, the bacterium was renamed and got its present name *Bacillus subtilis* by FERDINAND COHN [Coh72].
Bacillus subtilis is a rod shaped cell of a length of about 2 µm which is peritrichous flagellated. Its Gram positive cell wall has to withstand an inner cell pressure of about 20 atm [Ber]. A *Bacillus subtilis* cell has approximately 4100 genes. About half of them are involved in information processing, one-fifth in synthesis of cell envelope, determination of cell shape and division and one-tenth of the genes are related to cell energetics [K^+03].
Throughout the 1950s cultures of *Bacillus subtilis* were used as an alternative medicine due to the immuno-stimulatory effects of its cell matter. It has been found, that this bacterium has a significantly stimulatet broad spectrum immune activity upon digestion [C^+86]. It can promote healing benefits in humans, even though *Bacillus subtilis* does not belong to the native microbes that normally inhabit the human body. For example, *Bacillus subtilis* can be used to treat dysentery. But the popularity of using *Bacillus subtilis* as a medicinal product declined after the introduction of cheap consumer antibiotics, despite causing less chance of allergic reaction and significantly lower toxicity to normal gut flora [Kra].

As bacteria are known to cause diseases, for *Bacillus subtilis* this is only the case in severely immunocompromised patients [O$^+$98].
Non-toxigenic and non-pathogenic strains of *Bacillus subtilis* are widely available and have been safely used in a variety of food applications. The most famous food application of *Bacillus subtilis* is the japanese delicacy natto (Japanese fermented soy bean), known for its contribution to a healthy gut flora and vitamin K_2 intake [SYYS04].
Bacillus subtilis proliferate by dividing symmetrically, also called binary fission, to make two daughter cells or asymmetrically to produce a single endospore. The endospore is formed at times of nutritional stress to allow the organism to persist in the environment until conditions become favorable. An endospore can remain viable for decades and is resistant to unfavorable environmental conditions (e. g. drought, salinity, extreme pH, radiation and solvents) [MMP03]. Under beneficial conditions and adequate concentrations of nutrients and oxygen, the doubling time is about 45 minutes [Ber].

2.2 Conductivity

In electrolyte solutions current is transported by the movement of charge carriers (solvated ions) in an electrical field between two electrodes, which are charged unequal. Electrolytes are chemical compounds dissociated to ions when they are molten or solvated. By inserting a solid crystal (e. g. NaCl) into a solvent, for example water, the electrostatic attractive forces like the Coulomb force

$$\vec{F}_{\text{COULOMB}} = \frac{1}{4\pi\epsilon} \cdot \frac{q_1 \cdot q_2}{r^2} \cdot \frac{\vec{r}}{r}\,, \tag{2.2}$$

where q_i are the charge carrier and $\epsilon = \epsilon_0 \cdot \epsilon_r$, are weakened by the change of dielectric constants ϵ_r. In case of using water as solvent, the dielectric constant increases from the value for vacuum $\epsilon_{vacuum} = 1$ to the value for water $\epsilon_{H_2O} = 78,3$ (at 25 °C in homogeneous phase). Therefore, the electrolyte already dissociates to ions with a low energy addition (formation of loose charged atoms). However the dipolar character of water molecules is much more significant for a dissociation of a compound in water. This attribute leads to hydration (or rather general: solvation) [HV05].
When an electric field $\vec{E}$ is applied, the accelerated ions with the charge of ze_0 (z: charge number, e_0: elementary electric charge) succumb to a braking power, which increases with increasing ion velocity $\vec{v}$. The braking power taking effect is the Stokes' friction force:

$$\vec{F}_{Stokes} = 6\pi\eta r_I \vec{v}\,, \tag{2.3}$$

where r_I is the radius of solvated ions and η is the viscosity of surrounding medium.
A maximal constant ion velocity $\vec{v}_{max}$ is set after a short starting process. This constant

ion velocity establishes when the electrostatic force equals the friction force:

$$\begin{aligned} ze_0\vec{E} &= 6\pi\eta r_I \vec{v}_{max} \\ \Leftrightarrow \vec{v}_{max} &= \frac{ze_0\vec{E}}{6\pi\eta r_I} \,. \end{aligned} \tag{2.4}$$

The intensity of current in an electrolyte solution is given by

$$I = \frac{dQ}{dt} \Rightarrow I = \frac{dQ^+}{dt} + \frac{dQ^-}{dt} = Ae_0\left(n^+z^+v^+ + n^-z^-v^-\right) \,. \tag{2.5}$$

Here, A is the control surface in cm^2, $n^\pm$ is the number of charge carriers per cm^3, $z^\pm$ is the charge number of ion and $v^\pm$ is the velocity of ions in $\frac{\mathrm{cm}}{\mathrm{s}}$.
With respect to the concentrations of the included substances $c = \frac{n}{N_A}$, with $[c] = \frac{mol}{cm^3}$ and N_A as Avogadro constant, follows

$$I = Ae_0N_A\left(z^+v^+c^+ + z^-v^-c^-\right) \qquad [\text{HV05, NTA04}] \,. \tag{2.6}$$

The viscosity is temperature dependent. For a given composition and temperature the current in an electrolyte solution is proportional to the electric field strength E and therefore also proportional to the voltage U decreasing in the ionic conductor because of equation 2.4. This behavior can be written by

$$I = Y \cdot U \,. \tag{2.7}$$

Y describes the conductance value, which is composed of $Y = Y^+ + Y^-$. It equals the reciprocal value of an ohmic resistivity. The conductance value of an electrolyte depends on many factors. Thereby the kind of ions $\left(z^\pm, r_I^\pm\right)$, the concentrations $c^\pm$, the viscosity η as well as the temperature T and the dimensions of the ionic conductor (cross-section area A and distance of the electrodes d) are relevant. The conductance value can be written as

$$Y = Ae_0^2 \cdot \frac{N_A}{6\pi\eta}\left(\frac{\left(z^+\right)^2 c^+}{r_I^+} + \frac{\left(z^-\right)^2 c^-}{r_I^-}\right) \cdot \frac{1}{d} \,. \tag{2.8}$$

Because the viscosity depends on the temperature and the conductance value depends on the viscosity, the temperature influences the conductance value. When the temperature differs about 1 K, the conductance value changes already of about 3 % [HV05, NTA04].
Although the conductance value seems to be an ohmic resistivity because of its linear combination to the voltage, there cannot be observed a linear characteristic.
After a very shallow increase of the current at the beginning the current curve changes when the voltage of decomposition is exceeded. As of that voltage the resistivity of the ionic conductor drops hard. From there on the characteristic describes a fast increasing straight line. A change in conductivity would barely influence the developing of the

current curve [HV05].
In fact the developing of the curve is determined by two non-linear resistivities, which are in series with the resistivity of the electrolyte solution. These non-linear resistivities are given by the impedances $Z_L = i\omega L$ and $Z_C = -\frac{i}{\omega C}$ corresponding to the two electrodes, which limit the volume of the ionic conductor in one direction. The total resistance can be calculated by

$$R = |Z| \cos \varphi \,, \tag{2.9}$$

where

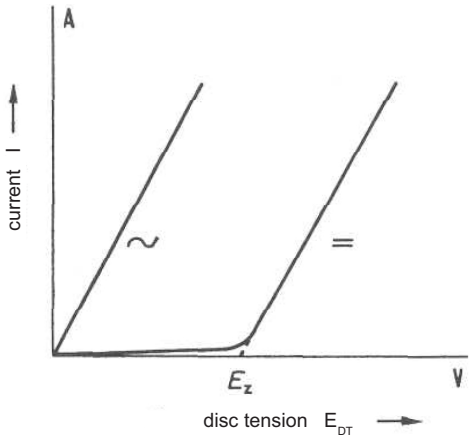

Figure 2-5: Electrolysis current I in dependence on the disc tension E_{DT} for alternating voltage (~) and direct voltage (=) [HV05].

$$|Z| = \sqrt{R^2 + (R_L - R_C)^2} = \sqrt{R^2 + \left(\omega L - \frac{1}{\omega C}\right)^2} \tag{2.10}$$

and φ is the phase-shift between the current and the voltage. To determine the resistivity of the electrolyte solution, the non-linear resistivities of the electrodes must be eliminated. This can be done with the help of alternating current. When a "disc tension" is applied to an electrochemical cell, so-called electrolytic double-layers occur at the electrodes because ions of contrary charge move towards the electrodes. With an applied alternating voltage, the double-layers change polarity with the frequency of the alternating voltage. When applying an alternating voltage $A_0 \sin(\omega t)$ with $A_0 < E_z$, where E_z is the decomposing field, the non-linear resistivity of the electrodes gets irrelevant because of $R_C = \frac{1}{\omega C}$ (ω: frequency of the alternating voltage). Therefore, the alternating current running through the electrochemical cell is just influenced by the ohmic resistivity R_E of the electrolyte. This causes a linear characteristic between current and voltage [HV05].
The frequency ω of the alternating voltage should not exceed a value of 50 kHz, because otherwise the inductances of the conductor circuit become to high ($R_L = \omega L$) [HV05].
The conductive value of an electrolyte can be written as

$$Y = \frac{A}{d} \cdot \kappa \,, \tag{2.11}$$

where A is the cross-section area, d is the distance between electrodes and κ is the conductivity $[\kappa] = \frac{1}{\Omega \cdot \mathrm{cm}}$. In priority the conductivity depends on the ionic concentration (see equation 2.6). Because of equations 2.7 and 2.11 the field strength inside the electrolyte solution results to

$$E = \frac{I}{A \cdot \kappa} = \frac{j}{\kappa} \quad \text{[HV05]} \tag{2.12}$$

with j as the current density and κ as the conductivity.

2.2.1 Electrolyte-conductivity in dependence on concentrations

Within an electrolyte there are electrostatic forces acting between the ions:

$$\vec{F}_{\text{COULOMB}} = \frac{1}{4\pi\epsilon} \cdot \frac{q_1 \cdot q_2}{r^2} \cdot \frac{\vec{r}}{r}\,, \tag{2.13}$$

where r is the distance between the ions and $q_i = z_i e_0$ is the charge of the ions. Because of these forces the ions constrain each other on their way through the electrolyte. Thus, with high ion concentration the conductivity value Y gets smaller again. Therefore, the conductivity in dependence on the ion concentration describes a curve which increases until reaching a maximum. After reaching this maximum the conductivity decreases slowly [HV05].

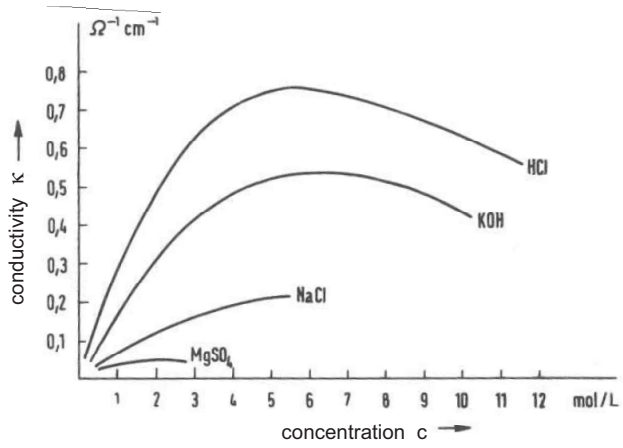

Figure 2-6: Conductivity of diluted electrolytes as a function of concentration at a temperature of $T = 18\,^{\circ}\text{C}$ [HV05].

In contrast to strong electrolytes, weak ones have a degree of dissociation depending on the electrolyte concentration. The degree of dissociation is defined as the dissociated fraction in relation to the total volume of electrolyte brought in solution. Also in relatively huge dilutions the values of dissociation degree are still small. Therefore, in weak electrolytes the conductivity in dependence on the concentration is mainly given by the development of the dissociation degree [HV05].

2.2.2 Debye-Hückel-Onsager theory of diluted electrolyte solutions

Solvated ions disperse themselves in a solution to reach an equilibrium state between the electrostatic force and the thermic movement of the ions [HV05, NTA04].
Due to the attractive and repulsive electric forces between the ions, their distribution in dilute solutions is not completely random. This ionic distribution was described quantitatively by DEBYE and HÜCKEL [NTA04].
Around each ion (central ion) a spherical-symmetrical cloud of ions, which are charged in the opposite way, is formed in a temporal average. Thereby, every ion participating

the ion cloud around a central ion is a central ion itself [HV05, NTA04].

When applying an electric field the equilibrium state of the charge carriers gets disordered by the acceleration of the central ion. After a relaxation time, within a new ion cloud is formed around the central ion, the equilibrium of charge is restored for a short term. However, the central ion always hurries its ion cloud a little ahead. In this way a so-called restoring force appears between the central ion and its ion cloud. This force is anti-proportional to the distance between the charge carriers (relaxation effect or effect of asymmetry) [HV05].

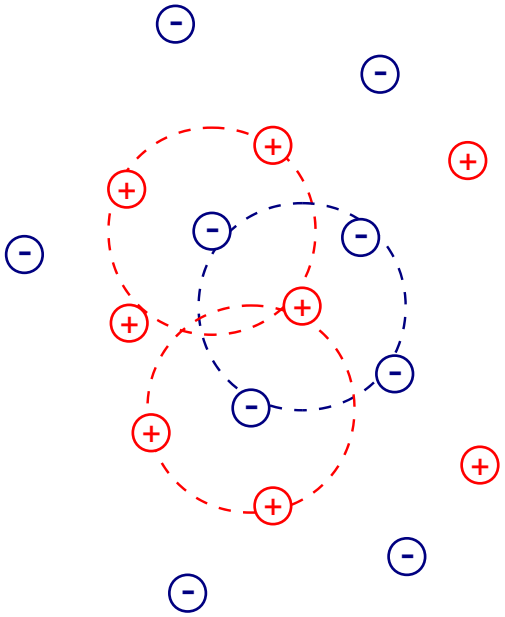

Figure 2-7: Two-dimensional scheme of ion configuration (central ion and surrounding ion cloud consisting of ions with opposite charge).

Apart from quantitative calculations of the electrostatic interactions between the central ion and its ion cloud in dependence on the concentration, the Stokes' braking force, appearing when ions move through the medium, is taken into account by the Debye-Hückel-Onsager theory (theory of electrolytic conductivity). Like the relaxation effect, the friction also depends on the ion concentration. With higher ion concentration more solvate shell movements of ions occur, wandering in opposite directions (so-called electrophoretic effect) [HV05].

When using spherical coordinates, the spacial distribution of the potential $\varphi(\vec{r})$ within an ion cloud can be described by the Poisson differential equation

$$\frac{1}{r^2} \cdot \frac{\partial}{\partial \vec{r}} \left(r^2 \frac{\partial \varphi(\vec{r})}{\partial \vec{r}} \right) = -\frac{\rho(\vec{r})}{\epsilon} \quad , \tag{2.14}$$

where $\rho(\vec{r})$ is the charge density ($\rho^+ - \rho^- \neq 0$) as a function of position and $\vec{r}$ is the radius vector and $\epsilon = \epsilon_0 \cdot \epsilon_r$ [HV05, NTA04].

In presence of the potential $\varphi(\vec{r})$, an ion i of the charge distribution, which has the charge $z_i e_0$, has the electric energy of $z_i e_0 \varphi(\vec{r})$ (electrical interaction energy).

The formation of ions, due to the stabilizing electric energy, is disturbed by random thermal motion of the ions and the solvent molecules, which counteract the electric effect and promote a random distribution of the ions. The ion density, resulting by the balance between these effects can be described by the Maxwell-Boltzmann distribution

$${}^1n_i(\vec{r}) = {}^1n_i^0 \cdot \exp\left(-\frac{z_i e_0 \varphi(\vec{r})}{k_B T} \right) \quad , \tag{2.15}$$

with ${}^1n_i^0$ as the number of ions i per cubic centimeter in uniformly distribution. The term k_BT (k_B: Boltzmann constant, T: Temperature) expresses the thermal energy of the ion [HV05, NTA04]. The charge density $\rho(\vec{r})$ equals the ion density multiplied by the ion charge, whereat it has to be summarized over all types of ions i:

$$\rho(\vec{r}) = \sum_i z_i e_0 \, {}^1n_i(\vec{r}) = \sum_i z_i e_0 \, {}^1n_i^0 \cdot \exp\left(-\frac{z_i e_0 \varphi(\vec{r})}{k_B T}\right) \quad . \tag{2.16}$$

DEBYE and FALKENHAGEN predicted that, when applying an alternating field of high frequency f with $\frac{1}{f}$ smaller than the relaxation time τ, an asymmetric formation of the central ion/ion cloud is no longer possible. Without the effect of asymmetry, the conductivity must increase. This effect of increasing conductivity is called Debye-Falkenhagen effect. Experiments have shown that this effect occurs for frequencies above 10^7-10^8 Hz. Hence, the relaxation time must be in the range of 10^{-8} s [HV05].
When an ion is accelerated by a high electric field and the ion needs less time to pass through an ion cloud than the time the ion cloud needs for its formation, the formation of an ion cloud is not possible. Above this critical field strength, one can observe an increase of conductivity in a range of several percent. This increase gets higher when the diameter of the ion cloud decreases (increase of the ion concentration). This phenomenon is known as Wien effect [HV05].

2.3 Potentials and structures of phase interfaces

This section treats potentials of membranes as well as potentials which can be found at electrodes of an electrochemical cell. When an electrode gets in contact with an electrolyte there are reactions leading to the generation of double-layers. In the following the generation of the double-layer, its capacity and the zeta-potential ζ are described.

2.3.1 Membrane potentials

When ions are involved in the stabilization of an osmotic equilibrium, an electrochemical equilibrium and the corresponding potential jump is generated in the semipermeable membrane, which separates two electrolyte solutions. The equilibrium state is established by diffusion of ions through the membrane. In equilibrium state the chemical and the electrochemical potential in both phases, which are separated by the membrane, must be identical. When ions are present in one phase, and these ions cannot diffuse through the membrane due to their size, there is a potential difference $\Delta\varphi = \varphi^{II} - \varphi^{I}$ at the membrane (Donnan potential) [HV05, KMM08].
In biological cells, normally there are so-called ion pumps, known as proteins. Proteins are able to create ion concentration differences between the membranes' inner and outer face and maintain this concentration gradient. This leads to a membrane potential [HV05]. So biological membranes behave similar to semipermeable membranes but

the potential of diffusion gives a larger part. The membrane potential can be written by

$$\Delta\varphi = \Delta\varphi^{II}_{\text{DONNAN}} + \Delta\varphi_{diff} - \Delta\varphi^{I}_{\text{DONNAN}} \quad . \tag{2.17}$$

It has to be considered, that for several ion types intra and extra cellular differences of concentrations can be generated. Therefore, the terms $\Delta\varphi^{II}_{\text{DONNAN}} - \Delta\varphi^{I}_{\text{DONNAN}}$ and $\Delta\varphi_{diff}$ consists of several parts which can be directed opposite to each other. Furthermore, charged particles bound to the surface (boundary layer) of the membrane also play a role [HV05].

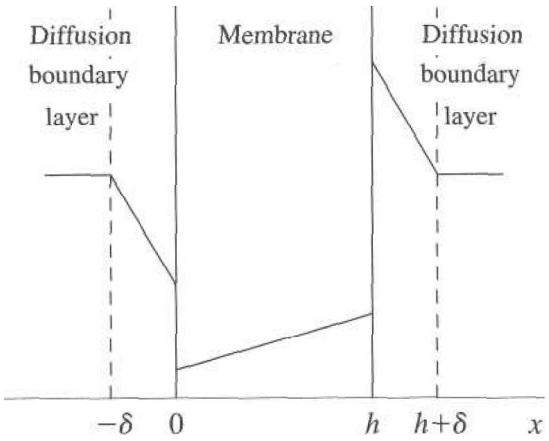

Figure 2-8: Scheme of the electrolyte concentration profile in a membrane system [KMM08].

The ion specific permeability of the membrane is controlled by the so-called ion canals which can open and close. Regarding a biological cell membrane of the macroscopic point of view it is a non-linear ion conductor. The membrane conductance value depends on its potential difference or difference of the ion concentration. Microscopic, the conductance value status of neighboring membrane parts can differ and therefore influence each other. This property is the base of the transmission of electric impulses through biological membranes [HV05].

2.3.2 Potentials of electrodes

When a metallic electrode gets in contact with an electrolyte solution, there can be reactions on the surface of the electrode. Even when no potential has been applied to the electrode to force current to flow, there is a potential difference between two electrodes, the so-called "surface over-potential" φ_s, which leads to a specific adsorption of ions at the electrode surfaces. In that way, a charged double-layer, which may be of the order of 1 to 10 nm in thickness, is generated to both sides of the phase interfaces. The generation of a double-layer by the adsorption of ions leads to a counterbalancing charge in a diffuse layer within the solution [NTA04].
The interior of the electrode and the electrolyte phase have different potentials, so

$\varphi_{electrode} \neq \varphi_{electrolyte}$. The difference $\Delta\varphi$ between the potentials of two phases $\varphi(I)$ and $\varphi(II)$ is known as Galvani voltage. When there are substances in a solution which form a redox pair, an equilibrium Galvani voltage can be found between an electrode and the electrolyte [HV05].
This equilibrium can be disturbed by applying a direct voltage between the electrode and a counter electrode. Due to the double-layer, there is a potential jump at the interface of the electrode. This potential jump can be varied by changing the electrode potential [NTA04]. The double-layer has a capacity, which can behave as a capacitor that is in parallel with the electrode reactions. By varying the electrode potential, the current passing from the electrode to the solution contributes to the charging of the double-layer capacity or take part in charge-transfer reactions (Faraday reactions). Thus, the generation of the double-layer increases or decreases or the double-layer changes the algebraic sign of its charge [HV05]. The diffuse part of the double-layer is part of the solution, and therefore mobile. When the diffuse double-layer interacts with an external electric field, the diffuse layer can be expected to move [NTA04].

The zeta-potential ζ

In an electrolytic double-layer on an electrode, the excess-ions inside the electrolyte barrier layer try to get close to the counter charge layer. An arrangement of the space charges in two parallel layers establishes. The distance between the centers of charge of the excess-ions to the electrode surface equals the half of the excess-ion-diameter $a/2$. The plane, which is formed by the charge emphasis of the electrolyte space charge, is called "Helmholtz plane" [HV05]. The "inner Helmholtz plane" (IHP) describes the position of the centers of the ions or molecules, which are adsorbed at the surface of the electrode, while the "outer Helmholtz plane" (OHP) is the locus of the centers of solvated ions at closest distance to the surface [NTA04].
The correlation between space charge density ρ and potential φ is given by the Poisson equation

$$\operatorname{div}\operatorname{grad}\varphi = -\frac{4\pi\rho}{\epsilon} \quad . \tag{2.18}$$

When regarding the ions of the OHP as punctual, there is a charge free space ($\rho = 0$) between this plane and the electrode. For this region, with $\rho = 0$, the integration over equation 2.18 results to $\frac{\mathrm{d}\varphi}{\mathrm{d}x} = const$ (x is the coordinate perpendicular to the electrode surface). So there is a linear potential transition between the electrode and the OHP [HV05].
But the model of the stiff Helmholtz double-layer is imperfect due to the thermal movement which dissipates this inflexible structure. Considering this effect, the (diffuse) ionic space charge ("diffuse double-layer") weakens with increasing distance to the elec-

trode surface (Gouy-Chapman theory)[‡], whereat the part, which is adjacent to the electrode, can be regarded as stiff again (according to STERN) [HV05, SS10].
The value $a/2$ is the smallest distance between the excess charge and the electrode ($x \geq \frac{a}{2}$). With $\beta = \left(x - \frac{a}{2}\right)$, for large β, the potential equals $\varphi(\beta) = \varphi_{electrolyte}$. For $\beta = 0$ the potential φ is $\varphi = \varphi(x = \frac{a}{2}) = \varphi_{OHP}$. The potential decreases exponentially within the diffuse double-layer from $\varphi = \varphi_{OHP}$ for $\beta = 0$ to $\varphi = \varphi_{electrolyte}$ for $\beta >> \frac{a}{2}$. Therefore, the Galvani voltage $\Delta\varphi$ between the electrode and the interior of the electrolyte solution is composed of two parts:

$$\Delta\varphi = (\varphi_{electrode} - \varphi_{OHP}) + \left(\varphi_{OHP} - \varphi_{electrolyte}\right) = \Delta\varphi_{stiff} + \Delta\varphi_{diffuse} \quad . \tag{2.19}$$

The potential difference $\varphi_{OHP} - \varphi_{electrolyte}$ between the OHP and the interior of the electrolyte is also known as **zeta-potential** ζ [HV05, NTA04]. So the Galvani voltage can be written by $\Delta\varphi = \Delta\varphi_{stiff} + \zeta$. At the distance $\beta = \lambda$ to the OHP, the potential difference between the OHP and the interior of the electrolyte is decreased to $1/e$ of its total value. This distance can be used as dimension of the diffuse double-layer thickness [HV05].
The thickness λ depends directly on the ionic strength $I = \frac{1}{2}\sum_i z_i^2 c_i$ of the solvent. In diluted electrolytes the dimensions of the diffuse layer can be about several 10 nm. But in solutions of a concentration of 0.1 mol/l, λ decreases to the dimension of the stiff layer-thickness. If the ionic strength is sufficient high, the complete double-layer can be approximated to be stiff and $\Delta\varphi_{diffuse} = \zeta$ can be neglected compared to the potential of the stiff double-layer $\Delta\varphi_{stiff}$ [HV05].
Ions, solvent dipoles as well as neutral molecules, which have a dipole characteristic, can be adsorbed on a metal surface when there is an van der Waals interaction with the metal or when there is a Coulomb interaction between the solvent components and the metal electrodes. The plane through the centers of adsorbed charges equals the IHP [HV05].

Double-layer capacity

In simplest case, the electrolytic double-layer can be compared to a parallel-plate capacitor with the capacity

$$C = \frac{Q}{U} \quad . \tag{2.20}$$

The charge Q equals the excess charge inside the solvent interface and the voltage U equals the potential difference between the electrode and the solvent. This potential difference is equivalent to the Galvani voltage $\Delta\varphi$ mentioned above, i. e. the double-layer

[‡] charge density weakens with increasing distance to the electrode by $\rho(x) = -\rho_s \kappa e^{-\kappa x}$ (ρ: charge density, ρ_s: surface charge density, κ: conductivity) [SS10]

capacity can be written by $C = \frac{Q}{\Delta\varphi} = \frac{Q}{\varphi - \varphi_{electrolyte}}$ [HV05, NTA04]. When the electrode potential is changed by a value $\mathrm{d}\varphi$, the change of the excess charge $\mathrm{d}Q$ depends on the already existing potential φ, i. e. $\mathrm{d}Q = \mathrm{d}Q(\varphi)$. Therefore, the so-called "differential double-layer capacity" C_d corresponds to

$$C_d = \frac{\mathrm{d}Q}{\mathrm{d}\varphi} \quad [\text{HV05, NTA04}] \,. \tag{2.21}$$

With $I = \frac{\mathrm{d}Q}{\mathrm{d}t}$, the capacity charge current I_C equals

$$I_C = \frac{\mathrm{d}Q(\varphi)}{\mathrm{d}t} = \frac{\partial Q}{\partial \varphi} \cdot \frac{\mathrm{d}\varphi}{\mathrm{d}t} = C_d \frac{\mathrm{d}\varphi}{\mathrm{d}t} \,. \tag{2.22}$$

The capacity of the Helmholtz layer can be approximated by the formula of a plate capacitor with an electrode area of 1 cm^2 and the plate distance d:

$$C = \frac{\epsilon}{d} \tag{2.23}$$

whereat ϵ is the dielectric permittivity. The dipoles of a solvent at the electrode surface and in the ion cloud of the solvate have a preferential orientation. The polarizability of the dipoles and therefore the value of the dielectric permittivity ϵ of the solvent decrease close to the electrode [HV05].
The stiff double-layer has to be described by two capacitors, which are connected in series (dipole-layer and layer between the IHP and OHP):

$$\frac{1}{C_{stiff}} = \frac{1}{C_{dipole}} + \frac{1}{C_{IHP-OHP}} \quad [\text{HV05, NTA04}] \,. \tag{2.24}$$

The capacity of the stiff double-layer does not only depend on the characteristics of the solution components but also on the material of the electrodes [HV05].
In diluted solutions, the capacity of the diffuse double-layer

$$C_{diffuse} = \frac{\epsilon}{\lambda} \tag{2.25}$$

has also to be taken into account in the series connection. Due to the fact, that $\lambda << \frac{a}{2}$, $C_{diffuse}$ is smaller than C_{stiff}. So, the total capacity decreases in diluted solutions.
Within an electrolytic double-layer, there can be high electric field strengths. When estimating that the thickness of the double-layer is several 10^{-8} cm and applying a voltage at the electrodes leading to a voltage difference of several 100 mV to the solvent, a mean field strength of

$$\frac{10^{-1}\,\mathrm{V}}{10^{-8}\,\mathrm{cm}} = 10^7\,\frac{\mathrm{V}}{\mathrm{cm}}$$

results within the layer. This field strength can already weaken electrostatic bonding forces in molecules [HV05].

Surface over-potential and the current density

The Butler-Volmer equation describes the dependence of the electrical current on the electrode potential. In this equation, it is considered that both a cathodic (reduction) and an anodic (oxidation) reaction occur on the same electrode.
The current density j depends on the surface over-potential φ_s , the solution composition adjacent to the electrode surface, the temperature and the nature of the electrode surface. The surface over-potential is given by with $\varphi_s = \varphi_{electrode} - \varphi_0$, where φ_0 is the equilibrium potential. The current density is represented by the Butler-Volmer equation

$$j_n = j_0 \left[e^{\frac{\alpha_a F \varphi_s}{k_B T}} - e^{-\frac{\alpha_c F \varphi_s}{k_B T}} \right] . \tag{2.26}$$

Here, j_0 is the exchange current density, which depends on the concentrations of reactants and products, temperature and the nature of the electrode-electrolyte interface as well as on impurities contaminating the electrode surface [HV05, NTA04]. Due to these dependences, j_0 can vary within a range from over $1\,\mathrm{mA/cm^2}$ to less than $10^{-7}\,\mathrm{mA/cm^2}$. F is the Faraday's constant $F = N_A \cdot e = 96\,485.3365\,\mathrm{C/mol}$. α_a and α_c are charge transfer coefficients for the cathodic and anodic reaction (additional kinetic parameters). They reflect how one direction of reaction is favored over the other by an applied potential. The transfer coefficients are related by

$$\alpha_a + \alpha_c = 1 . \tag{2.27}$$

For sufficiently large over-potentials a protective anodic oxide film forms on the electrode, which leads to a drop of the current density value. For higher over-potentials, the current density may increase again due to an anionic dissolution process or an electronically conducting film. In that case, the oxide film is removed from the surface of the electrode [NTA04].

2.4 Transport processes in electrolytic solutions

This section deals with the transport processes like migration and diffusion in electrolytic solutions. Besides of the basic diffusion laws for dilute solutions, thermal effects and transport properties as well as the corresponding fluid mechanics are described.

2.4.1 Infinitely diluted solutions

In infinitely diluted solutions, the medium consists of a nonionized solvent, ionized electrolytes and uncharged minor components.
Two of the known transport properties are the diffusion coefficient D_i and the mobility u_i, which denotes the average velocity of a species in the solution when acted by a force

of 1 N/mol independent of the force origin [NTA04].
The current density can be expressed by

$$\vec{j} = -F^2 \nabla\Phi \sum_i z_i^2 u_i c_i - F \sum_i z_i D_i \nabla c_i + F\vec{v} \sum_i z_i c_i \tag{2.28}$$

or when there are no concentration variations in the solution by

$$\vec{j} = -\kappa \nabla\Phi \ , \tag{2.29}$$

with the conductivity

$$\kappa = F^2 \sum_i z_i^2 u_i c_i \tag{2.30}$$

of the solution. The last term on the right side in equation 2.28 is zero due to electro-neutrality with

$$\sum_i z_i c_i = 0 \, . \tag{2.31}$$

Here, F is the Faraday constant, z_i is the charge number, c_i is the concentration of species i in $\frac{\text{mol}}{\text{cm}^3}$ and $\vec{v}$ is the bulk velocity of the fluid motion. Equation 2.29 is an expression of Ohm's law. It is valid for electrolytic solutions in the absence of concentration gradients, otherwise the current density is not proportional to the electric field and Ohm's law does not hold. In presence of concentration gradients, the diffusion current (second term in equation 2.28) plays a role. Due to the diffusion current, the current density could have a different direction from the electric field. With equations 2.30 and 2.31, equation 2.28 can be turned to

$$\nabla\Phi = -\underbrace{\frac{\vec{j}}{\kappa}}_{\nabla\Phi_{ohm}} \underbrace{- \frac{F}{\kappa} \sum_i z_i D_i \nabla c_i}_{\nabla\Phi_{diffusion}} \quad \text{[NTA04, KMM08].} \tag{2.32}$$

Even when there is no current present, there may be a potential gradient. The second term of equation 2.32 is known as the diffusion potential, which would be zero by electro-neutrality, if all the diffusion coefficients were equal [NTA04].
The potential gradient is related to the concentration gradient and the difference in diffusion coefficients for the diffusion of a salt.
Due to the fact, that the gradient of the electrochemical potential of species is the only driving force appropriate for diffusion and migration, it is to be expected that the ionic mobility and the diffusion coefficient are related to each other as described by the Nernst-Einstein equation

$$D_i = RTu_i \ , \tag{2.33}$$

with $R = 8.3143\,\mathrm{J/(mol\,K)}$ as the universal gas constant and the temperature T. This equation is only applicable at infinite dilution [NTA04].
The temperature dependence of ionic diffusion coefficients is approximated by the Stokes-Einstein relationship

$$D_i = \frac{RT}{6\pi\eta r_i} \ , \tag{2.34}$$

where η is the viscosity of the solution and r_i is the radius of a hydrated ion. As a consequence, the ionic diffusion coefficients and equivalent conductances can vary by 2-3 % per Kelvin (see also section 2.2) [NTA04].

2.4.2 Concentrated solutions

In dilute solutions the probability that two ions get close to each other is relatively small. In contrast, in concentrated solutions an ion is surrounded by both, solvent molecules and other ions. Thus, short-range interactions become important [KMM08].
Additional to the driving force there are frictional forces, which are proportional to the relative velocities of the components. Therefore, the thermodynamic driving force $-\nabla\mu_i$ for the motion of the solute (μ_i is the electrochemical potential of species i) produces no longer an acceleration of the ions but keeps them moving at a constant velocity $\vec{v}_i$. Both, the diffusion as well as the friction coefficients, depend on the composition of the electrolyte, the temperature and the pressure [KMM08].
The transport processes in concentrated solutions can be described by the Stefan-Maxwell approach

$$c_1 \nabla\mu_1 = K_{1,0}\left(\vec{v}_0 - \vec{v}_1\right) \ . \tag{2.35}$$

Here a two-component solution is considered, where the index $i = 0$ equals the solvent and $i = 1$ the solute. $K_{1,0}$ is the friction coefficient between solvent and solute.
For a multi-ionic system, equation 2.35 is augmented with the sum over all present ion species. The Stefan-Maxwell transport equations then are

$$c_i \nabla\mu_i = \sum_j K_{i,j}\left(\vec{v}_j - \vec{v}_i\right) \quad \text{[NTA04, KMM08].} \tag{2.36}$$

In this equation the sum also includes the solvent. With the Stefan-Maxwell diffusion coefficients $\bar{D}_{i,j}$ the friction coefficients $K_{i,j}$ can be written as

$$K_{i,j} = RTc_T \frac{x_i x_j}{\bar{D}_{i,j}} \ , \tag{2.37}$$

where c_T is the total molecular concentration (including the solvent), R is the universal gas constant, T is the temperature and $x_{i,j}$ is the molecular fraction of the component in the solution. With Onsager's reciprocal theorem follows $\bar{D}_{i,j} = \bar{D}_{j,i}$. The Stefan-

Maxwell equations only involve relative velocities and thus they are independent of the reference frame. But this also implies that additional equations are needed to describe the absolute motion of the solution [KMM08].

2.4.3 Transport properties

The electrode serves as a surface source or drain of the ion species involved in the electrode reactions, which entail a mass transport at electrodes. These electrode reactions lead to concentration differences close to the electrode which cause mass transport. The rate of an electrochemical reaction r_{ec} with the electrode is given by Faraday's law

$$r_{ec} = \frac{j}{nF} , \tag{2.38}$$

where r_{ec} is the reaction rate, j is the current density, n the number of electrons exchanged in the electrode reaction and F is the Faraday constant. The reaction rate and the mass transport are related to each other through the mass balance [KMM08].
The electric current density $\vec{j}$ is given by

$$\vec{j} = F \sum_i z_i c_i \vec{v}_i , \tag{2.39}$$

where i is an electro-active species, $\vec{v}_i$ is the velocity of the respective species and c_i its concentration. For infinitely dilute solutions there is one diffusion coefficient D_i for each solute species. These diffusion coefficients interact with each other. The mobility u_i is related to the diffusion coefficient by the Nernst-Einstein equation [NTA04].
For solutions of a single salt there are three transport properties. All three of them are functions of the concentration and the temperature. The diffusion coefficients for the ion-solvent interactions are constant, while for the ion-ion interaction the coefficient shows a $\sqrt{c}$-dependence (c: concentration). This dependence is characteristic for the Debye-Hückel-Onsager theory of ionic interactions in dilute solutions [NTA04].

2.4.4 Fluid mechanics

The diffusion and the migration fluxes are expressed by an average velocity of the fluid. The mass-average velocity $\vec{v}$ is defined as

$$\vec{v} = \frac{1}{\rho} \sum_i c_i M_i \vec{v}_i . \tag{2.40}$$

M_i is the molar mass of species i and ρ is the medium-density. The expression $\rho\vec{v}$ equals the mass-flux density in the fluid.
Within a medium there has to be a balance of mass. The law of mass conservation can

be expressed by

$$\frac{\partial \rho}{\partial t} = -\nabla \cdot (\rho \vec{v}) \ . \tag{2.41}$$

This equation reduces to $\nabla \vec{v} = 0$, when the medium-density ρ is constant in space and time [NTA04, KMM08]. When the density and the viscosity of a fluid are constant, the law of conservation of momentum is given by the Navier-Stokes equation

$$\frac{d\vec{v}(r,t)}{dt} = \frac{\partial \vec{v}}{\partial t} + \vec{v} \cdot \nabla \vec{v} = -\frac{1}{\rho} \nabla p + \nu \nabla^2 \vec{v} + \vec{f} \, , \tag{2.42}$$

where p is the thermodynamic pressure, $\nu = \frac{\eta}{\rho}$ is the *kinematic viscosity* of the fluid and $\vec{f}$ represents body forces (per unit volume), e. g. gravity, acting on the fluid. The rate of change of momentum of a fluid element is equal to the applied force (pressure gradient and body forces) [NTA04].
There can be other forces included in the momentum balance, too. If the fluid is not electrically neutral, the electrical force

$$\rho_e \vec{E} = \epsilon (\nabla \vec{E}) \vec{E} = \epsilon \left(\nabla^2 \Phi \right) \nabla \Phi \tag{2.43}$$

must also be taken into account for the law of momentum. In addition, in some electrochemical systems the body forces $\vec{f}$ also include the magnetic force (Lorentz force)

$$\vec{F}_L = \vec{j} \times \vec{B} \, , \tag{2.44}$$

where $\vec{j}$ is the current density within the solution and $\vec{B}$ is the magnetic induction in $\mathrm{Vs/m^2}$. At the same time, the magnetic field may itself be due to the current flow in the system [NTA04].
Because the electric field can be expressed by $\vec{E} = \frac{\vec{j}}{\kappa} + \frac{F}{\kappa} \sum_i z_i D_i \nabla c_i$, the electric charge density ρ_e in equation 2.43 can be written by

$$\frac{\rho_e}{\epsilon} = -\left(\vec{j} + F \sum_i z_i D_i \nabla c_i \right) \cdot \frac{\nabla \kappa}{\kappa^2} + \frac{F}{\kappa} \sum_i z_i D_i \nabla^2 c_i \, . \tag{2.45}$$

The concentrations c_i and the conductivity κ only vary in the thin diffusion layers near electrodes. Thus, only in these regions the electric charge density differs from zero. But even near the electrodes the charge density is small because the permittivity ϵ is small. Since, with a supporting electrolyte, κ will be large compared to the variations in κ, the electric effect will be largest with a binary electrolyte [NTA04].

2.5 Transport in membranes

When two compartments α and β are separated by a membrane and the compartments are ideally mixed, the homogeneous solute concentrations c^α and c^β are constant if the solutions are stirred (steady state). Otherwise, the concentrations vary in time as a result of transport across the membrane. This again leads to a time dependence of the transport process [KMM08].
If the compartment volumes V^α and V^β are large compared to the membrane volume, the solute flow leads to very slow time variations of the concentrations $c^\alpha(t)$ and $c^\beta(t)$. In that case, $c^\alpha(t)$ and $c^\beta(t)$ can be considered as constant as far as the transport across the membrane is concerned (quasi-steady-state) [KMM08].
Charged membranes, or ion-exchange-membranes, are either cation or anion selective. The selectivity depends on the inserted fixed acidic or basic dissociating groups within the membrane matrix. There are weak groups, such as carboxyl and amino groups, and strong groups like sulphonate groups. These groups lead to fixed-charge distributions that may depend on the composition of the solution filling the membrane phase. Membranes which have negatively charged (anionic) groups repel anions electrostatically and attract cations. In that way the fixed membrane charge is compensated. This is vice versa for membranes with cationic groups. If the ions in the solution, which are filling the membrane, are of the opposite sign to the fixed charge groups within the membrane, they are denoted as counter ions and if the solution-ions have similar charge to the fixed charge groups in the membrane, they are called co-ions [KMM08].
For the distribution of an ionic species i the Donnan-equilibrium condition establishes between the internal (int) and external (ext) solutions that its electrochemical potential is the same in the two phases

$$\mu_i^{int} = \mu_i^{ext} \,. \tag{2.46}$$

For membranes which have a high content of water, it can be assumed that the activity coefficients f_i and the standard chemical potentials μ_i^0 are the same in both phases, internal and external. The activity coefficients are correlated to the thermodynamic activity a_i of the species i by

$$a_i = f_i \cdot \frac{c_i}{c_0} \,, \tag{2.47}$$

where c_0 is necessary to ensure that both the activity and the activity coefficient are dimensionless. The thermodynamic activity is defined by the chemical potential μ_i and the chemical potential of species i in the chosen standard state (μ_i^0):

$$a_i = exp\left(\frac{\mu_i - \mu_i^0}{RT}\right) . \tag{2.48}$$

Here R is the gas constant and T the thermodynamic temperature.

If the activity coefficients f_i and standard chemical potentials μ_i^0 internal and external are the same, the distribution equilibria are described by

$$c_i^{int} = c_i^{ext} \cdot e^{-z_i \frac{F}{RT} \Delta\Phi_D} \tag{2.49}$$

$$c_{\pm,12}^{int} = c_{\pm,12}^{ext} , \tag{2.50}$$

where $\Delta\Phi_D = \Phi^{int} - \Phi^{ext}$ is the Donnan-potential and $c_{\pm,12}$ is the mean electrolyte concentration.
The stoichiometric electrolyte concentration in the membrane phase c_{12}^{int} is smaller than in the external phase $c_{12}^{ext} = \frac{c_1^{ext}}{\nu_1} = \frac{c_2^{ext}}{\nu_2}$, where ν_i is the number of ions of species i:

$$c_{12}^{int} = \frac{c_2^{int}}{\nu_2} = c_{12}^{ext} \cdot e^{-z_2 \frac{F}{RT} \Delta\Phi_D} \leq c_{12}^{ext} . \tag{2.51}$$

This phenomenon, known as Donnan exclusion, is responsible for the selectivity of ion-exchange membranes with respect to the transfer of charged species across them. Between the internal and the external phases there may exist a significant pressure difference. Due to the equilibrium condition for water, $\mu_0^{int} = \mu_0^{ext}$, the Donnan pressure difference Δp_D must follow the osmotic pressure difference by

$$\Delta p_D = p^{int} - p^{ext} = \pi^{int} - \pi^{ext} = \Delta\pi_D , \tag{2.52}$$

where π is the osmotic pressure. It can be assumed that the water partial molar volume is approximately the same in both phases. The difference in the osmotic pressure is given by

$$\Delta\pi_D \approx RT \left(\sum_i c_i^{int} - \sum_i c_i^{ext} \right) . \tag{2.53}$$

Ion-exchange membranes are able to equilibrate with the bathing solution by replacing the counter ions inside by those present in the solution, whereat the counter ions have to diffuse in and out of the membrane [KMM08].
Real membranes have a certain degree of heterogeneity which could result from an uneven distribution of fixed-charge groups throughout the membrane volume or from the initial structure of the membrane. In charged porous membranes the charge groups are on the pore walls and the solution inside the pores is not homogenous [KMM08].
When the electric potential inside the membrane is a function of position, $\Phi^{int}(\vec{r})$, the ionic concentrations inside the membrane are given by

$$c_i^{int}(\vec{r}) = c_{12}^{ext} \cdot e^{-z_i \frac{F}{RT} \left(\Phi^{int} - \Phi^{ext} \right)} , \tag{2.54}$$

where Φ^{ext} is the electric potential in the bulk external solution [KMM08].
To describe the heterogeneity of the membrane, it can be assumed that the membrane can be described as an array of parallel, cylindrical capillaries of radius b with an uni-

form surface-charge concentration σ on the pore walls. It is considered that the membrane is in equilibrium with a bathing solution of a concentration c_{12}^{ext}. The relation between the surface-charge density σ and the fixed-charge concentration c_{int} of the membrane is

$$z_{int}c_{int} = \frac{2\sigma}{bF} \,. \tag{2.55}$$

When the electric potential inside the membrane is a function of a radial position coordinate r that measures the distance to the pore axis, the potential distribution is obtained by the Poisson-Boltzmann equation

$$\frac{1}{r}\frac{d}{dr}\left(r\frac{d\Phi}{dr}\right) = \frac{z_2 F}{4\pi\epsilon}\left(c_1 - c_2\right) = \frac{2z_2 F c_{12}^{ext}}{4\pi\epsilon}\sinh(\varphi) \,, \tag{2.56}$$

where $\varphi(r) = z_2\frac{F}{RT}\left(\Phi(r) - \Phi^{ext}\right)$ is the dimensionless electric potential. This variation of the electric potential inside the membrane leads to a poorer co-ion exclusion than predicted by the Donnan theory [KMM08].

2.6 Adsorption of ions, dipoles, and neutral molecules on metal surfaces

Out of a microscopic view adsorption on metal electrodes is due to specific interactions of solvent particles with so-called active centers (e. g. surface states with bonding forces are not saturated because of their position at crystallographic steps or lattice defects). The electronic structure of the metal atoms itself plays a role, too [HV05].
Substances which can be adsorbed (adsorbates) can not only be gases like hydrogen, chlorine, nitrogen or oxygen, but also organic molecules like alcohols or acids. Furthermore, ions like Cu^+ ions can be adsorbed and even atom-overlays of e. g. lead (Pb), sulfur (S) and selenium (Se) are possible [HV05]. Adsorption can be caused by electrostatic interactions, chemical interactions and sometimes adsorption is caused by weaker interactions such as van der Waals forces. The adsorption of charged particles of the solvent involves at least a partial desolvation. Therefore, anions are adsorbed more likely than cations[§] [SS10].
The amount of adsorbed species is given in terms of the coverage Θ. The coverage describes the relation of the surface which is covered by adsorbates to the over-all electrode surface [HV05, SS10]. So the coverage has values of $0 \leq \Theta \leq 1$, whereat $1 - \Theta$ equals the free surface fraction [HV05]. The relation between the covered and the free

[§] cations tend to have a firmer solvation sheath than anions

surface of the electrode is given by the Langmuir isotherm

$$\frac{\Theta}{1-\Theta} = \frac{c}{c_0} e^{\left(\frac{\mu_{sol}-\mu_{ad}}{k_B T}\right)}, \tag{2.57}$$

where $\mu_{ad} = E_{ad} + k_B T \ln\left(\frac{\Theta}{1-\Theta}\right)$ is the chemical potential of the adsorbate (E_{ad}: adsorption energy per particle) and $\mu_{sol} = \mu_0 + k_B T \ln\left(\frac{c}{c_0}\right)$ is the chemical potential for an ideal solute. The difference $\Delta\mu = \mu_{sol} - \mu_{ad}$ depends on the potential Φ of the electrode. c is the concentration and the unit c_0 makes the argument $\frac{c}{c_0}$ of the logarithm dimensionless. When including the interactions between the adsorbates, one can assume that $\Delta\mu_{ad}$ is proportional to Θ by $\mu_{ad} = \mu_{ad}^0 + \lambda\Theta$, whereat λ is a constant. λ is positive if the adsorbed particles repel and negative if they attract each other. The resulting isotherm, also known as Frumkin isotherm is

$$\frac{\Theta}{1-\Theta} = \frac{c}{c_0} e^{\left(\frac{\mu_{sol}-\mu_{ad}}{k_B T}\right)} e^{\frac{\lambda}{RT}\Theta} \text{ [SS10].} \tag{2.58}$$

When the solvent contains positive, negative and uncharged particles and the charged particles are not under a specific adsorption but the uncharged particles are, the neutral particles can interact with the electrode surface without disruption. By changing the potential at the electrode in positive direction, anions are attracted into the double-layer at the electrodes and if applicable onto the surface under displacement of already adsorbed neutral particles. A negative potential at the electrode may lead to an adsorption of cations [HV05].

The structure of an over-layer resulting by adsorption on a simple crystalline surface depends on various factors such as the sizes of the adsorbate and substrate atoms or molecules and the interactions between the involved particles. If the interactions between the adsorbed species is repulsive, the over-layer has a homogeneous structure. But in presence of attractive forces the adsorbed particles tend to form islands or patches on the electrode surface [SS10].

The construction of a metallic surface during an electrochemical process on an electrode is named *electro-crystallization*. This surface construction is due to a material exchange which is parallel to the exchange of charge. The over-layer is growing layer by layer, whereat there are two mechanisms known for the development of layers or growth steps. On one hand there can be the two-dimensional nucleation whereat a new net layer develops on the surface, and on the other hand there can be a broadening of a growth step which arise from a screw dislocation and wind itself to a non-vanishing spiral as shown in figure 2-9 [HV05].

Mostly, on an electrode surface there can be found several screw dislocations which lead to a surface roughening. The deposit of ions on the electrode surface is preferential at positions where there are high electric field strengths. A roughening of the electrode surface is advantaged by the presence of solutions of low ionic concentration. In contrast, the deposit out of high concentrated solutions may lead to a smoothing of the electrode surface [HV05].

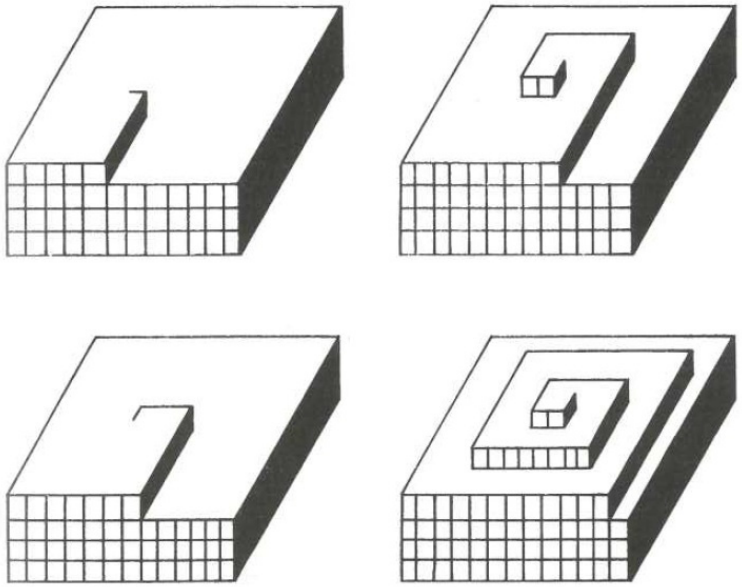

Figure 2-9: Scheme of the crystal-surface growth at presence of screw dislocations / spiral growth in a shape of pyramids [HV05].

Metal ions are not the only kind of ions which can be adsorbed by electrodes during an electrochemical process. There also can be an adsorption of organic molecules. When an electrode gets in contact with an aqueous solution containing a neutral aliphatic compound, the aliphatic chains are squeezed out towards the surface by the hydrogen-bounded water structure. But the dipole moment of an aliphatic compound is lower than that of water. When the electrode surface-charge is high, the polar water molecules are drawn towards the surface by electrostatic forces. At the same moment, the adsorbed molecules are expelled by the water molecules [SS10].
The inverse process to the deposition is the dissolution of metal, where metal atoms pass from lattice sites into the loose surface state. Thereat, the adsorption atom is already partly hydrated. After electron delivery to the metal electrode, the metal atom goes fully hydrated into solution [HV05].

Chapter 3

Methods for DNA transfer into cells

Up to now, there is no clear understanding of the mechanisms by which membrane breakdown is achieved [SD88], [KS86].
Many different methods were developed to transfer DNA molecules into biological cells. One of the newest methods is to transform cells with the help of a femtosecond laser. Thereat a temporary doorway can be opened into living cells so that DNA can get inside without harming the cells. UDAY TIRLAPUR and KARSTEN KÖNIG, who developed this method in 2002, used an infrared laser to cut a hole in Chinese Hamster Ovary (CHO) cells by a series of ultrashort laser pulses. They were able to transform single cells by transferring a green fluorescent protein (EGFP) into the treated cell. Those cells, which did not receive laser surgery did not produce the glowing protein. To porate cells by laser pulses is very effective and its selectivity is a great improvement over existing methods for gene transfer into cells, whereat it is not possible to target individual cells within a suspension [TK02, Har02].
Of the established methods for gene transfer into cells, the two most common ones are the $CaCl_2$-method for the biochemical techniques on the one hand and on the other hand the principle of electroporation. Due to the fact that a lot of cell types cannot be transformed by the $CaCl_2$-method but by electroporation, electroporation is the more frequent used technique. Another advantage of electroporation compared to the $CaCl_2$-method are the much higher transformation efficiencies.
In the following two sections the state of the art of the $CaCl_2$-method and electroporation will be presented. Thereat, the focus lies on the description of the electroporation process.

3.1 The $CaCl_2$-method

The laboratory technique of calcium chloride ($CaCl_2$) transformation increases the ability of a cell to incorporate plasmid DNA and allows it to be genetically transformed [DE79]. In presence of calcium ions, bacteria can be made competent to take up DNA

without the use of a phage. This competence is effective for linear and circular DNA molecules [MH70].
For calcium chloride transformation, bacteria are prepared by chilling the cells in the presence of Ca^{2+} by treating them with $CaCl_2$ solution to make them permeable to plasmid DNA [CCH72].
In the case of *E.coli* the cells grown to an optical density of 0.85 at a wavelength of 590 nm are washed in a 10 mM NaCl solution of a volume which equals the half of the cell volume. After centrifugation, the bacteria were resuspended in half their volume of 0.03 M $CaCl_2$ and kept at a temperature of 0 °C for 20 minutes. The *E.coli* are sedimented and resuspended again in 0.03 M $CaCl_2$ but for this time in a tenth of the volume of the cells. After a second incubation at 0 °C for 60 minutes and the addition of DNA, the bacteria are subjected to a heat pulse at 42 °C for a time duration of 2 minutes to enable the uptake of the DNA. The second incubation at 0 °C resulted in a fourfold increase in transformation efficiency whether or not DNA was already added to the cells. The effectiveness using chemical treatment methods varies widely among different types of prokaryotic cells. For *E.coli* transformation efficiencies of 10^5 to 10^6 transformants per microgram of DNA could be obtained [CCH72], [MH70]. By modifying the procedure, DAGERT and EHRLICH found in 1979, that competent *E.coli* cells which were prepared with a prolonged incubation in calcium chloride with a duration of about 24 hours yield over 10^7 transformants per µg DNA. Thereat no additional manipulations are required as compared with the standard method described above [DE79]. The achieved efficiency of *E.coli* transformation seldom exceeded about 10^8 transformants per microgram of nucleic acids and is frequently much less [Dow93].
The exact mechanism of the transformation with the calcium chloride method is not completely understood up to now. But it is known, that the cells have to be kept cool during the procedure. It is believed that the cool temperatures stimulate the attachment of DNA at the cell surface. The cold temperature also assists to change the physical characters of the membrane, like a reduced membrane fluidity, which facilitates the passage of DNA molecules through the membrane. It is assumed that the calcium ions play an important role to neutralize the negative electric charge of the phosphate groups of the cell membrane as well as of the DNA molecules which would repel each other otherwise due to their corresponding charge. During the heat shock, the DNA molecules get inside the cells. The heat shock produces a temperature gradient which can be compared to an opened door of a heated chamber in winter. By this way, the cells are transformed and obtain new characters like resistances to specific antibiotics [TP07].

3.2 The electroporation process

Gene transfer by electroporation is a useful alternative to chemical methods. A great range of species of eukaryotes and prokaryotes have been successfully electroporated by the use of electric fields. Many strains of *E.coli* are electro-competent to efficiencies

of 10^9 to 10^{10} transformants per µg of DNA [DMR88, Dru94]. This was determined by applying electric fields of very high amplitudes on *E.coli* with pBR- and pUC-variants as plasmid DNA [DMR88]. Transformation efficiencies can be reached which are as high as 80 % of the surviving cells and DNA capacities of nearly 10 µg/ml are possible [Dow93, Dru94].
Compared to biochemical techniques, electroporation is very simple and often efficiencies greater than those reached with chemical methods are available [TS11, N$^+$82, SD88, DMR88]. For example, some strains of *E.coli* yield only 10^8 to 10^9 transformants per µg of DNA with methods of chemical treatment, while by electroporation efficiencies up to 10^{10} transformants per µg are reached [DMR88]. Many types of eukaryotes and prokaryotes cannot be transfected or transformed by chemical methods but by electroporation [SD88].
When biological cells, eukaryotes as well as prokaryotes, are exposed to an electric field the components of the cell membrane become polarized. Across the membrane, a voltage potential develops which leads to a membrane breakdown in localized areas when the potential difference exceeds a threshold value. By this the cell membrane becomes permeable [HS67, Y$^+$00]. When the membrane becomes permeable, the resistance drops and the voltages within the system redistribute, while the membrane capacitance change is small [C$^+$82, FWW94]. At the moment whereat the membrane permeabilization and therefore the membrane conductance is maximal, the widely separated pores occupy only about 0.1 % of the electroporated membrane [FWW94, H$^+$91]. For most cells the charging times are of the order of 1 µs [Wea00]. The membrane of a cell, which has the thickness of about 5 nm and a dielectric constant of $\epsilon_r = 5$, can be regarded as an insulator which separates two conducting aqueous phases. It can be represented as a capacitance and a resistance which are arranged parallel, whereat the specific capacity of the membranes of biological cells assumes a value of 1 $\frac{\mu F}{cm^2}$ [Zim82]. As long as the magnitude or the duration of the applied electric field does not exceed a critical limit, the permeability of the cells is reversible [LNR77, SD88, Dru94]. When the electric field exceeds the critical limit, the cells are irreversibly damaged due to lysis [N$^+$82, HS67, SH68, SD88].
The effect of permeabilizing cells by the use of an electric field is known as "electroporation". As shown in former research, a voltage difference across the cell membrane of 0.2-1.5 V induced by an applied high voltage field is required for the forming of pores [TT81, SD88, KS86, Ros98]. Primary created pores have a radius of $r_p \approx 1$ nm [Wea00]. The required potential difference may depend on the composition of the cell membrane, temperature and the duration of appliance of the electric field [SD88]. When a strong external electric field is applied to a cell, the membrane becomes polarized due to the movement of ions and formation of dipoles along the electric field lines [TT81, LNR77, SD88, Wea00]. The ions accumulate on the membrane surface and thus generating a transmembrane potential [TT81, Zim82]. When applying a rapidly changing voltage on a cell, e. g. an AC field, fewer and fewer dipoles will be formed or reoriented in time, which leads to dielectric dispersion. This dispersion, which depends

on the dielectric and the mobility of the dipoles in it, is characterized by the dielectric relaxation time, given by $\tau = \frac{1}{2\pi f_0}$, with f_0 as the frequency of the AC field at the dispersion. This frequency dependence of the dielectric constant and the conductivity exhibits three dispersions known as α-, β- and γ-dispersions [Zim82].

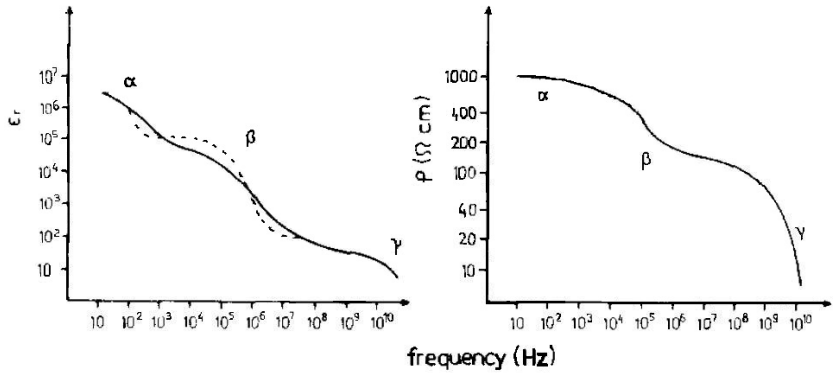

Figure 3-1: Frequency dependence of the dielectric constant ϵ_r and of the specific resistance ρ of a tissue [Zim82].

The α-dispersion in the lower frequency range is related to the relaxation of the cell membrane caused by the charge displacements in and around the membranes. The β-dispersion, the so-called Maxwell-Wagner dispersion, in the medium frequency range is due to charging processes at the interfaces of the membranes. Aside from the main dispersions, secondary dispersion ranges between the β- and γ-dispersion, which are not always easily to distinguish, arise from interfacial relaxations of sub-cellular components as well as from dipole rotation of macromolecules (proteins) and lipid molecules and the water bound to these molecules. Due to low ionic strength of the suspension used for the dielectrophoresis and fusion of cells the dispersions may be shifted to lower frequency ranges, because of changes in the relaxation times [Zim82].
The capacity and the high resistivity of the membrane force the current to flow around the cells at low frequencies. With increasing frequencies, the membrane capacity offers progressively less resistance and at high frequencies, the conductive cell interior contributes to the total conductance [Zim82].

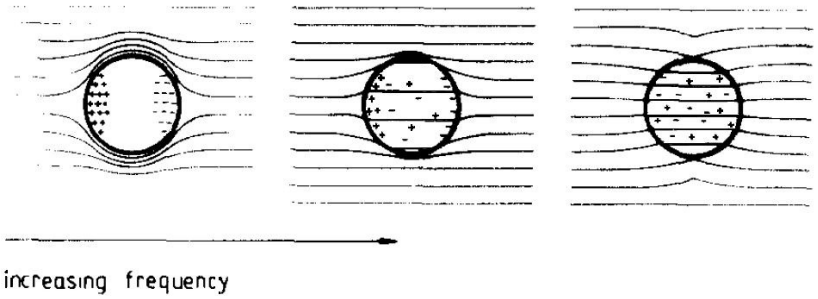

Figure 3-2: Frequency dependence of the current flow around and through a spherical cell [Zim82].

The electric conductance of the membrane increases when the frequency raises while the dielectric constant ϵ_r exhibits the opposite behavior. At low frequencies, the charged particles in the cell interior are virtually free of field and a charge (ion) distribution occurs. In this case, the cell behaves like a large dipole. With increasing frequencies, the charge separation becomes less strict, since the ion movement takes time and the impedance of the cell membrane reduces. The dielectric constant measured for the whole system is quite small [Zim82].
The generation of a dipole at low frequencies causes a membrane potential difference between the cell interior and the cell exterior, and a field-induced dipole can exert a force on other dipoles in its vicinity. Depending on the experimental conditions, both of these effects can occur separately or together with the production of heat due to friction (Joule heating) and by dielectric losses [Zim82]. The permeability of the cell membrane is attributed to the field-induced transmembrane potential. No other effects such as Joule heating or the shock wave associated with the voltage discharge are involved to the forming of pores [TT81]. Through the pores of the electroporated cell membrane, molecules can be introduced or escape [SD88].
Membrane recovery is generally dependent on temperature. Some pores, induced by electroporation, remain open for long times. So ions and molecules can continue to cross the cell membrane by diffusion and electrically driven associated with diffusion potentials until the pores have closed again [Wea00].
The process of electroporation has become an established method to transfer nucleic acids into eukaryotic (transfection) and prokaryotic cells (transformation) [SD88].
Through the induced pores which have a minimum radius of approximately 1 nm, not only DNA but also small ions such as Na^+ and Ca^- can be transported [Wea00].
When a spherical membrane-bound particle with a membrane of the thickness d, an inner radius a and an outer radius b is placed in a plane electric field of the strength E, the voltage difference ΔU across the membrane at a point P can be written by

$$\Delta U = \left\{ \left[1 + \frac{1 + \lambda - 2\lambda^2}{9 + 2(1-\lambda)^2 \cdot 3\frac{d}{b}} \right] b - \left[\frac{\left(1 + \lambda + 2\lambda^2\right)\left(1 - 2\frac{d}{b}\right) + 9\lambda}{9 + 2(1-\lambda)^2 \cdot 3\frac{d}{b}} \right] a \right\} E \,. \quad (3.1)$$

The parameter λ describes the ratio between the membrane conductivity and the external buffer conductivity. The conductivity of the initial buffer of the particle is supposed to be the same as that one of the external buffer. Assuming that the conductivity of the membrane is much smaller than that of the fluids inside and outside the cell, it can be considered to be zero which means that $\lambda = 0$. Further it can be considered that the thickness of the membrane can be neglected compared to the outer radius. In this case, the induced membrane potential at sub-threshold external fields is given by a solution to Laplace's equation as

$$\Delta U = 1.5 \cdot r \cdot E \cdot \cos\theta \,. \quad (3.2)$$

This formula is often referred to as Schwan's equation. Here r is now the outer radius of the particle and θ is the angle between the vector to a point P on the cell membrane and the direction of the electric field, whereat the origin of the vector $\vec{P}$ of the point P equals the geometric center of the cell. Hence, the maximum voltage difference U_{max} can be found across the membrane when $\cos\theta = \pm 1$. So the maximum potential difference is at the points $\theta = 0$ and $\theta = \pi$ in line with the field direction [N$^+$82, TT81, SH68, KS86, GLW86, Ros98]. Therefore the maximum voltage difference ΔU_{max} can be calculated by

$$U_{max} = 1.5 \cdot r \cdot E \,. \tag{3.3}$$

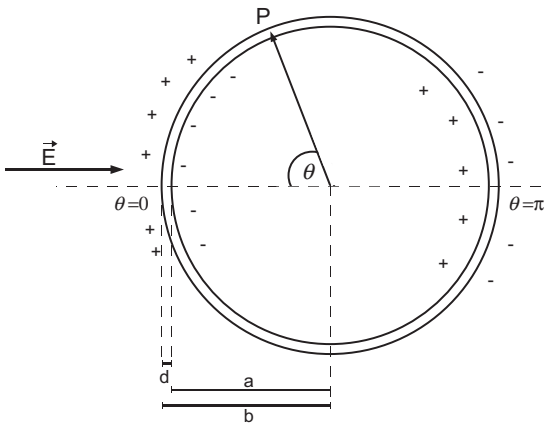

Figure 3-3: Draft of a biological cell treated with an electric field.

With this conditions the value of U_{max} for a given electric field is determined by the radius of the cell. So an applied electric field of 2 kV/cm will place a maximum voltage difference of $U_{max} = 3$ V across the plasma membrane of a cell with the radius r =10 µm, while the same electric field strength causes only a voltage difference $U_{max} = 30$ mV across the membrane of a cell with the radius r =0.1 µm [KS86]. So efficient transfection of eukaryotes and transformation of prokaryotes depend on the optimization of the electrical and biological parameters for each individual cell type [SD88]. But Schwan's equation is not exact for cells in suspension, which are exposed to an electric field. Due to the presence of other cells within the suspension, the electric field outside a cell is no longer homogeneous. So the induced transmembrane voltage depends not only on the geometrical and electrical properties of the cell itself but also on the cell density in the suspension [SSM98, PPM02].

Permeabilization of cells can be achieved, when exposing cells to an appropriate electric field having a duration of 1-2 µs. If all cells of a heterogeneous suspension should be electroporated, the critical voltage potential across the plasma membrane of the smallest cell in the population must be achieved with the risk of damage to the larger cells. Using this method on immobilized cells may restrict the ability to make multiple membrane lesions as a consequence of repeated exposures to the applied electric field. For cells which are in suspension, multiple membrane lesions are available due to cellular tumbling [KS86].

In the formation of hydrophilic (aqueous) pores, the lipides adjacent to the aqueous inside of the pore reorient in a manner that their hydrophilic heads are facing the pore, while their hydrophobic tails are hidden inside the membrane [KSN96].

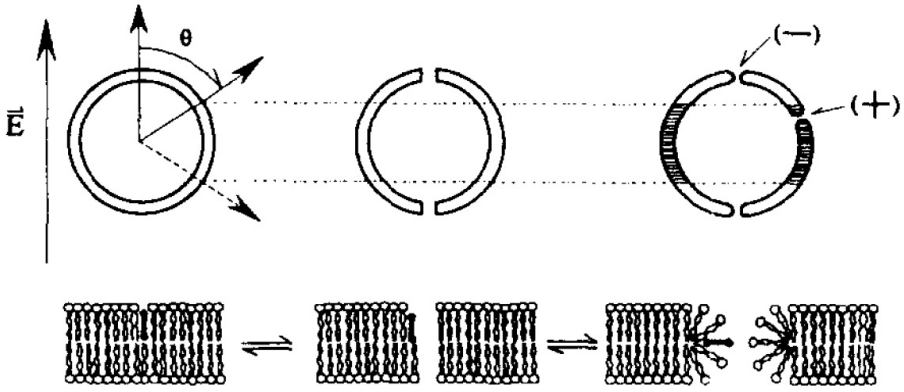

Figure 3-4: Scheme for the molecular rearrangement of the lipids in the pore edges and for the lipid cluster phase transitions [KSN96].

To electroporate cells, they can be exposed briefly to an intense electric field by rapid passage through a steady field or by pulsing the field through a static cell suspension [KS86]. If the discharge of a capacitor is used to produce a pulsed electric field, the applied field decays exponentially. The voltage declines over time as a function of the time constant τ, which is a convenient expression of the duration of the pulse, by

$$U(t) = U_0 \cdot e^{-\frac{t}{\tau}} . \tag{3.4}$$

τ is a product of the capacitance C of the capacitor in farads and the ohmic resistance of the cell suspension R ($\tau = RC$) and describes the time required for the voltage to decline to $1/e$, which equals 37% of the peak amplitude [LNR77, SD88, KS86, DMR88]. A larger capacitor or higher resistance in the circuit leads to longer pulses. The voltage drops as a function of the electric field strength E and the size of the electroporation cell. The electric field strength is related to the potential of the electrodes by

$$E = \frac{U}{d} , \tag{3.5}$$

where d is the distance between the electrodes and U the applied voltage [SD88]. When the electrode gap is fixed during the applied electric pulse, the field strength follows the voltage decline of the capacitor:

$$E(t) = E_0 \cdot e^{-\frac{t}{\tau}} . \tag{3.6}$$

The sample resistance can be determined by its ionic strength and the geometry of the sample chamber and the electrodes. The capacitor discharge of a given size capacitor into a medium with higher ionic strength and therefore a lower resistance will produce a pulse with a shorter time constant τ [TT81, SD88].
Hence, the transmembrane potential can be written as

$$\Delta U = 1.5 \cdot r \cdot \cos\theta \cdot E_0 \cdot e^{-\frac{t}{\tau}} . \tag{3.7}$$

The initial applied electric field strength E_0 and the time constant of the capacitor dischargement τ are two of the most important electric variables affecting electroporation. The electric field strength can be adjusted by varying the voltage to which the capacitor is charged or the distance between the electrodes. Due to the specificity of the capacitor the voltage cannot be varied without limits. The time constant τ can be regulated by changing the size of the capacitor or the resistance of the sample. The flexibility of the obtaining E_0 and τ is not unlimited. Changing the ionic strength of the cell suspension, which should be electroporated, can have a reducing influence on the viability of the cells [SD88].
When the membrane is permeabilized by electroporation, the membrane becomes conductive by means of the induced transient pores. Thus, the induced membrane potential is reduced. Equation 3.3 is only valid as far as the ratio λ between the membrane conductivity and the external buffer conductivity is zero (see equation 3.1). If the membrane becomes as conductive as the buffer ($\lambda = 1$), one obtains

$$\Delta U = (b - a) \cdot E \,, \tag{3.8}$$

with a and b as the inner and outer radii of the cell [TT81].
To prolonging the life of the capacitor and minimize the heating of the cell suspension during electroporation, the applied voltage should be kept as low as possible by decreasing the spacing between the electrodes. An applied electric field of 20 kV/cm, which is needed to produce an equivalent voltage gradient in a cell with the radius of r =1 µm to electroporate it, can be obtained best by discharging a capacitor charged to 2 kV and an electrode distance of 1 mm. By decreasing the spacing between the electrodes and increasing the cross sectional area of solution at the electrode surfaces to obtain a reasonable working volume of the cell suspension, the resistance will be decreased. To get a minimal value for the time constant, not to heat the cell substance, either the size of the capacitors or the resistance of the medium must be increased [KS86]. The ionic strength determines the current by the time constant τ but also the rate of heating of the sample [SD88]. When modifying the ionic strength of the medium it must be ensured that the conductivity of the medium is still greater that that of the cellular membranes [KS86].
The effective size and the stability of the pores in the membrane, caused by electroporation, is crucial to the cell preparations. The pore size can be estimated in larger cells by determination of the rate at which substances enter and leave the cell through the electroporated membrane. As an example, the rate of leakage of several markers from adrenal medullary cells, electroporated by an electric field of 2 kV/cm, indicates an effective pore size of approximately 4 nm. Due to the fact that the rates of marker entry or leakage are too fast, this approach cannot easily be used for small cells [KS86].
Small changes in the electric field strength can have a great influence on the yield of transformants. The transfection of eukaryotes, or transformation in the case of prokaryotes, increases with higher electric field strength, peaks and then sharply declines. The

sensitivity to an electric pulse varies for different types of cells. The electric field strength as well as the time constant τ of the pulse affect cell viability and transformation frequency. Increasing one of these variables or the number of applied pulses, transformation and cell death increase up to a point where the cell death by protoplast lysis becomes excessive and the efficiency of the transformants declines. So an optimal combination of electric field strength and time constant must be experimentally determined for each cell type to produce maximum transformation [SD88].
There are many parameters influencing the electroporation efficiency of cells. It is known that the presence of divalent cations stabilize membranes of eukaryotes which may make the cell membrane more resistant to electroporation. But the presence of divalent cations also have an influence on electroporation of bacteria. Electroporation of *Campylobacter* is strongly inhibited by just 1 mM Ca^{+2}, Mn^{+2} or Mg^{+2} while electroporation of *E.coli* is unaffected up to 10 mM of these cations [SD88].
To detect the formation of pores by electroporation molecules and/or DNA fragments are brought into the suspension of cells. When these particles pass through a pore in the cell membrane, the cell becomes transformed and gets a specific new character. This specific feature allows to separate transformed from non-transformed cells and therefore gives a hint to the success rate of electroporation.
The molecules can pass through an electroporated membrane by several ways, whereat there are three general mechanisms of transmembrane transport:

- Diffusion
- Electrophoresis
- Osmosis

In case of diffusion, the molecules passing through the membrane are driven by the molecular concentration difference across the membrane. When the passing molecules are driven by an electric potential difference across the membrane, the corresponding mechanism is the electrophoresis and in case of osmosis the driving force is the osmotic pressure difference across the cell membrane.
In most experimental studies it is said, that the main component of small molecules transported through an electroporated membrane is diffusion [TAC94, N^{+}98, GT99].
For macromolecules the mechanism of diffusion is often insufficient to pass through the membrane adequately. But it is known that the presence of electrophoretic forces can improve the uptake of macromolecules significantly [RT98, S^{+}02]. Mostly, electrophoretic transport of macromolecules proceeds during the applied voltage pulse. To achieve sufficient molecule/DNA uptake, the used pulses have durations of milliseconds to tens of milliseconds [RT98, R^{+}98].
For some types of eukaryotic as well as of prokaryotic cells it has been reported that electroporation was more efficient at temperatures of 0-4 °C. For example *E.coli* have at least 100-fold higher transformation efficiencies when electroporated at a temperature

of 0-4 °C than when pulsed at room temperature (20-25 °C), which may be an effect related to the state of membranes or a consequence of the additional joule heating that occurs during the pulsing process [SD88].
Another parameter affecting on the transformation efficiency is the form of DNA which should be introduced into the cells by electroporation. So there is a difference when using supercoiled circular plasmid DNA or linearized DNA which probably behaves as a much larger molecule even though it has the same molecular mass as the supercoiled plasmid. Due to the possible role of DNA topology in the electroporation process, it is difficult to compare electroporation of lambda DNA and plasmid DNA [SD88].
The efficiency of transformation is also dependent on the concentration of DNA inside the medium. With an increase of DNA concentration there is an increase of transformants [SD88, DMR88, Z$^+$11, FTW85]. With *E.coli* the number of transformants increases linearly with DNA concentration, as can be seen in figure 3-5 [SD88]. But the transformation probability becomes non-linear above one plasmid per cell and saturation occurs at approximately 150 plasmids per cell [Han83]. So above a certain concentration of DNA a saturation of transformants can be observed. In this way the transformation rate which is calculated by the number of transformants divided by the amount of DNA in microgram reaches a maximum and decreases again [Z$^+$11]. This phenomenon occurs with several types of bacteria cells. It was not only observed for *E.coli* but also on *Streptococci* [SD88]. The amount of DNA leading to this saturation varies for each type of cells. However, the concentration of DNA that saturates the transformation system is much higher for electroporation than for chemically-mediated transformation [SD88].

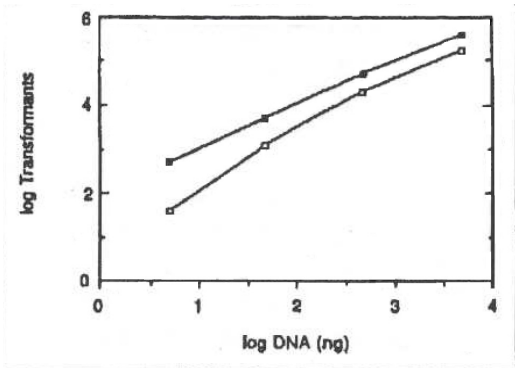

(a) different DNA pBR322 concentrations added to 0.8 ml of *E.coli* LE392 (c=2 · 10^{9}cells/ml) at applied field strength of 6 kV/cm (■) and 5 kV/cm (□) of a pulse duration of 5 ms

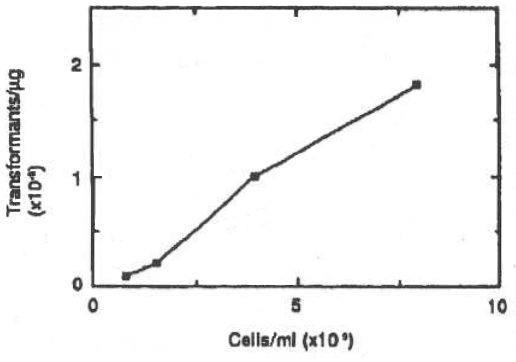

(b) different cell concentrations with pBR322 DNA (c=0.1 µg/ml) at an applied field strength of 6 kV/cm of a duration of 5 ms

Figure 3-5: Transformed *E.coli* LE392 with pBR322 DNA selected on ampicillin which were electroporated with single exponential pulses [SD88].

The size of DNA molecules might have an effect on the electroporation efficiency but the absolute size limit of DNA which can be transferred into cells by electroporation is not known [SD88]. It could be observed, that with increasing plasmid size transfor-

mation efficiencies of *E.coli* declines linearly [Han83]. Though, it was shown, that two separate plasmids containing different selectable markers can be transferred simultaneously into cells [SD88].
To electroporate prokaryotes several waveforms of electric pulses are effective. So electric pulses with an exponential decay as well as pulses of square wave, whereat the voltage is raised to a given amplitude maintaining for a specific time (pulse width) and then returned to zero, can be used. Due to the smaller size of bacterial cells compared to eukaryotes, higher electric field strength are required for electroporation as can be calculated by equation 3.3. For example, for a pulse with exponential decay of a duration of 5 ms, transformation of *E.coli* is not detectable until an applied field strength of at least 3 kV/cm (see figure 3-6a). Maximum transformation could be observed at 10 kV/cm. In comparison, for cultured mammalian cells the highest transformation efficiencies occurred at a range of $E_0 = 0.5\text{-}1.0\,\text{kV/cm}$ at the same pulse duration [SD88]. It was shown that longer pulses (longer time constants τ) reduce the voltage requirement for transformation of cells. The dependence of transformation on τ and the compensating effect on transformation of the field strength and τ can be seen in figures 3-6b and 3-6c. As this effect was also observed in transformation of several types of cells, this seems to be a general phenomenon.

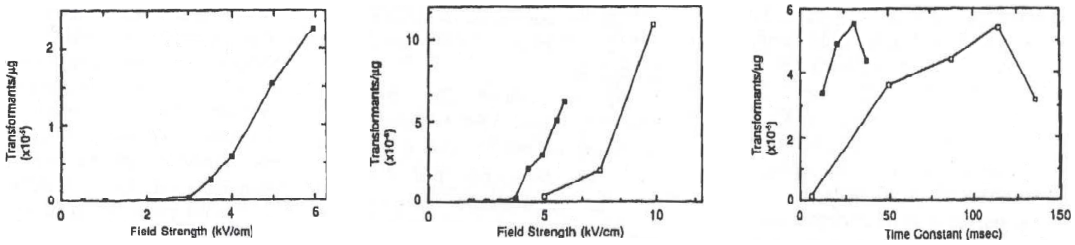

(a) Pulses with a duration of 5 ms **(b)** Pulse durations of 4.6 ms (□) and 13 ms (■) **(c)** Electric fields of 3.75 kV/cm (□) and 6.25 kV/cm (■)

Figure 3-6: Transformed *E.coli* LE392 with pBR322 DNA selected on ampicillin which were electroporated with single exponential pulses [SD88].

When cells are permeabilized by electroporation, they can be transformed when DNA slips inside. In the case of mammalian cells the applied electric field induces a complex reaction between the cell membrane and the DNA strain carrying plasmid, which is accumulated at the cell interface by electrophoretic forces. These electrophoretic forces effect the insertion of the plasmid into the cell by crossing the membrane [K^+91, S^+92b]. In contrast, results of measurements with *E.coli* showed no influence of electrophoretic forces on the insertion process of plasmids into the bacteria cells [W^+94].

Chapter 4

Experimental arrangement and preparation of the samples

This chapter deals with the preparation of the bacteria samples and the experimental arrangement. In the experiments *E.coli* C600 and *Bacillus subtilis* 168 were electroporated with pDsRed-Express plasmid DNA or pBluescript II KS +. Before the bacteria samples could be used for electroporation they had to be made electro-competent. Therefore, the bacteria need to be washed several times with double-distilled water as explained in section 4.1.
Furthermore, the different configurations of experimental arrangement used for the electroporation of the bacteria preparations are presented. A small volume of bacteria suspension was electroporated within commercially available electroporation cuvettes with inserted aluminum electrodes. The voltage needed for electroporation was generated by a voltage generator which was rebuilt from a commercial one. An oscilloscope measured the current and the voltage within the electroporation cuvette. With the help of the current and voltage data and the determination of the transformation efficiency of the bacteria the relation between transformation efficiency, electric field strength, conductivity of the bacteria suspension, current density and charge was ascertained. Details about the experimental setup can be found in section 4.2.

4.1 Preparation of the bacteria samples

In former research [Dow88, Dow93] was mentioned, that it is necessary to make bacteria "electro competent". For electroporation experiments bacteria have to be washed with water or a low conductivity medium in order to reduce the salts and the conductivity to get a high resistance of several 1000 Ω.
In this section it is explained how *E.coli* C600 and *Bacillus subtilis* 168 were treated to make them electro-competent.

4.1.1 Preparation of electro-competent *E.coli* C600

E.coli C600 of a glycerin-permanent culture were spread on a LB-plate without additions and incubated for 16 hours at 37 °C. To prepare the LB-plate, 15 g Agar-Agar (Kobe I) (ROTH, Germany) and 25 g LB broth powder (Luria/Miller) (ROTH, Germany) were suspended in 1 l double distilled water and autoclaved for 20 minutes at 121 °C on a liquid cycle before pouring it into petridishes ($\varnothing = 9$ cm). From this plate one of the formed colonies was picked and put into 10 ml of LB-medium. The LB-medium was prepared by suspending 25 g LB broth powder (Luria/Miller) (ROTH, Germany) in 1 l double distilled water and autoclave this mixture for 20 minutes at 121 °C on a liquid cycle. To get a pre-culture of *E.coli* bacteria, the LB-medium, which contained the picked up colony, was given into a shaking incubator (GESELLSCHAFT FÜR LABORTECHNIK MBH, GFL 3031) at 200 rpm and a temperature of 37 °C for 16 hours.
Out of this pre-culture 1 ml was given into several Erlenmeyer flasks filled with 250 ml of LB-medium. Afterwards these Erlenmeyer flasks were put into the shaking incubator at 37 °C and 150 rpm. When an OD_{600} (optical density at a wavelength of 600 nm) of a value between 0.6 and 0.7 was reached (measured with EPPENDORF, BioPhotometer *plus*), the Erlenmeyer flasks were put on ice for at least 30 min.
It was found, that the stage of the growth cycle at which cells are harvested is critical to success. There is a narrow window in the cell concentration at harvest. Above or below this window, the transformation efficiency drops off rapidly. For *E.coli* the optimal stage of the growth cycle occurs at a cell concentration corresponding to an optical density of 0.6 at a wavelength of 600 nm [B$^+$07].
The content of the Erlenmeyer flasks was filled in cooled centrifuge beakers (volume: 250 ml) and centrifuged at 4 °C for 15 min with $5000 \cdot g$. The supernatant was discarded. For the washing process the bacteria, which are left in the centrifuge beakers, were elutriated with 250 ml ice-cold autoclaved distilled water, each. The suspension was centrifuged again under the same conditions. To wash bacteria a second or more times the resulting pellet was imbibed again in 250 ml of ice-cold autoclaved distilled water and centrifuged (4 °C, 15 min, $5000 \cdot g$).
After the last washing process the pellet of each centrifuge beaker was resuspensed with 1350 µl of double distilled water. To avoid the damage of the bacteria, when storing them in the freezer (−80 °C) for later use, glycerin was added (10:1, 10 parts of bacteria suspension and 1 part glycerin).

4.1.2 Preparation of electro-competent *Bacillus subtilis* 168

Bacillus subtilis 168 were made electro-competent in a similar way like *E.coli*. For the pre-culture one colony of *Bacillus subtilis* 168 was picked from a LB-Agar-plate and put into 10 ml of LB-medium. This mixture was given into a rotating shaker (GESELLSCHAFT FÜR LABORTECHNIK MBH, GFL 3031) at 200 rpm and a temperature of 37 °C. After 6 hours the temperature was decreased to 30 °C whereat the pre-culture was mixed for

another 66 hours. While *E.coli* have an optimal growth temperature at about 37 °C, for *Bacillus subtilis* the ideal temperature ranges from 28-30 °C [NRC99].
Out of this pre-culture 1 ml was given in several Erlenmeyer flasks filled with 250 ml of LB-medium. In the Erlenmeyer flasks *Bacillus subtilis* 168 was grown by mixing them in the rotating shaker at 37 °C to an OD_{600} (optical density at a wavelength of $\lambda = 600\,\text{nm}$) of 1.5 (measured with EPPENDORF, BioPhotometer *plus*). The *Bacillus subtilis* 168 cells were harvested and washed twice the same way as *E.coli* C600.
In 1991, STEPHENSON *et al.* found, that *Bacillus subtilis* 168 showed best transformation efficiencies when suspended in 30 % polyethylene-glycol (PEG). For *B. subtilis* 168 suspended in glycerin, transformation efficiencies were very low [SJ91].
Therefore, in contrary to *E.coli* C600 to which glycerin was added, *Bacillus subtilis* 168 were resuspended in 33 % PEG 6000 (CARL ROTH GMBH + CO. KG) in a ratio of 10:1 (10 parts of PEG and 1 part of *B. subtilis* 168) to store them in the freezer at $-80\,^{\circ}\text{C}$ for later use.

4.2 Experimental arrangement

In this section the details of the experimental setup for the electroporation of *E.coli* C600 and *Bacillus subtilis* 168 are described.
To determine the dependence of the transformation efficiency of *E.coli* C600 and *Bacillus subtilis* 168 on several physical parameters two experimental setups were used which differ only by the used voltage generator and the resistance.
To detect transformation efficiencies of *E.coli* C600 and *Bacillus subtilis* 168 in dependence on the electric field and the current density, an experimental arrangement was used as shown in figure 4-1. Commercially available cuvettes of synthetic material with inserted aluminum electrodes (BIO-BUDGET TECHNOLOGIES GMBH, electroporation cuvettes with long electrodes, electrode dimensions: 1 cm×1 cm, 1 mm distance) were used for electroporation. The sample with a volume of 100 µl had to be given between the electrodes to fill up the cuvette gap (d=1 mm).
The bacteria were electroporated with an electric field, generated by a voltage generator, which performs single pulses with an abrupt increase $\left(\frac{\Delta U}{\Delta t} = 1500\,\frac{\text{V}}{\mu\text{s}}\right)$ and an exponential decrease (decay time $\tau = 3\,\text{ms}$). The generated voltage can be adjusted between 50 V and 3000 V. The voltage generator is a reproduction of a commercial one.
The electroporation cuvette and a resistance of $1\,\Omega$ are connected in series with the generator. In order to protect the oscilloscope, which was connected parallel to the generator and the resistivity, a probe (also parallel to the generator) and a protection circuit was placed in the construction. With the probe the voltage was decreased by a factor of 1000.
The voltage between the electrodes of the cuvette was recorded with the oscilloscope (TEKTRONIX, TDS 3014, 100 MHz, 1.25 GS/s). In order to get the current, the voltage over the measuring resistance was measured by the oscilloscope. With the data of the

measured voltage and current, the current density and the resistivity or conductivity inside the electroporation cuvette was calculated by $R = U/I$.

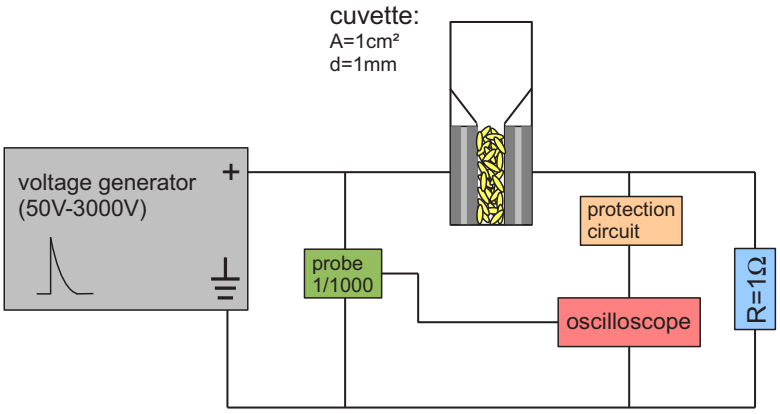

Figure 4-1: Layout of the measurement construction

To electroporate bacteria, only a small number of aliquots were taken at once out of the freezer (−80 °C) and thawed on ice. It is important, that the bacteria do not get warmer than about 4 °C due to the fact, that *E.coli* have 100-fold higher transformation efficiencies when electroporated at a temperature of 0-4 °C than when pulsed at room temperature (20-25 °C) [SD88], as mentioned in section 3.2.
Within one preparation of cells it is possible, that there is a difference in cell-density and quality of the cells. To get optimal results, some different (mostly 3 or more) aliquots of bacteria were mixed together. DNA (c=10 ng/µl) was added to the bacteria in a ratio of 1:50. *E.coli* C600 were transformed with pDsRed-Express plasmid DNA, while *Bacillus subtilis* 168 were transformed with pBluescript II KS +.
After electroporation of a volume of 100 µl, the treated bacteria were washed out of the cuvette with 1 ml of LB+ (Luria-Bertani with glucose (10 mM)), filled into EPPENDORF vessels (Eppi) (→ total volume: 1100 µl) and put onto ice again. In case of using pDsRed-Express as DNA, in all Eppis 11 µl of 100 mM IPTG (isopropyl-β-D-thiogalactopyranoside) was added, after all electroporation processes of one series of measurement were performed.
IPTG is a highly stable synthetic, non-fermentable analog of lactose which inactivates the *lacZ* repressor and induces synthesis of β-galactosidase *. Consequently, there is a transcription of the *lac* operon. IPTG induces the expression of cloned genes that are under control of the *lac* promoter [Fer10, SR01]. When pDsRed-Express is used for electroporation, the addition of IPTG leads to the expression of the Ds-Red-Express gene and a red fluorescence of the transformed bacteria which could be observed several hours after the transformation.
Afterwards, the Eppis filled with electroporated bacteria were left in a thermomixer (EPPENDORF, Thermomixer comfort) for 30 min at 1000 rpm and a temperature of 37 °C

* enzyme that promotes lactose utilization

for recovery of the bacteria from the "electroshock" and for expression of the ampicillin resistance.
To detect the transformed cells the electroporated sample (20-50 µl) was spread on LB-Agar-plates containing Ampicillin, because in both cases (using pBluescript II KS + or pDsRed-Express as DNA) the transformed bacteria become resistant to Ampicillin. Therefore, only the transformed *E.coli*/*Bacillus subtilis* can survive on the Ampicillin-Agar-plates and form a colony.
To determine the number of survivors, the treated bacteria were diluted and spread on LB-Agar-plates without Ampicillin.
The inoculated Agar-plates were given into an incubator at a temperature of 37 °C for about 16 hours. Then, the formed colonies were large enough to be counted visually.
Figure 4-2 shows a small part of the Ampicillin-Agar-plates from one series of measurements, on which colonies of transformed *E.coli* C600 with pDsRed-Express DNA were counted.

Figure 4-2: Ampicillin-Agar-plates with transformed *E.coli* C600 with pDsRed-Express DNA.

A similar experimental arrangement was used to determine the influence of the applied charge on the transformation efficiency of *E.coli* C600 with pDsRed-Express plasmid DNA. Therefore, the setup presented in figure 4-1 was minimal modified by exchanging the voltage generator.
Instead of a generator, which produces single pulses with an exponential decay, an alternating current (AC) square wave generator was inserted.
This self-made square wave generator is able to produce a rectangular high voltage of up to ± 1.5 kV with a slope of 3600 V/µs. Furthermore, the frequency and the duty-cycle could be adjusted.

The experimental arrangement shown in figure 4-3 is used for the experiments presented in section 5.7 to 5.10. There, the rectangular shape of one positive to one negative change of the voltage will be called "pulse".
The ohmic resistance of 1 Ω was replaced by another ohmic resistance of 10 Ω, which was already embedded in the square wave generator. The experimental arrangement with the square wave generator is shown in figure 4-3.

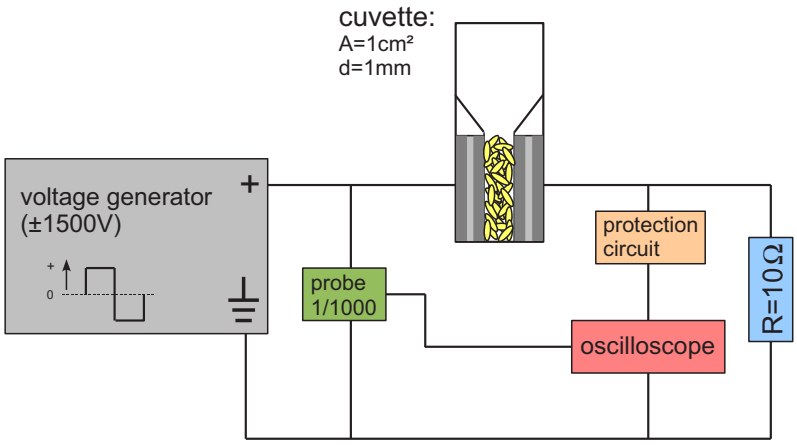

Figure 4-3: Arrangement of measurement with square wave generator.

For further measurements to determine the relation between the transformation efficiency of *E.coli* C600 with pDsRed-Express plasmid DNA and the applied amount of charge, the square wave generator was modified later. The voltage generator then could produce voltage pulses of only positive amplitudes up to 1.5 kV.

Chapter 5

Electroporation in dependence on the electric field, current density and the charge

This chapter deals with the experiments made with the arrangement presented in section 4.2 and the out-coming results. In the following, the transformation efficiencies of *E.coli* C600 and *Bacillus subtilis* 168 were detected in dependence on the electric field strength, the current density, the conductivity of the bacteria suspension and the amount of charge which was applied to the bacteria suspension.
In sections 5.1 to 5.5.4 for the described experiments the measurement setup pictured in figure 4-1 was used. In section 5.1 the transformation rate of *E.coli* C600 with pBluescript II KS + will be compared with transformation results of eukaryotic cells transformed by the electroporation method. Section 5.2 treats with the behavior of conductivity measured within an electroporation cuvette when using one and the same cuvette several times to electroporate bacteria.
To determine the relationship between the transformation efficiency and the current density, it is necessary to know the conductivity of the bacteria suspension. Therefore, the conductivity has to be measured before the bacteria get open by electroporation as well as during the electroporation process itself. Due to the fact, that a small voltage pulse has to be applied on the bacteria suspension to measure its conductivity, the threshold value whereat the bacteria cells start to open has to be determined. For this reason, the transformation efficiencies for *E.coli* C600 with pBluescript II KS + will be detailed ascertained for low applied electric fields in section 5.3.
In section 5.5 the transformation efficiencies of *E.coli* C600 with pDsRed-Express plasmid DNA and *Bacillus subtilis* 168 with pBluescript II KS + will be determined in dependence on the current density. Thereat, the conductivity of the bacteria suspensions will be varied in different ways. On the one hand, the conductivity will be increased by adding several concentrations of different kinds of salt solution to the bacteria suspen-

sion. On the other hand the conductivity will be modified by washing *E.coli* C600 more or less while making them electro-competent.
Afterwards, the transformation efficiency of *E.coli* C600 with pDsRed-Express will be examined in dependence on the applied amount of charge. For this kind of experiment, a measurement setup will be used as shown in figure 4-3. The corresponding results will be presented in sections 5.7 to 5.10. Furthermore, the effect of using an electroporation cuvette several times to electroporate bacteria will be measured in a more detailed way with the help of the experimental arrangement shown in figure 4-3.

5.1 Electroporation of *E.coli* C600 in comparison to other cells

In 1982 NEUMANN *et al.* examined the transfer of DNA, carrying the thymidin-kinase-gene, into mutated mouse cells (LTK^-). It was shown, that the transformation efficiency increased with the electric field strength up to an optimum and decreased again. The decrease can be explained because of the damage of cells due to the formation of irreversible pores [N^+82].
A similar behavior was observed when *E.coli* C600 were electroporated by using a voltage generator producing voltage pulses with an exponential decay (see experimental arrangement in figure 4-1). In this example the DNA transferred into the cells was pDsRed-Express (CLONTECH LABORATORIES, INC., California, USA). Optimal transformation efficiencies were found at about 21 kV/cm.

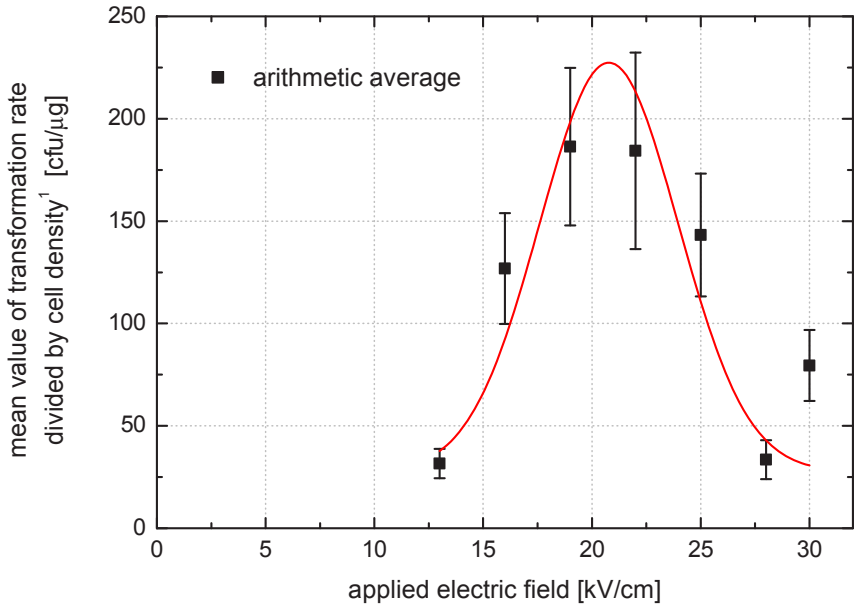

Figure 5-1: Transformation rate of electroporated *E.coli* C600 with pDsRed-Express as DNA ([1]cell density per µl of aliquot).

5.2 Conductivity and the influence of electroporation cuvettes

When using cuvettes with aluminum electrodes, one can easily measure the conductivity of the bacteria suspension during the electroporation process. For this the current and the voltage at the cuvette were recorded by an oscilloscope (see figure 4-1). The conductivity can be calculated dividing the voltage maxima by the respective current maxima.
Here only one electric pulse with an exponential decay was applied to electroporate *E.coli* of the strain C600 (100 µl) with 2 µl pBluescript KS II+ as DNA. The used electrode surface in the cuvette was 1 cm^2.
For several electroporation processes of *E.coli* C600 one and the same cuvette was used. After each electroporation (always applying an electric field of 13 kV/cm, which equals a voltage of 1300 V) the cuvette was washed with ethanol (70 %) and distilled water. It was dried with high pressured synthetic air before it was used again for the next electroporation process. This procedure was repeated twelve times.
In figure 5-2 the conductivity of bacteria suspension is shown in dependence on the number of measurement. The conductivity decreases linearly with each usage of the cuvette.

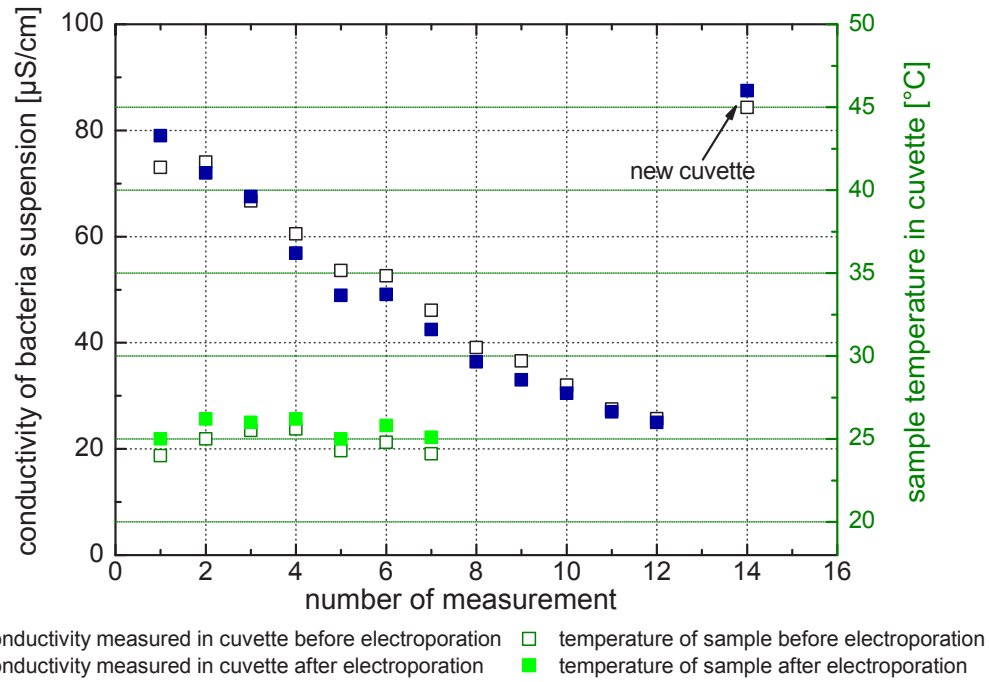

Figure 5-2: Conductivity of bacteria suspension measured in the cuvette before and after the electroporation with $E = 13\,kV/cm$ when using the same cuvette several times with cleaning in between the measurements.

In general, the conductivity depends linearly on the viscosity and the viscosity of the suspension depends on the temperature. So the temperature influences the conduc-

tivity directly. Therefore, for the first seven usages of the cuvette, the temperature of the bacteria suspension was measured directly before the electroporation and immediately after the process with a thermocouple element (NEWPORT ELECTRONICS GMBH, K-type, NiCr-NiAl, 0.5 mm diameter). The delay between the electric pulse and the measurement was only a few seconds. There was no heat exchange of the solution with the conductive electrodes. A further measurement of temperature, which was done again one minute after the electric pulse, provided the same temperature as directly after the electroporation.
When the temperature differs about 1 K the conductivity of the medium changes already about 3 % [HV05].
In figure 5-2, it can be noticed that the difference of temperature due to the electroporation process is quite small. As far as it can be observed, the real change in temperature due to the electroporation process is less than 1 K and therefore negligible. So there is no large effect on conductivity to be expected.
Although the temperatures of the bacteria suspension are more or less the same for all measurements, the measured conductivity decreases linearly. As the suspension filled in the cuvette was taken from one and the same bacteria preparation, the conductivity of the suspension should be the same for all measurements. Therefore, the decrease of conductivity must be caused by a change of the electroporation cuvette itself, e.g. by a deposit of dielectric material on the electrodes. To avoid errors measuring the conductivity of the bacteria suspension, a new cuvette was used for each electroporation in the following measurements.

5.3 Threshold value of electric field to electroporate *E.coli* C600

To find out the conductivity of the bacteria suspension it is necessary to apply an electric pulse on the sample. Therefore one has to know, at which electric field strength transformation of *E.coli* C600 appears for the first time. For easy handling and to save time, the measurement of the conductivity could be done with the electroporation equipment. In this experimental arrangement (see figure 4-1), the generator cannot produce electric pulses smaller than 50 V. An electric pulse of 50 V equals an electric field strength of $E = 0.5\,\mathrm{kV/cm}$ inside the cuvette. For this reason it was necessary to check, if there is already transformation of *E.coli* when using an electric field strength of 0.5 kV/cm to measure the conductivity of the bacteria suspension.
In former experiments with single pulse electroporation it was found, that in a mixture of *E.coli* LE392 and pBR322 plasmid DNA transformation starts with an electric field strength of about 3 kV/cm and a pulse duration of 5 ms [SD88].
Electroporation of *E.coli* of the strain C600 with pBluescript II KS + (STRATAGENE, California, USA) as DNA showed a similar behavior. When using a single pulse with an exponential decay, transformation of *E.coli* was not detectable until an electric field strength of 3.5 kV/cm and a decay time $\tau \approx 3\,\mathrm{ms}$, as can be seen in figure 5-3. Here the

samples were centrifuged after a recovering-time of 30 min and the supernatant was eliminated. The complete bacteria suspension which was left of a sample (100 µl) was spread on just one LB-Amp-Agar-plate (concentration of Ampicillin: $c_{Amp} = \frac{100\,\mu g}{ml}$) per sample.

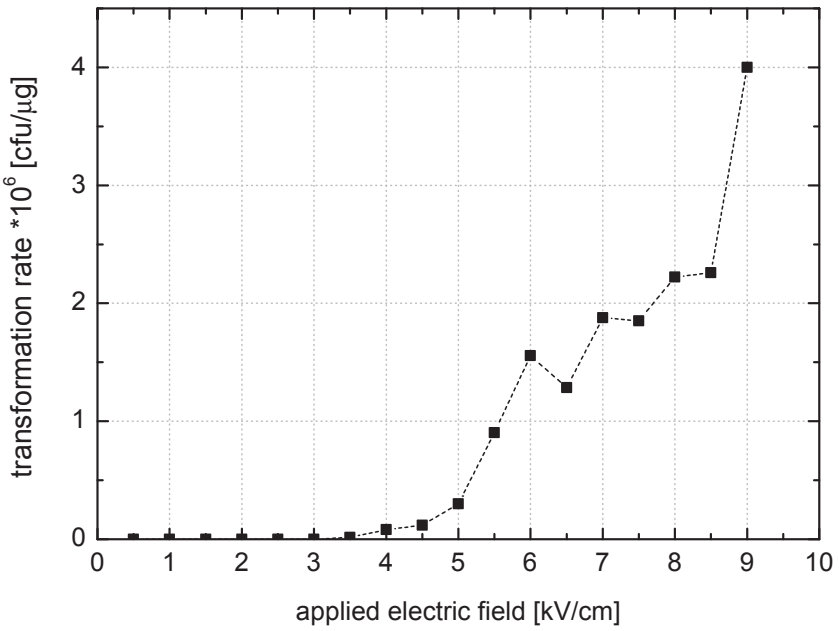

Figure 5-3: Experiment to find the threshold value where transformation starts.

Based on this observation a small electric pulse with a field strength of 0.5 kV/cm could be applied before every electroporation process to measure the conductivity. This was done for all following experiments.
However, transformed *E.coli* deliver β-lactamase to the surrounding area. For that reason an area of non-transformed bacteria colonies can be found around one colony of transformed *E.coli*. Because of these so-called "satellite colonies" it is more complicated to count the transformed colonies.
To simplify the detection, DNA for electroporation of *E.coli* C600 was changed. Instead of pBluescript II KS + DNA (2961 bp), pDsRed-Express (3311 bp) was used for the following experiments. As both plasmids have nearly the same size and their expression is under the control of the same promoter, the transformation efficiency by electroporating *E.coli* is expected to be almost the same.
Using pDsRed-Express plasmid-DNA in electroporation experiments of *E.coli* has a great advantage. While transformed bacteria with pBluescript II KS + are colored white, those with pDsRed-Express get pink. In that way it is easy to distinguish between transformed *E.coli* and their "satellite-colonies" which are still white. Figure 5-4 shows an example for *E.coli* C600 transformed with pBluescript II KS + (5-4a) and with pDsRed-Express (5-4b and 5-4c).

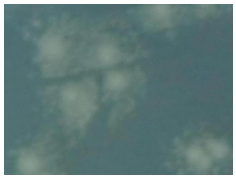

(a) colonies with pBluescript II KS +

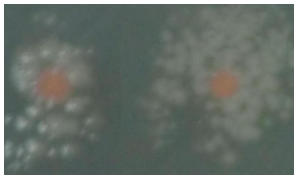

(b) colonies with pDsRed-Express

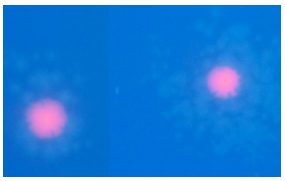

(c) colonies with pDsRed-Express illuminated with UV light

Figure 5-4: Transformed *E.coli* C600 with pBluescript II KS + (left) and pDsRed-Express (middle and right) as DNA.

The fact, that *E.coli* C600 transformed with pDsRed-Express fluoresce in a red color, when illuminated with UV light, opens up the possibility to detect the transformation efficiency in a lot of different ways. For example, the transformation rate could be identified by a cell-analyzer. Thereat, the cells are illuminated with lasers emitting light of different wave length while flowing through a capillary tube. The cell-analyzer then detects the fluorescent cells with photomultiplier and count the transformed cells.
Another possibility would be to detect the transformation efficiency by measuring the light intensity of the fluorescing cells by a camera connected to a microscope, whereat the bacteria are illuminated with UV light on the microscope slide. Figure 5-5 shows a photograph of *E.coli* C600 which were transformed with pDsRed-Express plasmid DNA and illuminated with UV on a microscope slide.

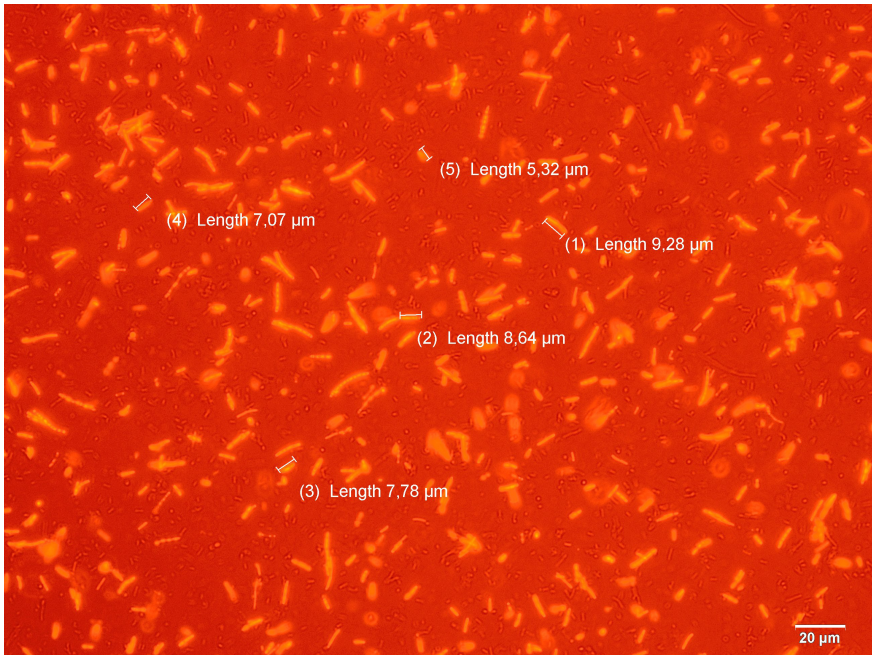

Figure 5-5: *E.coli* C600 transformed with pDsRed-Express illuminated with UV light regarded with a microscope.

In the following experiments the transformation efficiency of *E.coli* C600 with pDsRed-Express and *Bacillus subtilis* with pBluescript II KS + was detected by spreading the samples on LB-Agar-plates containing Ampicillin and counting the formed colonies by eye as shown in figure 4-2.

5.4 Electroporation in dependence on electric field strength and current density

If DNA, often plasmid DNA, is transferred into a cell, the cell will be transformed. In this way the cell gets new attributes normally not be found this way in nature. Consequently, it is possible to find out if a transfer of DNA into cells has happened and how many cells have been transformed (transformation efficiency).
As described in former experiments [TT81, N^+82] the formation of pores is related to the electric potential in the cell membrane itself. Therefore, the electric field strength inside the cell membrane, induced by the external field, seems to be the key factor to find the optimal transformation efficiency.
When using a voltage generator, which produces single pulses with an exponential decay, and the gap between the electrodes is fixed during the applied electric pulse, the electric field strength can be described by

$$E(t) = E_0 \cdot e^{-\frac{t}{\tau}} \ . \tag{5.1}$$

The sample resistance R can be determined by its ionic strength and the geometry of the sample chamber and the electrodes. The capacitor discharge of a given size capacitor into a medium with higher ionic strength and therefore a lower resistance will produce a pulse with a shorter time constant τ, which is correlated to the ohmic resistance and the capacitor by $\tau = R \cdot C$ [TT81, SD88].
Up to now, the efficiency of electro-transformation was only considered in dependence on the electric field strength. There are many studies, for example by DOWER *et. al* in 1988, who measured the number of transformants by applying single voltage pulses with an exponential decay. On the one hand, they changed the amplitude of the applied electric field strength E_0 with a fixed decay time τ and on the other hand they varied the decay time at a constant amplitude E_0 by changing the size of the capacitor and the resistance, which were in parallel with the sample [DMR88].
Before filling the bacteria-DNA mixture into the cuvettes, the suspension is stirred. Thus, there are no concentration gradients present. Therefore, the applied electric field strength can be written in dependence on the resistivity of the medium containing the cells and the current density by

$$\begin{aligned} & E &&= \frac{U}{d} = \frac{R \cdot I}{d} = \frac{\rho \cdot d \cdot I}{A \cdot d} = \frac{\rho I}{A} = \rho \cdot j \\ \Leftrightarrow \quad & j &&= \frac{E}{\rho} = \kappa \cdot E \ , \end{aligned} \tag{5.2}$$

where E is the electric field strength, U the voltage, d the distance between electrodes, R the ohmic resistance, I the current, A the surface of the electrode, ρ the resistivity of the medium, j the current density, and κ the conductivity of the medium (see section 2.4.1/equation 2.32).

Therefore, it can be assumed that the transformation efficiency depends on the conductivity of the medium containing the bacteria and the DNA, which should be introduced into the cells, and the current density of the applied electric field.
Until today, only the killing but not the transformation of cells was examined in dependence on current density. It was assumed that the killing of cells does not depend on the current density [SH67, KT77].
As observed before, the amount of killed bacteria in dependence on the electric field is different for different species [SH67]. Therefore the optimum of the transformation efficiency certainly varies by using various organisms. This variation is due to the different sizes of cells [SD88].

5.5 Experiments with bacteria suspensions of different conductivities

In the following experiments the conductivity of the bacteria suspension was changed in different ways. On one hand the conductivity was changed by adding salt to the bacteria suspension as done with a NaCl solution. On the other hand the conductivity was influenced by washing the cells in different ways before electroporation while making the bacteria electro-competent.

5.5.1 Electroporation of *E.coli* C600 with addition of NaCl-solution

Transformation in dependence on the electric field strength

To find out if the maximum bacteria transformation rate (TR) * depends on the current density and conductivity of the bacteria suspension (see equation 5.2) a mixture of *E.coli* C600 and pDsRed-Express DNA was electroporated with addition of several volumes of 10 mM NaCl solution. Therefore, aliquots of one and the same preparation of electro-competent *E.coli* C600 (cell-density: $\rho_{cells} = (6,43 \pm 1,22) \cdot 10^5\,\mu l^{-1}$) were used for three measurement series. To avoid great differences in cell-density three aliquots with a volume of 100 µl (so all in all 300 µl of *E.coli*) were mixed together with 6 µl pDsRed-Express DNA. For the first series of measurements no NaCl was added. In the second series of measurements 18 µl of NaCl solution (10 mM) were given into the mixture of *E.coli* (300 µl) and DNA (6 µl), and for the third one 36 µl of NaCl solution (10 mM).
For all series of measurements out of the mixture of *E.coli*+pDsRed-Express (+NaCl solution) (volume of about 300 µl) a volume of 100 µl was taken to be electroporated in a new cuvette with an electrode size of 1 cm^2 and an electrode distance of 1 mm. The applied electric field strength varied from 6 kV/cm to 30 kV/cm.

* $TR = \frac{\text{colony forming units [cfu]}}{\text{amount of used DNA [µg]}}$

After the recovering time of 30 minutes at 37 °C, for each sample, five LB-Agar plates containing Ampicillin were spread with 50 µl of the electroporated bacteria solution. Subsequentley the LB-Amp-Agar-plates were stored in an incubator at a temperature of 37 °C for 16 hours. In this time the transformed *E.coli* formed a colony while the non-transformed cells died, because they were not resistant to Ampicillin.
The colonies of the transformed cells were counted visually.
Figure 5-6 shows the mean values of transformation rate with the corresponding root mean square deviation for all three series of measurements in dependence on the electric field strength. The data points of the averaged transformation efficiencies are numbered consecutively. As all bacteria were taken from the same preparation they are expected to behave in the same way if conductivity is irrelevant for transformation.

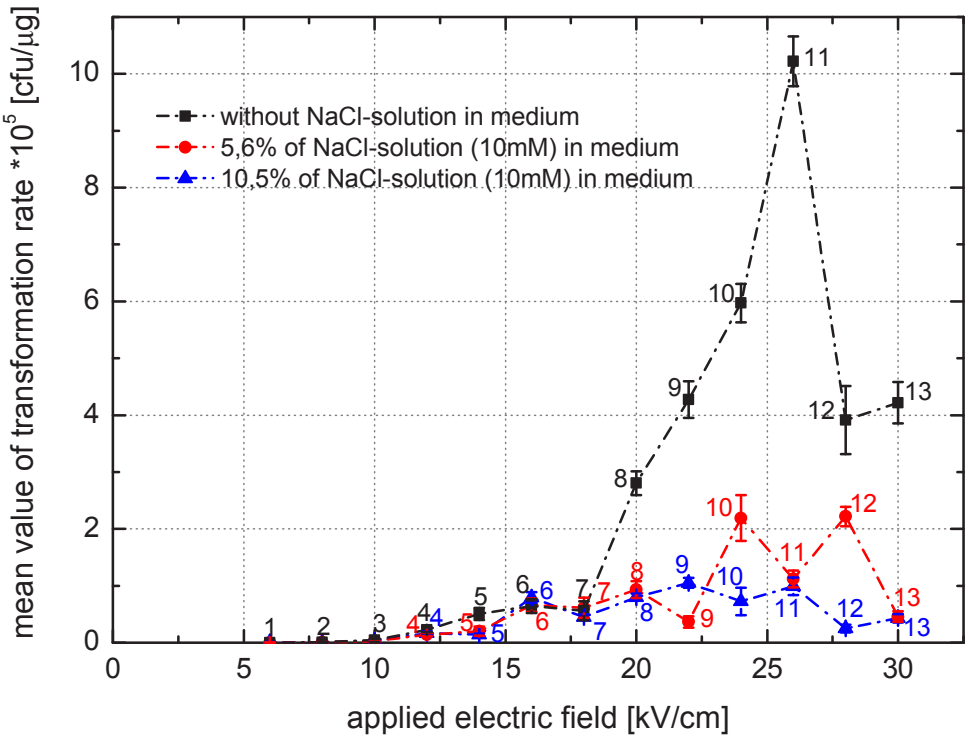

Figure 5-6: Arithmetic average of *E.coli* C600 transformation rate with pDsRed-Express DNA and addition of different volumes of NaCl solution (10 mM).

In fact, no clear maximum for the transformation rate in dependence on the electric field strength can be observed for the series of measurements with NaCl added in the bacteria suspension in comparison to the one without addition of salt. So in this aspect, except of the change in magnitude of the transformation rate, no effect of the presence of NaCl solution in the bacteria suspension can be seen.
It was already said by FROMM *et al.* [FTW85] that an adjustment of salt concentration influences the electroporation efficiency. In this experiment an increase of NaCl solu-

tion in the cell suspension leads to a decrease of the amplitude of the transformation efficiency.
In figure 5-7 the number of colonies of surviving and transformed *E.coli* C600, which could be counted on LB-Agar-plates†, when 10 µl of the sample‡ was spread on them, can be compared. For all three series of measurements the number of survivors is nearly the same while the number of transformed *E.coli* decreases with increasing NaCl concentration.

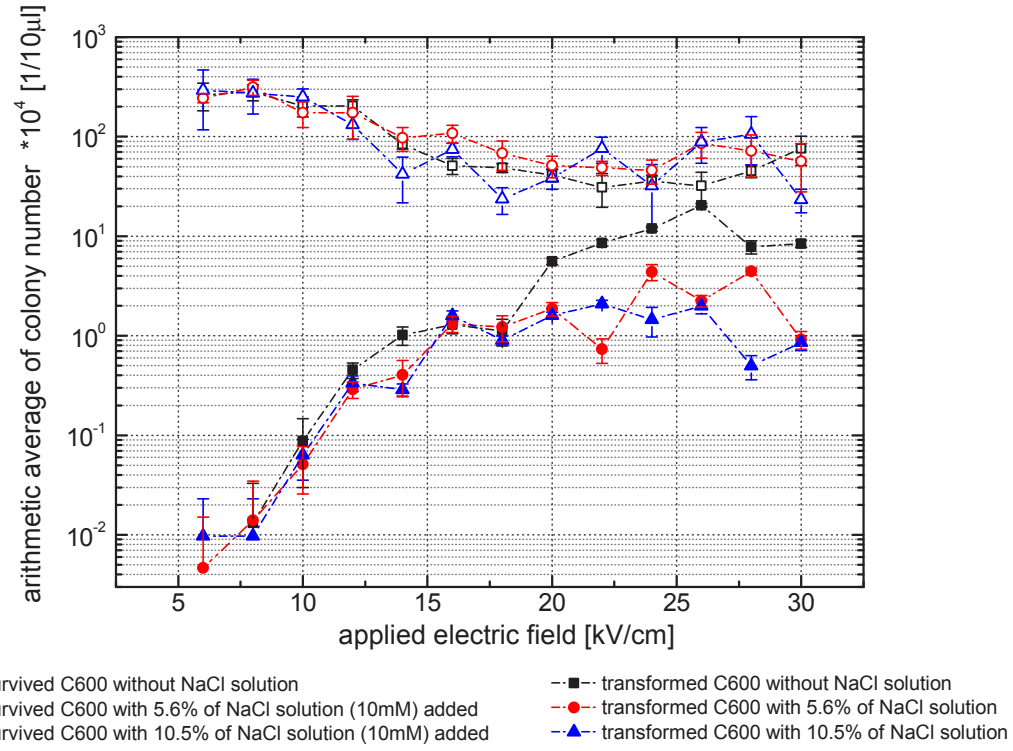

Figure 5-7: Number of surviving (□ ,○, △) and transformed (■, ●, ▲) *E.coli* C600 with pDsRed-Express for a volume of 10 µl per sample (100 µl of electroporated medium (*E.coli* C600 and pDsRed-Express (50:1)) with 1 ml LB+).

Due to the logarithmic scale in figure 5-7, it cannot be seen clearly, that the number of survivors is nearly the same for all three series of measurements. Therefore the data points of survivors are shown once again on a linear scale in figure 5-8.

† Agar plates to identify transformed cells contain ampicillin, while the number of survivors where detected with Agar plates without ampicillin content.
‡ sample: 100 µl of electroporated suspension and 1 ml of LB+ (LB-medium with glucose)

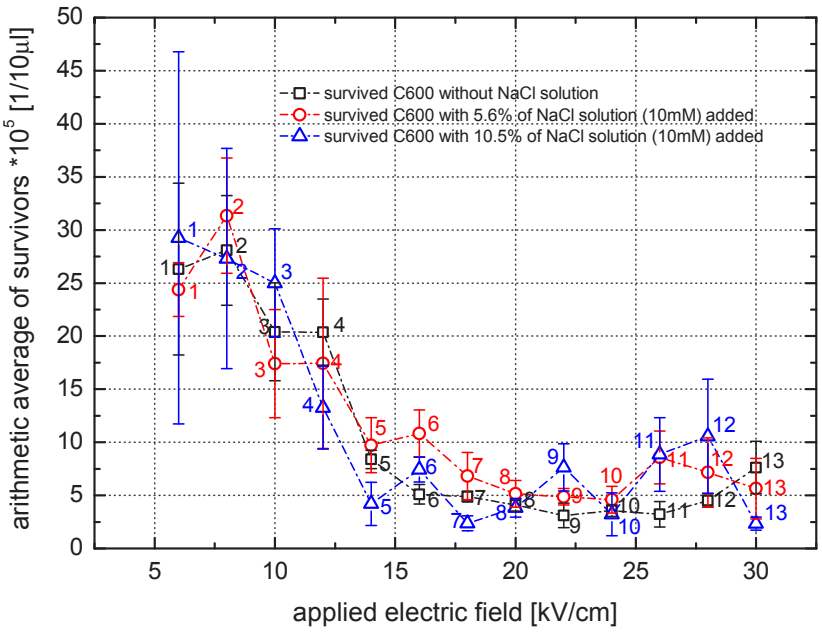

Figure 5-8: Number of surviving colonies per 10 µl of sample for different concentrations of added NaCl-solution.

Transformation in dependence on current density

For each electroporation the voltage and the current were recorded with an oscilloscope (see measurement construction in figure 4-1). Out of these data the current density and the conductivity of the medium in the cuvette during the electroporation process was calculated.

The conductivities of the bacteria suspension were measured before the electroporation process by applying a small electric pulse of 0.5 kV/cm (50 V) for all three series of measurements. Without addition of NaCl solution the conductivity of the bacteria suspension was (46.327 ± 2.051) µS/cm, (65.863 ± 7.761) µS/cm with 5.6 % of NaCl solution and (80.271 ± 4.263) µS/cm with 10.5 % of NaCl solution. The conductivities equal arithmetic averages resulting of five values measured by applying an electric field of the strength of 0.5 kV/cm. Due to the fact, that first electroporation of *E.coli* C600 was observed when applying an electric field strength of 3.5 kV/cm (see section 5.3), there is no electroporation at an electric field strength of 0.5 kV/cm. Hence, these measured conductivity values are equivalent to the conductivities of the bacteria suspension before the cell membrane was electropermeabilized and a cytoplasmic ion leakage was present.

In contrary to the diagram with the transformation rate in dependence on the electric field strength (figure 5-6), clear differences in the position of the maximum transformation rate for different concentrations of NaCl solution in the bacteria suspension, and

therefore for different conductivities, can be observed when plotting the mean values of the transformation rate in dependence on the related current density (see figure 5-9). This difference gets more obvious when enumerating the measuring points. In the diagram where the transformation rate is shown in dependence on the electric field strength (figure 5-6) the measuring points were counted continuously with increasing electric field strength.
In figure 5-9, where the transformation rate is shown in dependence on the current density, the numbers of the data points equals the enumeration in figure 5-6. When comparing these two diagrams directly, one could find, that some of the data points are shifted in figure 5-9 compared to figure 5-6. So an increase of the electric field strength does not implicate an increase of the current density. For this phenomenon there can be many reasons, e.g. size and quality of the bacteria, air bubbles in the cuvette or a difference in the quality of the cuvettes.

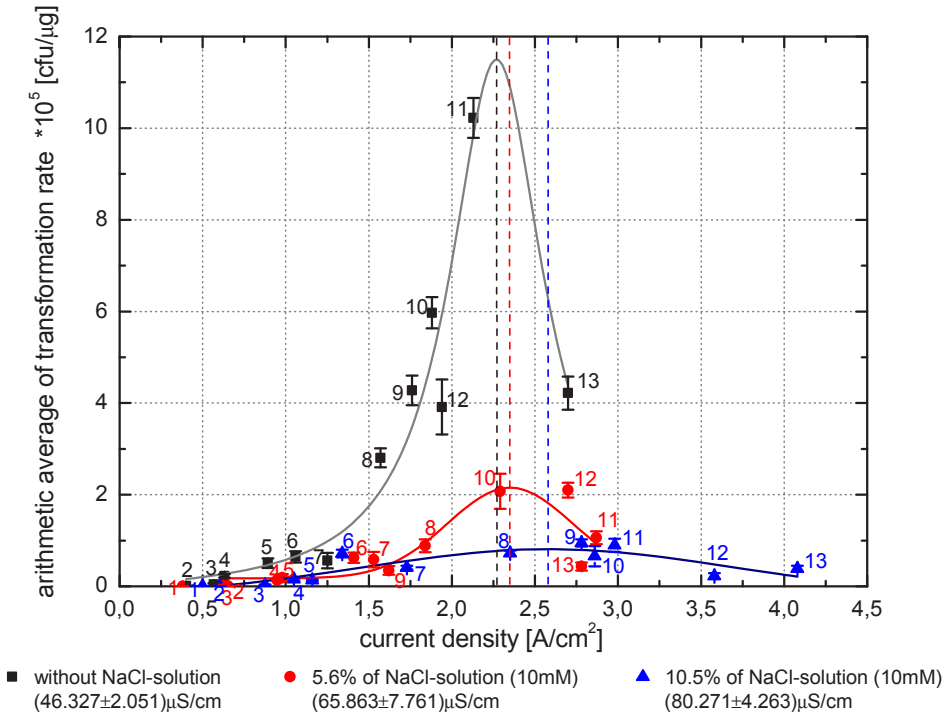

Figure 5-9: Mean values of transformation rate for *E.coli* C600 of the same preparation but different additions of a 10 mM-NaCl solution in dependence on current density.

Despite the fact that with higher NaCl concentration the magnitude of the transformation rate decreases, one can observe that with higher conductivity, higher current densities are necessary for achieving maximal transformation. Consequently, the transformation of *E.coli* bacteria depends on current density and conductivity as assumed before. It can be seen that equation 5.2 is valid for transformation of *E.coli* C600.
The shift of the data points cannot only be observed for the transformation rate but also for the number of surviving *E.coli*. Figure 5-10 shows the number of survivors for all three measurement series in dependence on the current density.

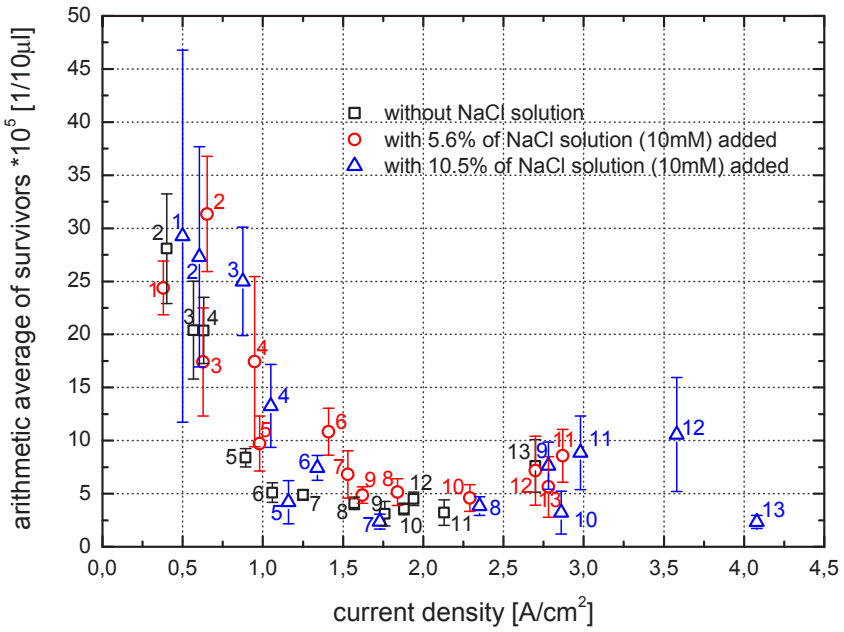

Figure 5-10: Number of surviving colonies per 10 µl of the sample for different concentrations of added NaCl-solution in dependence on current density.

This shift reveals that the surviving of *E.coli* depends on current density after all. This observation is in conflict with that one from SALE and HAMILTON [SH67], who said that the killing of bacteria does not depend on current density. This difference in measurement results may be caused by the respective experimental arrangements.

5.5.2 Electroporation of *E.coli* C600 washed in different ways

In this experiment the impact of washing bacteria on the transformation rate and survival is examined. In order to do that, electro-competent *E.coli* C600 were prepared by washing them one to three times.

To find out the dependence between maximal transformation and conductivity of the bacteria medium (changed by washing the bacteria a different number of times), an electroporation experiment with three series of measurements was carried out. For this experiment a high amount of *E.coli* C600 from one preparation was divided into three equal volumes and washed with distilled water in different ways. For the first series the volume of bacteria was washed just once, for the second twice and for the third three times in a manner as described in section 4.1.

For every electroporation a new cuvette was used filled with a volume of 100 µl suspension (mixture of *E.coli* C600 and pDsRed-Express (c=10 ng/µl) in a ratio of 50:1). Here also three aliquots of 100 µl were mixed together in advance to avoid larger differences in conductivity and quality of the cells.

Plotting the mean values of the transformation rate in dependence on the applied elec-

tric field, the maximum for bacteria washed twice occurs at higher fields than for those washed three times. Therefore, it cannot be said, which electric field is necessary to get maximal transformation when only knowing the conductivity.

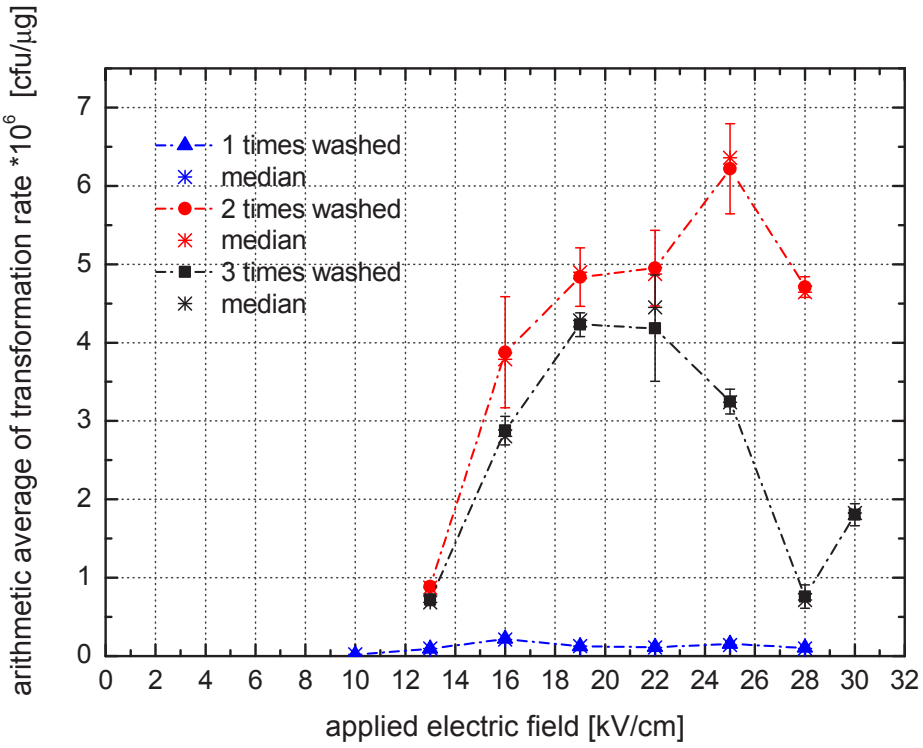

Figure 5-11: Transformation rate of *E.coli* C600 with pDsRed-Express without regarding on cell densities.

The magnitude of transformation rate differs for the different series of measurements. As bacteria were washed in different ways, the cell density in the used aliquots is not the same for differently washed *E.coli*. Bacteria used in the first series of measurement (washed just once) had a cell density of $\rho_{cells} = (15,317 \pm 2,076) \cdot 10^5\,\mu l^{-1}$. *E.coli* which were washed twice had a cell density of $\rho_{cells} = (9,251 \pm 0,450) \cdot 10^4\,\mu l^{-1}$ and those which were washed three times had a cell density of $\rho_{cells} = (2,269 \pm 0,462) \cdot 10^4\,\mu l^{-1}$. These differences in cell density can be explained, as some *E.coli* cells get lost during the washing process. This can already be observed, when regarding the number of colonies of transformed *E.coli* on the LB-Amp-Agar-plates containing Ampicillin as shown in figure 5-12. For *E.coli* C600 washed once, the highest amount of transformed colonies is for 16 kV/cm. When regarding the LB-Amp-Agar-plates of the three times washed *E.coli*, the maximal transformation rate can be found with an applied electric field strength of 19 kV/cm and 22 kV/cm.

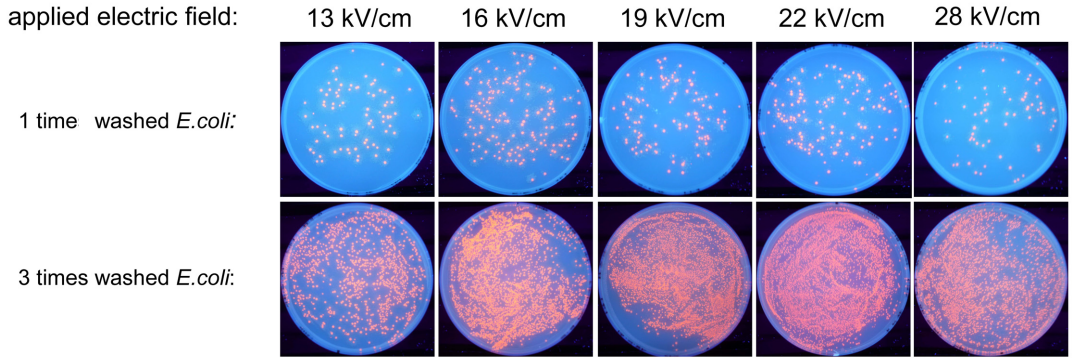

Figure 5-12: Pictures of transformed *E.coli* C600 with pDsRed-Express on LB-Agar-plates containing Ampicillin. The Agar-plates were illuminated by a UV-lamp (BENDA, Wiesloch, Germany, type N-36M). For both series of measurement 50 µl of sample (100 µl of mixture *E.coli* C600 and pDsRed-Express (50:1) with 1ml LB+) was spread on each Agar-plate.

Scaling the transformation rate respectively to the cell density of the used preparation (each value of transformation rate was divided by the value of the belonging cell density), shown in figure 5-13, gives information about the relation of transformation efficiency and the washing of bacteria.

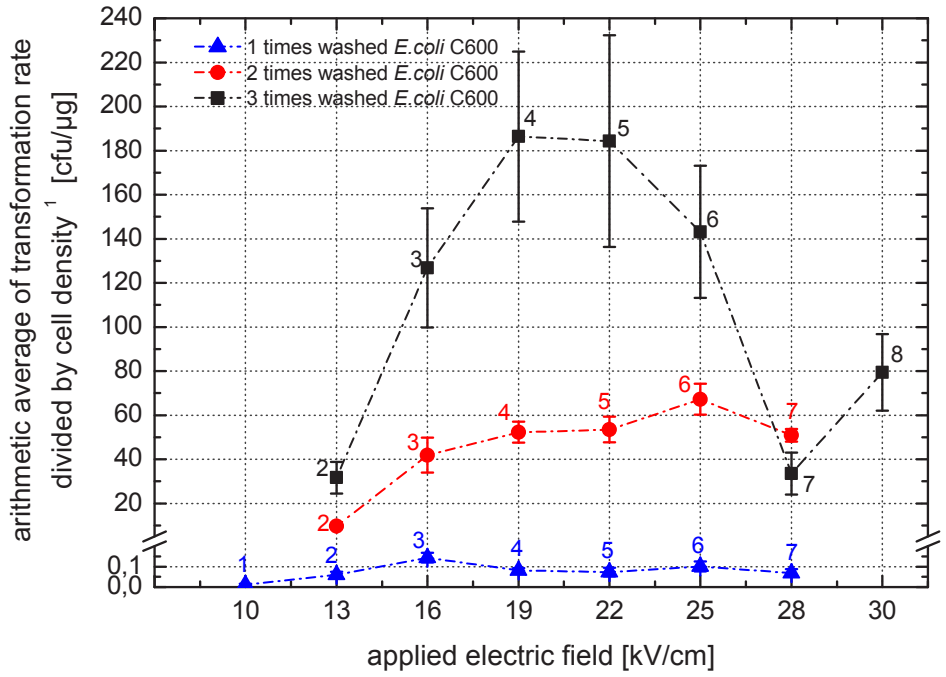

Figure 5-13: Transformation efficiency of *E.coli* C600 with pDsRed-Express which was washed in three different ways before electroporation with regard to the different cell-densities of each series of measurement ([1]cell density per µl of aliquot).

Washing the *E.coli* C600 more often leads to higher transformation efficiencies. When regarding the related current densities in figure 5-14, it can be found, that the transformation maximum is shifted to higher current densities for lesser washed bacteria, which have therefore higher conductivities. The measured conductivity of the *E.coli* washed just once was $(52.188 \pm 2.842)\,\mu S/cm$, $(24.945 \pm 1.194)\,\mu S/cm$ for those washed twice and $(20.635 \pm 1.375)\,\mu S/cm$ for the *E.coli* washed three times. The observed shift to higher current densities for higher conductivities is conform with that one regarding the transformation maxima, when NaCl solution (10 mM) was added to the bacteria suspension (see figure 5-9).

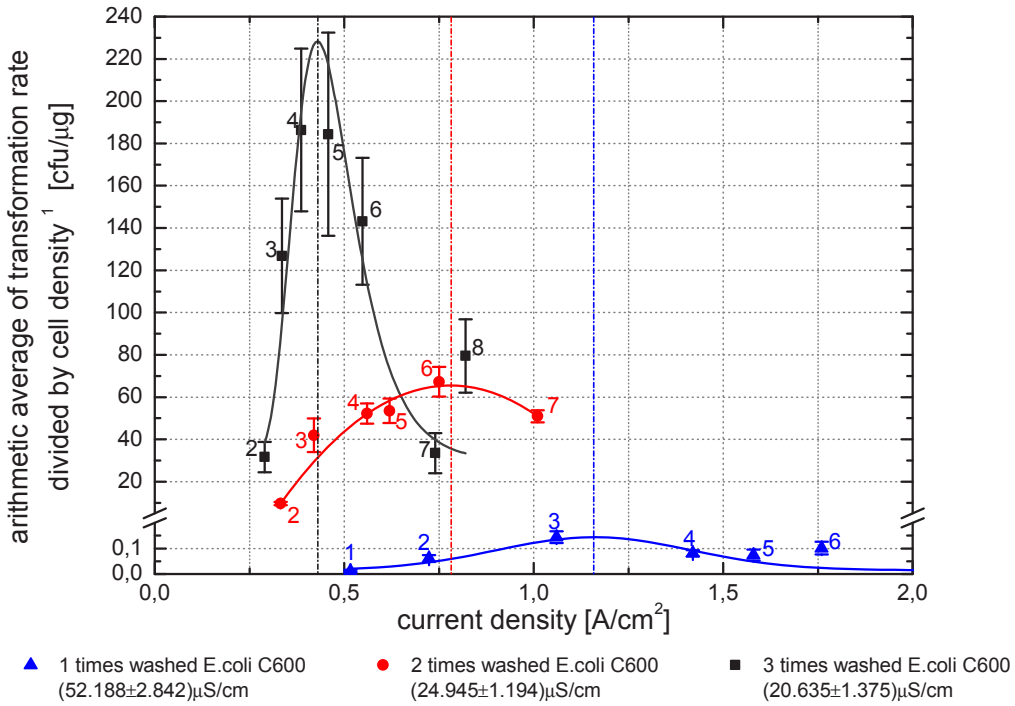

Figure 5-14: Transformation rate of *E.coli* C600 washed in different ways in dependence on current density with regard on the respective cell density ([1]cell density per µl of aliquot).

In this case the magnitude of transformation rate for *E.coli* C600, washed in different ways, correlates with the number of bacteria surviving the electroporation process. Figure 5-15 shows that washing bacteria more often leads to a higher number of survivors. A comparison with the experiment adding NaCl solution to the bacteria suspension shows that in both cases higher conductivity leads to smaller transformation rates with higher concentrations of salts. But in contrary to the washing-experiment, adding NaCl has no effect on the number of surviving *E.coli* (see figure 5-8).

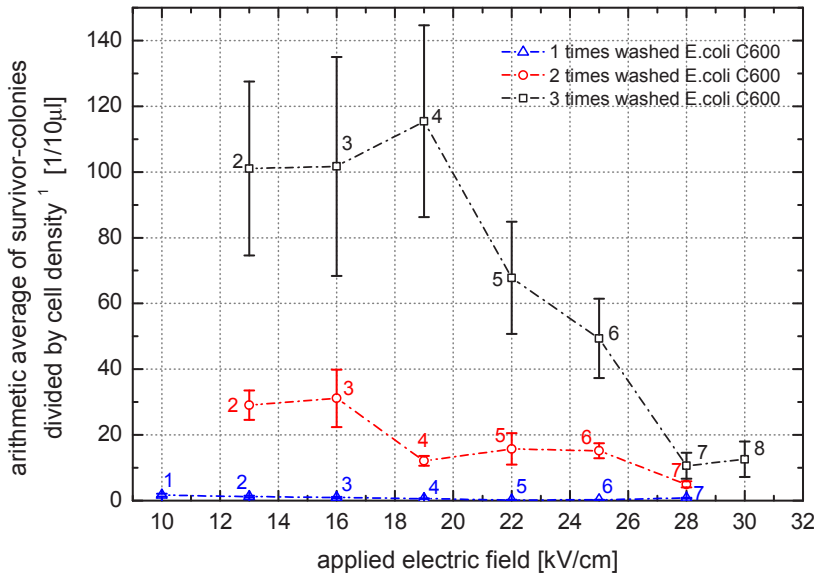

Figure 5-15: Number of surviving colonies of different washed *E.coli* in dependence on the applied electric field ([1]cell density per µl of aliquot).

Just as in the measurement adding NaCl solution to the bacteria suspension, in this experiment the number of surviving *E.coli* depends on the current density. Comparing figure 5-15 and figure 5-16 the shifting of data points for the number of survivors can be seen clearly.

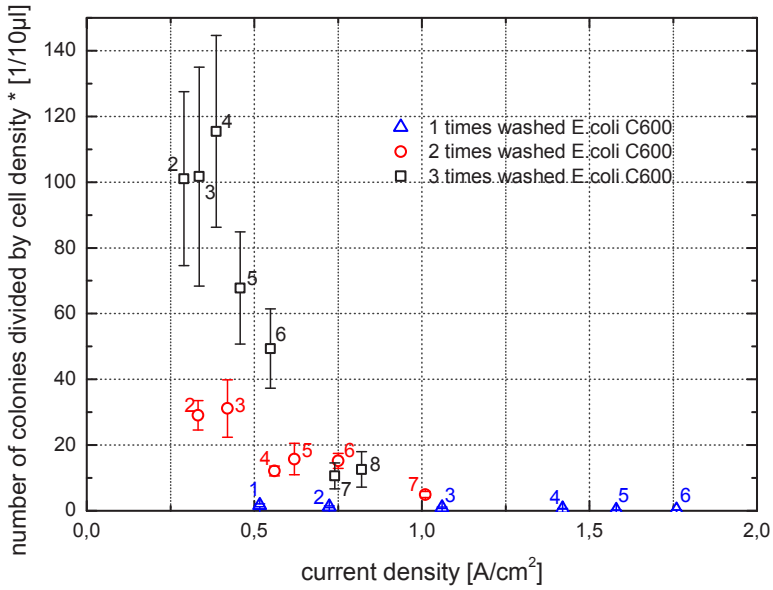

Figure 5-16: Number of surviving *E.coli* in dependence on current density (*cell density per µl of aliquot).

In 1988 CALVIN and HANAWALT [CH88] found that increasing of the cell density at a given field strength leads to an increase of the transformation rate and at the same time to a decrease of the number of survivors.
Washing the *E.coli* several times leads to a decrease of the cell density. Therefore less washing should lead to higher transformation efficiencies. However, in this experiment the magnitude of transformants decreased when the cells were less washed. So the salts in the cell suspension which are eliminated by washing have a more dominant influence on transformation than cell density.
In this experiment the number of survivors decreased when washing the bacteria less but it cannot be said if this effect is due to the decreasing cell density when washing the *E.coli* more often or due to the mixture of several salts in the sample.

5.5.3 Electroporation of *E.coli* C600 with addition of several salt solutions

In the following experiment, *E.coli* C600 were added with several concentrations of different kinds of salt solution (see table 5-1) and electroporated with pDsRed-Express plasmid DNA using the experimental arrangement which was shown in figure 4-1 (voltage pulses with exponential decay).
It was observed, that the position of maximal transformation efficiency shifted in dependence on the current density to higher values with increasing conductivity for all kinds of added salt solution. This observation is conform with the behavior described in sections 5.5.1 and 5.5.2. Thus, the shift of the transformation efficiency maximum position is independent on the kind of added salt solution.
The pre-electroporation conductivity of the bacteria suspension was measured by applying a low voltage of 50 V, which equals an electric field of 0.5 kV/cm.
Here *E.coli* C600 were transformed with pDsRed-Express plasmid DNA ($c = 10\,\mathrm{ng/\mu l}$). The ratio between the volumes of the bacteria sample and the added DNA was 50:1.

added salt	volume of added salt solution [%]	conductivity [µS/cm]
none	0	$50,236 \pm 1,968$
NaCl	5	$65,797 \pm 1,932$
	10	$87,418 \pm 9,001$
	15	$114,386 \pm 8,722$
KCl	5	$53,217 \pm 2,334$
	10	$80,838 \pm 6,662$
	15	$110,560 \pm 2,318$
$MgCl_26H_2O$	5	$79,150 \pm 3,544$
	10	$113,751 \pm 7,306$
	15	$155,752 \pm 14,402$

Table 5-1: Volume percentage of 10 mM salt solution added to each sample and the resulting conductivities of the bacteria suspension.

The results of the measurement can be seen in figure 5-17. The current density was measured at the current maximum at the start of the exponential decay.

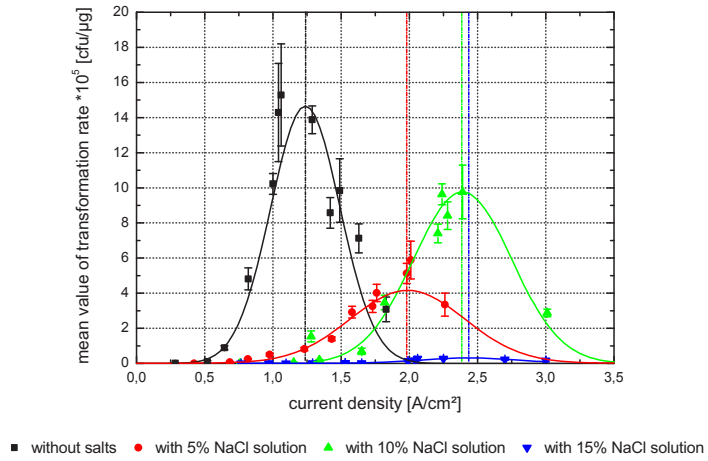

(a) Addition of NaCl solution.

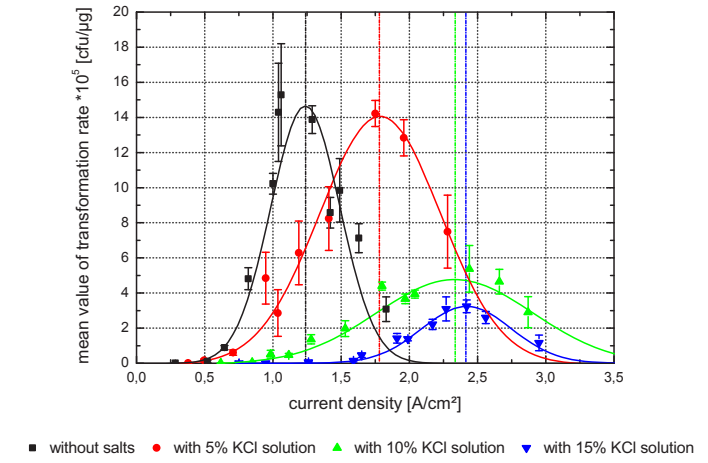

(b) Addition of KCl solution.

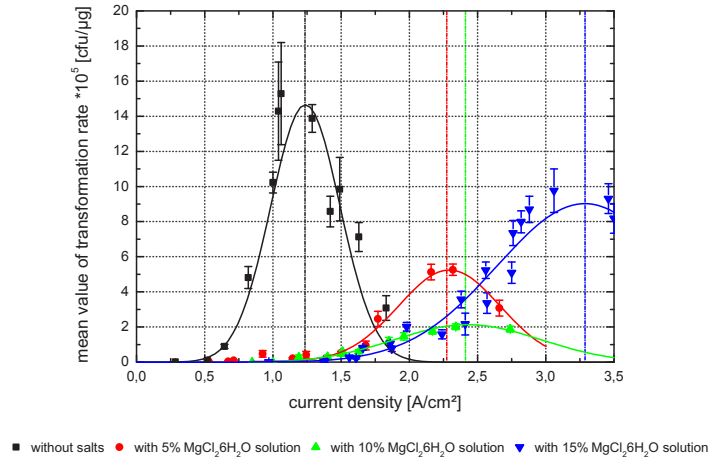

(c) Addition of $MgCl_2 6\,H_2O$ solution.

Figure 5-17: Transformation efficiencies of *E.coli* C600 + pDsRed-Express plasmid DNA with several concentration of different salt solutions.

In contrast to the observation made in sections 5.5.1 and 5.5.2 the magnitude of transformation efficiency does not always decrease with increasing salt concentration. This leads to the conclusion, that there is no dependence of the magnitude of transformation rate on the conductivity of the bacteria suspension.
The only obvious relation, which was observed, was the shift of the transformation peak position in dependence on the current density with changing conductivities.
Based on this and preliminary experiments, like those in sections 5.5.1 and 5.5.2, a diagram was developed which can be used to predict the electric field, which has to be applied to reach maximal transformation efficiencies of *E.coli* C600 transformed with pDsRed-Express plasmid DNA (see figure 5-20).
The conductivity of the bacteria suspension (black points ■ in figure 5-20) was measured before the electroporation process for each sample with a small electric field of 0.5 kV/cm (50 V), which causes no transformation.
To determine the current density needed to reach maximal transformation efficiencies, the transformation rate of the *E.coli* C600 was plotted in dependence on the current density and approximated by a Gaussian as can be seen in figure 5-18. The peak position of the Gaussian equals the current density for maximal transformation efficiency.

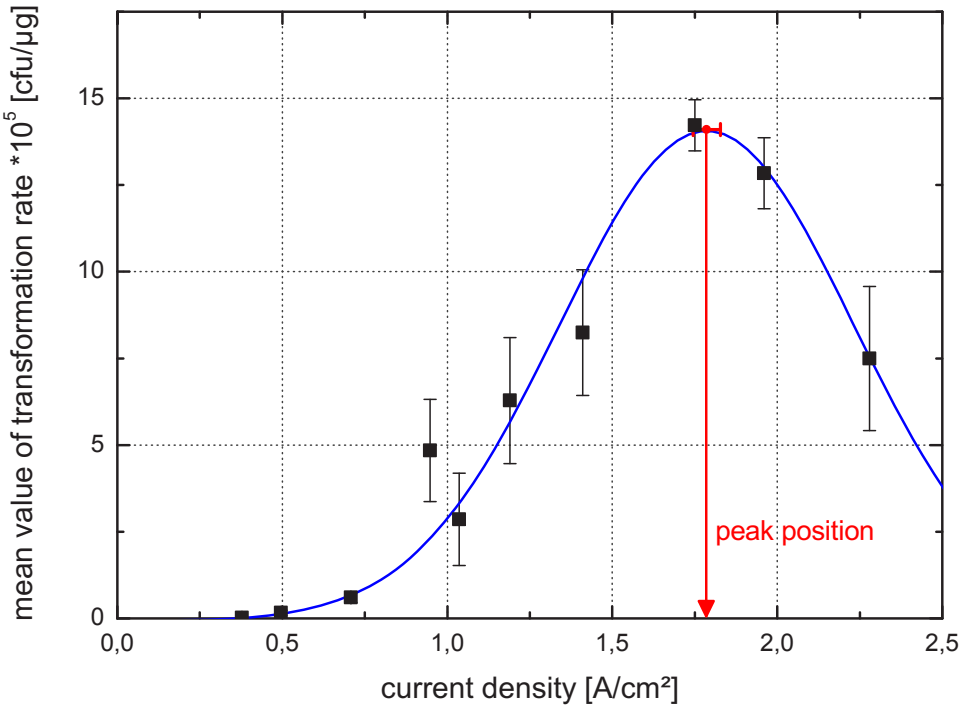

Figure 5-18: Determination of the current density needed to reach maximal transformation efficiency (■ : mean value of transformation rate).

During the electroporation process the cells are opened, whereat charged particles can slip out of the cell and increase the conductivity of the suspension. The conductivity of the bacteria suspension during the electroporation was measured for each process when applying electric fields of different magnitudes.
It could be observed, that the conductivity of bacteria suspensions of equal composition, measured during the electroporation process, increases linearly with increasing current density (figure 5-19).

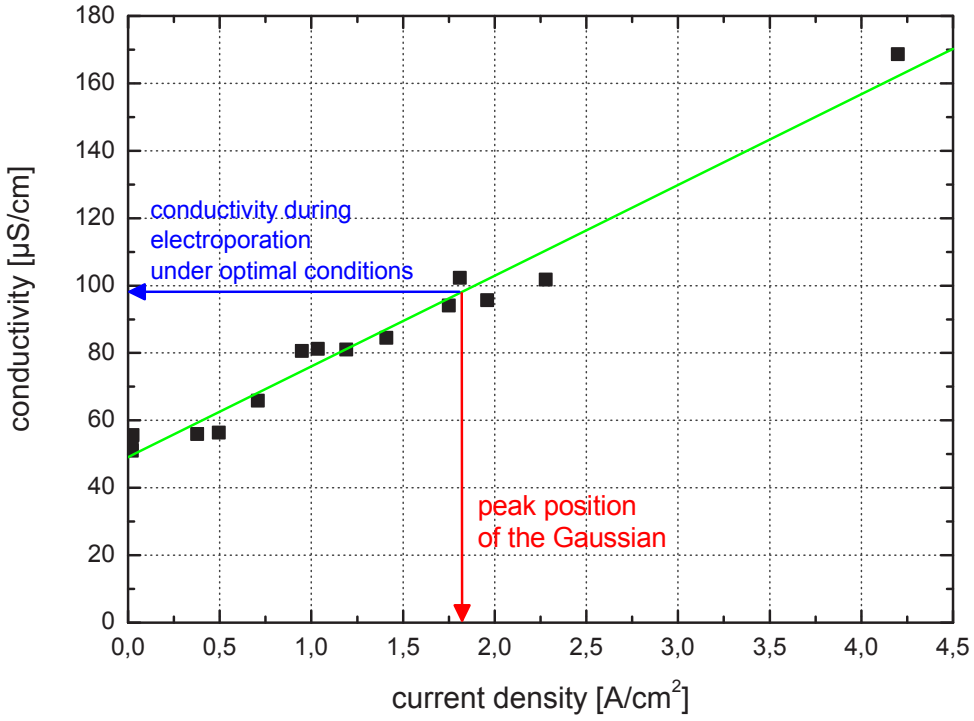

Figure 5-19: Conductivity of *E.coli* C600 of one and the same preparation during the electroporation process for several applied electric fields in dependence of the corresponding measured current density. The origin of the blue and the red arrow equals the value corresponding to the maximal transformation efficiency for this mixture of *E.coli* C600 and pDsRed-Express.

For easier understanding, this linear correlation is called "**LinFit**" further on.
To calculate the conductivity during the electroporation process for optimal conditions, the value of the current density at the peak position of the Gaussian was inserted into the function of **LinFit**. The calculated values of the conductivity during the electroporation process under optimal conditions are inserted as red points ● in figure 5-20.
The pre-electroporation conductivities (black points ■) and the conductivities of the suspension, which are reached under optimal conditions during the electroporation process (red points ●) were fitted on the abscissa and the correlated values of current density (peak position of the Gaussian) on the ordinate of a cartesian diagram.

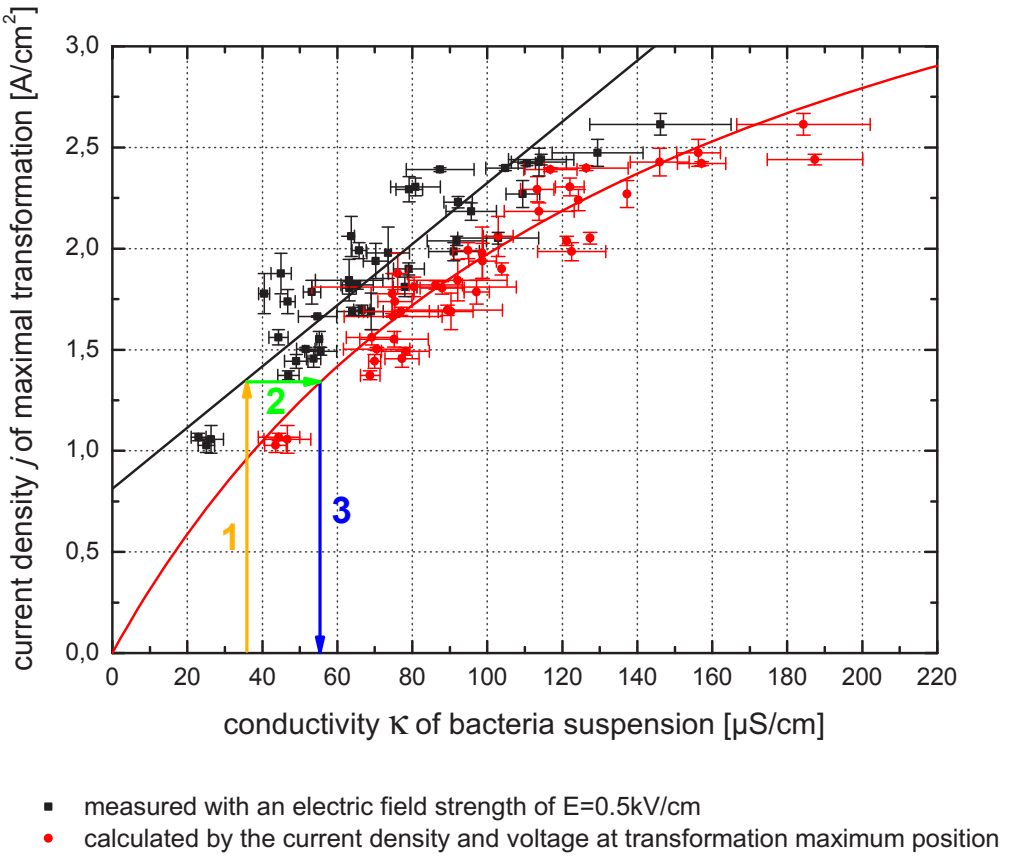

Figure 5-20: Calibration graph for optimal electroporation of *E.coli* C600 with pDsRed-Express plasmid DNA.

When the pre-electroporation conductivity of the suspension is known, with this graphic, it is possible to determine an electric field range, wherein optimal transformation efficiencies can be reached for *E.coli* C600 with pDsRed-Express plasmid DNA.
When regarding the linear dependence between the pre-electroporation conductivities and the current density (black curve), it can be seen which current density is needed for maximal transformation efficiency as shown by the example of the orange arrow (1).
For this current density value, the conductivity of the suspension during the electroporation can be read in the diagram with the help of the approximating hyperbola (red curve) as shown in the example by the green arrow (2) and the blue arrow (3).
The hyperbola function describes a curve by

$$j = \frac{a \cdot \kappa}{b + \kappa} \quad , \tag{5.3}$$

whereat $a = (4,788 \pm 0,329)\ \frac{\mathrm{A}}{\mathrm{cm}^2}$ and $b = (142,736 \pm 16,165)\ \frac{\mu\mathrm{S}}{\mathrm{cm}}$ are constants and κ is the conductivity of the bacteria suspension during the electroporation process.
When inserting equation 5.3 into equation 5.2, the electric field, which has to be applied

to reach maximal transformation efficiencies, can be calculated by

$$E = \frac{j}{\kappa} = \frac{a}{b+\kappa} \quad . \tag{5.4}$$

Then the voltage, to which the voltage generator should be adjusted, can be determined by $U = E \cdot d$, whereat d is the distance between the electrodes.
The absolute error of the voltage σ_U can be calculated by gaussian error propagation:

$$\sigma_U = d \cdot \sigma_E \tag{5.5}$$

with

$$\sigma_E = \sqrt{\left(\frac{1}{b+\kappa}\right)^2 \cdot \sigma_a^2 + \left(\frac{-a}{(b+\kappa)^2}\right)^2 \cdot \left(\sigma_b^2 + \sigma_\kappa^2\right)} \quad . \tag{5.6}$$

The parameters σ_E, σ_a, σ_b and σ_κ correspond to the absolute errors of the electric field, the conductivity κ and the constants a and b of the approximating hyperbola in figure 5-20.
To prove the correctness of the developed calibration graph (figure 5-20) if it is really possible to predict the electric field range, wherein optimal transformation efficiencies can be reached for *E.coli* C600 with pDsRed-Express plasmid DNA, a series of measurements was done with six samples of unknown compositions.
Of one and the same preparation of *E.coli* C600 to a volume of 640 µl, 12.8 µl of pDsRed-Express (c=10 ng/µl) and 100 µl of a mixture of double-distilled water and a 10 mM NaCl solution of unknown concentration was added.
Before electroporation, the conductivity of each sample was measured for a volume of 100 µl within the electroporation cuvette at an electric field of $E = 0.5\,\mathrm{kV/cm}$. Afterwards the samples were electroporated. Therefore single voltage pulses of different amplitudes were applied to sample volumes of 100 µl. So for each sample the electroporation efficiencies were determined, which were reached for five different applied voltages. The voltages were within a range, which was estimated by reading the prospective conductivity during the electroporation process out of figure 5-20 and inserting it into equation 5.4.
Figures 5-21a and 5-21b show the transformation efficiencies for all six samples in dependence on the electric field and the current density.
The colored bulks at the bottom of the graphics show the predicted range for each sample, within the correspondent maximal transformation efficiency should be found.
It can be seen, that the maximal transformation efficiency for each sample is within or nearly within the range of the electric field or current density, which is marked by the corresponding bulk. Therefore, it can be assumed, that the calibration graph works quite fine.

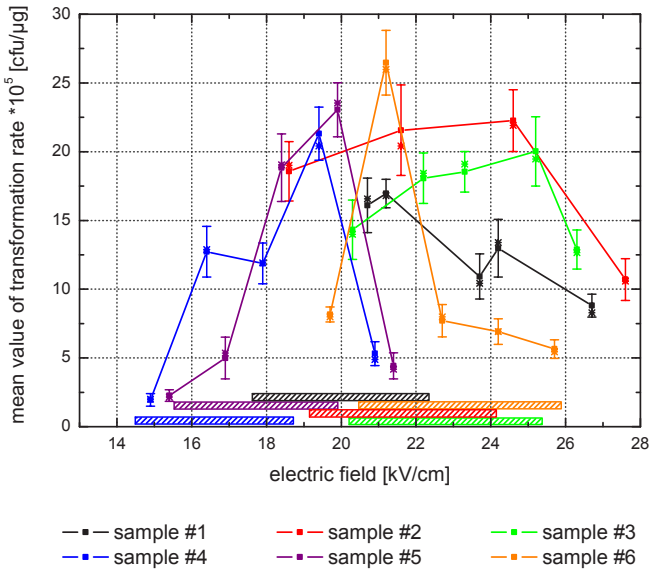

(a) Transformation rate in dependence on electric field.

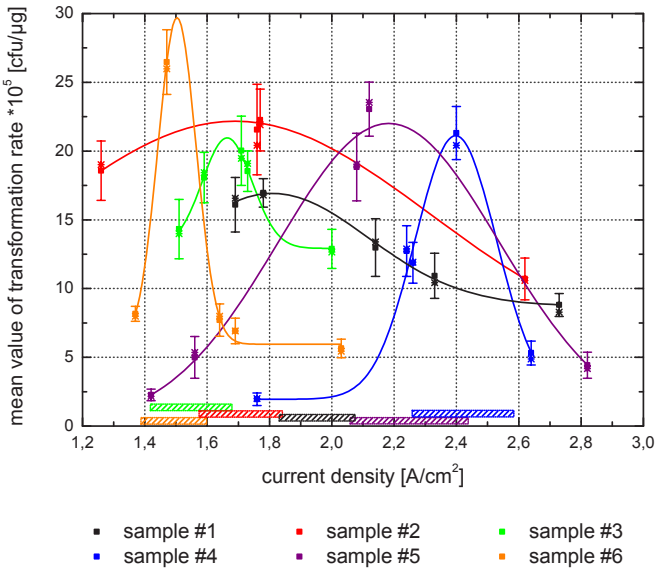

(b) Transformation rate in dependence on current density.

Figure 5-21: Transformation efficiency of electroporated *E.coli* C600 with pDsRed-Express plasmid DNA, to which several concentrations of NaCl solution were added, in dependence on the applied electric field and the current density.

The shift of the gaussian peak position in figure 5-21b is consistent with former observations. As can be seen, when comparing the conductivities in table 5-2, which shows the mixing ratios of the double-distilled water and the 10 mM NaCl added to each sample as well as the resulting conductivity, the value of current density where the peak position can be found increases with increasing conductivity.

sample	NaCl solution : H_2O [%]	conductivity [µS/cm]
#1	50:50	$78,040 \pm 3,198$
#2	25:75	$63,998 \pm 4,108$
#3	0:100	$54,692 \pm 5,097$
#4	100:0	$104,761 \pm 5,207$
#5	75:25	$95,689 \pm 6,726$
#6	0:100	$51,551 \pm 2,465$

Table 5-2: Mixing ratio between NaCl solution and double-distilled water, which was added to each sample and the resulting conductivities of the bacteria suspension.

5.5.4 Transformation of *Bacillus subtilis* 168 in dependence on current density

Bacillus subtilis 168 were electroporated with pBluescript KS II+ plasmid DNA with the help of the same experimental arrangement like *E.coli* C600 (see figure 4-1).
Electroporation of *Bacillus subtilis* 168 showed a very similar behavior like electroporation of *E.coli* C600.
The conductivity of the bacteria suspension was changed by adding different volumes of 10 mM NaCl solution. The pre-electroporation conductivity of each sample was measured by applying a small electric field of $E = 0.5\,\mathrm{kV/cm}$ causing only very low transformation, which is negligible compared to the transformation efficiency reached for higher electric fields.

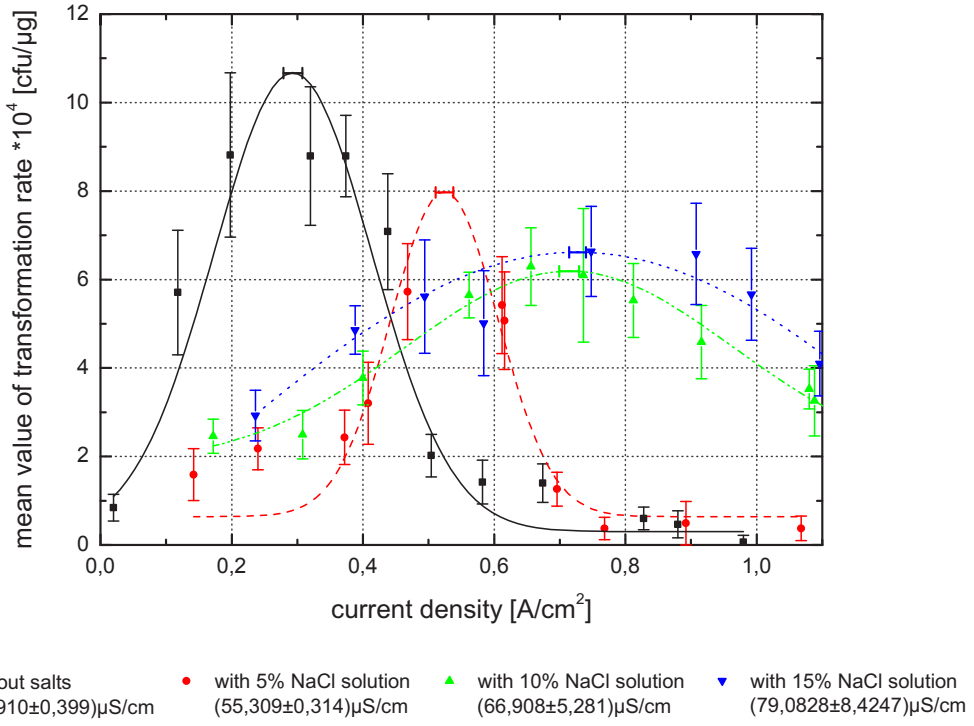

Figure 5-22: Transformation efficiencies of *Bacillus subtilis* 168 of several conductivities transformed with pBluescript KS II+ in dependence on current density.

Regarding the transformation efficiencies of *Bacillus subtilis* 168 of different conductivities in dependence on the current density (as shown in figure 5-22) it can be seen, that with increasing conductivity higher current densities are needed to reach the transformation maximum.
Thereat the current densities are corresponding to the current and the voltage maximum before the exponential decay.
Maximal transformation efficiencies of *Bacillus subtilis* 168 can already be found at current densities, which are 10 times smaller than those needed for maximal transformation efficiencies of *E.coli* C600. Apart from that, their behaviors are quite the same.
The smaller distance between the Gaussian peak positions, corresponding to the two highest NaCl solution volume concentrations added to the bacteria suspension, may be explained by the conductivity behavior of salt solutions of different concentrations.
With increasing volume of salt solution the concentration of ions increases, too. Due to electrostatic forces the ions constrain each other on their way through the electrolyte, which leads to the fact that with high ion concentrations the conductivity value gets smaller again. Therefore the conductivity in dependence on the ion concentration describes a curve which increases first until reaching a maximum. After reaching this maximum the conductivity decreases slowly (see figure 2-6) [HV05].
Therefore, the distances between the Gaussian peak positions mirror the conductivity behavior of NaCl solutions of different concentrations.

5.6 Charge dependent electroporation

As in section 5.4 in dependence on the current density, the applied electric field strength can also be written in dependence on the amount of charge by

$$\begin{aligned} & E = \frac{U}{d} = \frac{R \cdot I}{d} = \frac{\rho \cdot d \cdot I}{A \cdot d} \\ \Leftrightarrow \quad & E = \frac{\rho I}{A} = \frac{\rho \cdot q \cdot t}{A} \quad , \end{aligned} \tag{5.7}$$

where E is the electric field strength, U is the voltage, d is the distance between electrodes, R is the ohmic resistance, I is the current, A is the surface of the electrode, ρ is the resistivity of the medium, q is the charge, and t is the time.
Due to equation 5.7 it can be assumed that the amount of charges applied to the bacteria cells is the essential parameter to reach maximal transformation efficiency.
To verify this assumption, *E.coli* C600 with pDsRed-Express plasmid DNA were electroporated with square wave pulses. The corresponding arrangement of measurement is shown in figure 4-3.

5.7 Electroporation of *E.coli* C600 in dependence on the applied frequency

E.coli C600 were electroporated with pDsRed-Express plasmid DNA by applying several square wave pulses of different frequencies. The duty-cycle of the bipolar voltage generator was adjusted, to 50 : 50. That means that the percentage of the positive and the negative fraction of the pulse duration is in a ratio of 50 % : 50 %. The electric field strength was $E = \pm 5.5\,\mathrm{kV/cm}$.
Figure 5-23a and 5-23b show the transformation efficiencies and survivors for all five adjusted frequencies in dependence on the number of applied voltage pulses.

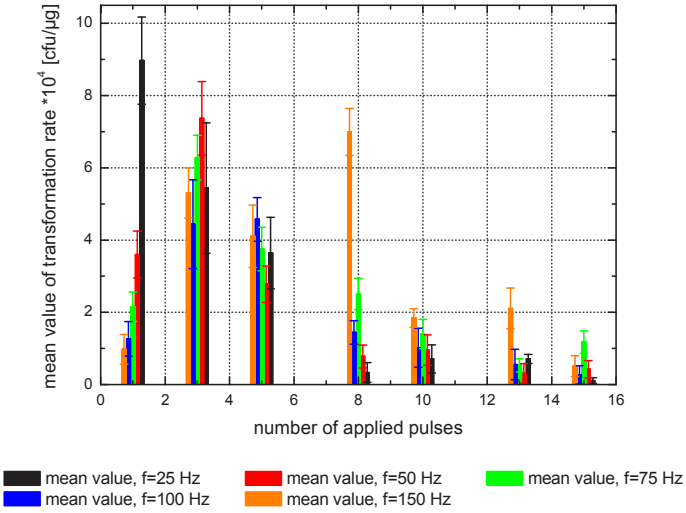

(a) Transformation efficiency

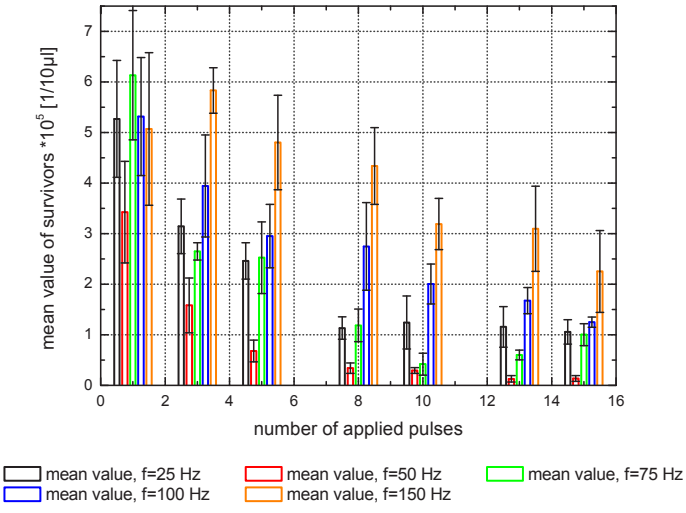

(b) Survivors

Figure 5-23: Transformation efficiencies and survivors for several frequencies in dependence on the number of applied voltage pulses (duty-cycle: 50% positive, 50% negative; electric field strength: $E = \pm 5.5\,\mathrm{kV/cm}$)

It can be seen, that for each frequency another number of applied voltage pulses is needed to reach maximal transformation efficiency. There seems to be a tendency, that for increasing frequency a higher number of pulses is necessary.
In this context it can be assumed, that with smaller frequencies the number of survivors should decrease faster with the number of applied voltage pulses than with larger frequencies. But comparing the results of all frequencies in figure 5-23b shows, that this assumption is not fulfilled.
When plotting the data of figure 5-23a and 5-23b in dependence of the measuring time (see figures 5-24a and 5-24b) the behavior of the transformation rate opens up new vistas.

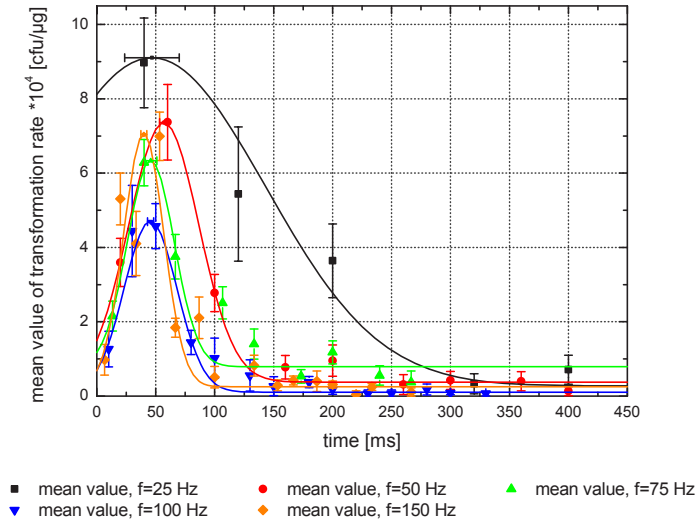

(a) Transformation efficiency

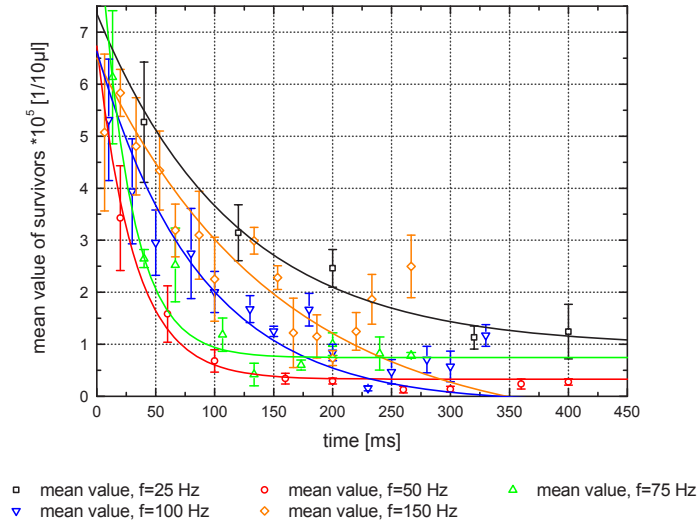

(b) Survivors

Figure 5-24: Transformation efficiencies and survivors for several frequencies in dependence on the measuring time (duty-cycle: 50% positive, 50% negative; electric field: $E = \pm 5.5\,\mathrm{kV/cm}$)

As shown in figure 5-24a, for all frequencies, the transformation maximum occurs after a measuring time of about 50 ms.

When regarding the amplitudes of the transformation efficiencies, one could believe that applying smaller frequencies leads to a higher number of transformants when taking the results for 150 Hz for an error in measurement. But the survivors diagrammed in figure 5-24b, show no dependence of the amplitudes on the applied frequency. Therefore, it has to be assumed that for this range of applied frequencies the behavior of the amplitudes of transformants just occurs due to the fact that the data points of the transformation rate is the arithmetic mean value calculated from the results of only five Ampicillin-Agar-plates. But it cannot be said that the magnitude of transformation efficiency is completely independent on the applied frequency. As described in section 3.2 (also see figure 3-2), there is a decreasing formation of dipoles when applying a rapidly changing voltage which leads to dielectric dispersion. So for very high frequencies the amplitude of the transformation rate may decrease to zero.
Regarding the conductivities in dependence on the measuring time, it can be observed, that they behave in the same way for all frequencies. Apart from the oscillation of the graphs with the frequency adjusted to the voltage generator, the conductivities all follow the same course. Their development is shown in figure 5-25. At the beginning the conductivity increases up to a maximum, then saturates and finally decreases again. This behavior can be explained by the fact, that with increasing measuring time more bacteria cells are opened and therefore the ion concentration increases within the suspension. With a higher amount of ions, the conductivity increases, but at a critical value, the ions begin to constrain each other on their way through the suspension due to electrostatic forces (see section 2.2.1/figure 2-6). Thus, with high ion concentrations the conductivity value gets smaller again. So the conductivity in dependence on the ion concentration describes a curve which increases until reaching a maximum and after reaching this maximum the conductivity decreases slowly [HV05]. Another possible explanation for the decrease of the conductivity could be, that some of the electroporated cells close again and encapsulate ions of the suspension.

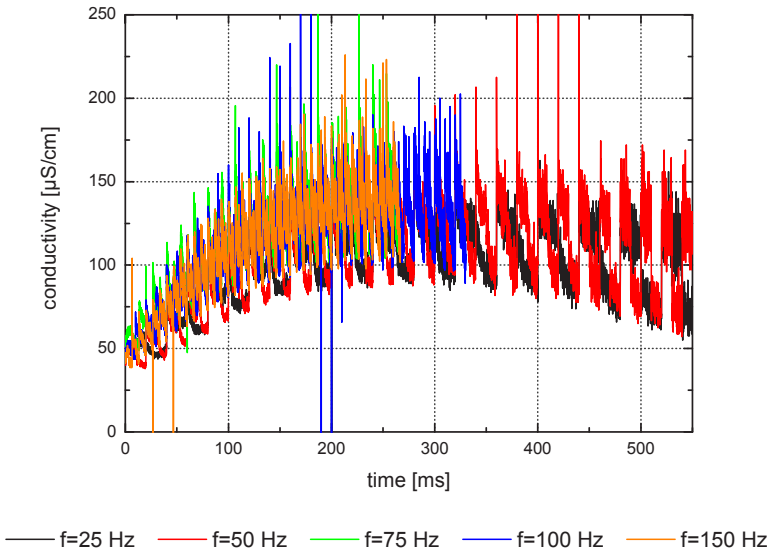

Figure 5-25: Conductivity in dependence on the measuring time

Comparing figures 5-24a, 5-24b and 5-25, it can be seen, that maximal transformation occurs at a measuring time when there are only about 50 % survivors of the initial cell amount left and the value of conductivity was increased of about 50 % of its initial value.
The fact, that the transformation maxima for all frequencies occurred at the same time, and taking equation 5.7 into account, lead to the assumption, that the transformation of *E.coli* C600 depends on the amount of charge. The transformation rate in dependence on the amount of charge is shown in figure 5-26. The charge was determined by integrating the measured current over the time.

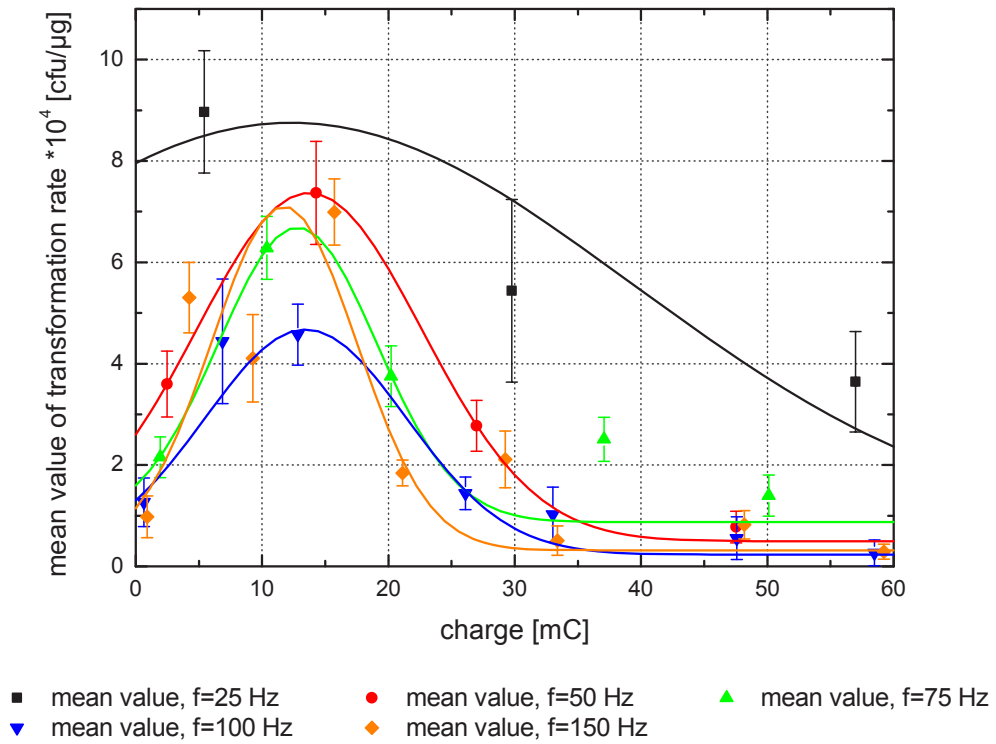

Figure 5-26: Transformation efficiencies for several frequencies in dependence on the amount of the applied charge (zoom-in to the important part of data-points)

For all applied frequencies, the maxima of transformation efficiency accumulate at a value of 15 mC. Out of the observation made by figure 5-24a and 5-26, it can be assumed that transformation of *E.coli* C600 with pDsRed-Express plasmid DNA does not depend on the adjusted frequency but on the duration of treatment and the amount of applied charge. This assumption could be manifested by the experimental results presented in section 5.10.

5.8 Conductivity and changes on the electrode surface

For all experiments the current and the voltage during the process was measured in dependence on the measuring time with an oscilloscope. Figure 5-27 shows the development of the current and voltage curve for the electroporation of *E.coli* C600 with pDsRed-Express plasmid DNA. The applied electric field was $E = \pm 5.5\,\mathrm{kV/cm}$ (voltage $U = \pm 550\,\mathrm{V}$, electrode surface $A = 1\,\mathrm{cm}^2$, electrode distance $d = 1\,\mathrm{mm}$). The frequency was $f = 25\,\mathrm{Hz}$ and the number of applied voltage pulses was $n = 10$.

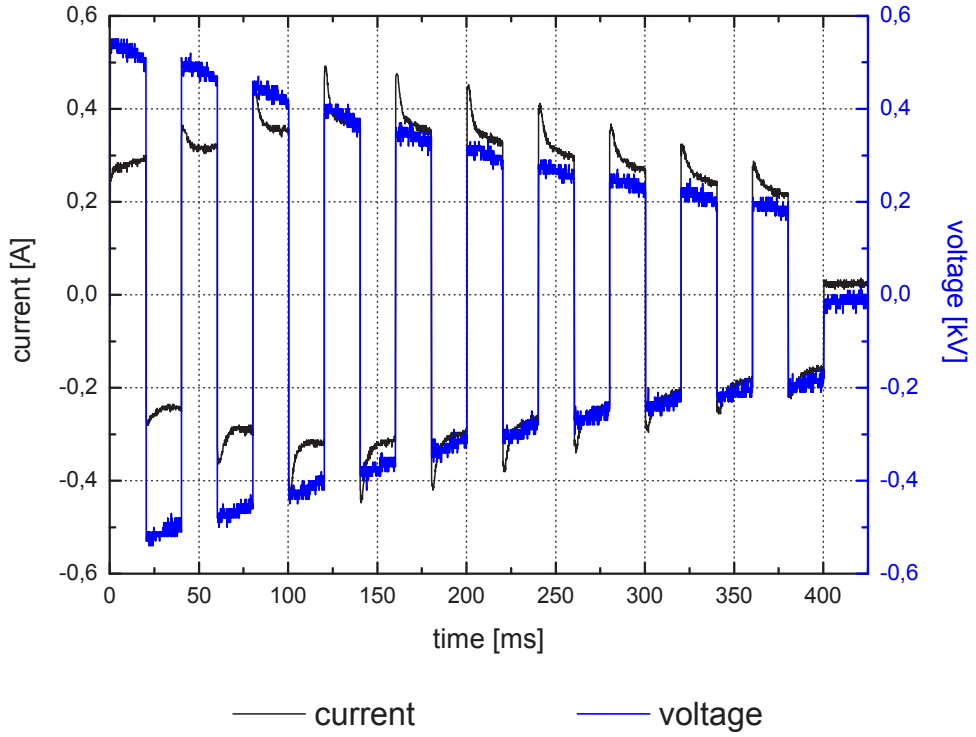

Figure 5-27: Current and voltage measured during the electroporation process of *E.coli* C600 with pDsRed-Express plasmid DNA ($E = \pm 5.5\,\mathrm{kV/cm}$, $f = 25\,\mathrm{Hz}$, $n = 10$)

The magnitude of the voltage decreases from pulse to pulse and the pulses have no horizontal plateau. This behavior is caused by the power supply of the voltage generator. The magnitude of the current pulses increase at first, reach a maximum and then decrease again. It should be emphasized that the shape of the current pulses do not equal the shape of the voltage pulses. In fact, on top of the current pulses there is an exponential decay which is different for each pulse.

In systems of direct current, the current follows the shape of the voltage curve. The observed exponential behavior on top of the current pulses leads to the assumption that there is a dielectric layer accumulating on the electrode surfaces. These dielectric layers establish a capacitor in between the electrodes. The exponential decay then equals the decay curve of a capacitor.

The difference in the decay times of the current pulses can be explained by a change in

the relative permittivity ϵ_r of this capacitor. If the relative permittivity of the dielectric barrier increases, due to the deposit of particles out of the bacteria suspension, the magnitude of the current pulse peaks increases and the pulse decay time has to be shorter. In figure 5-27 each pulse has a duration of 40 ms. In case of a current passing a dielectric layer, the current should decrease to zero during each half-cycle of a pulse. Actually, this cannot be observed. In fact, the current decreases exponentially at first and then follows the shape of the voltage pulse. But the current does not decrease to zero level. This leads to the assumption, that in this case there is a combination of a direct current and a current initiated by a displacement current.
For a capacitor, the electric field strength decays by

$$E(t) = E_0 \cdot e^{-\frac{t}{\tau}} \ , \tag{5.8}$$

whereat E_0 is the electric field strength at the moment $t = 0$ and τ is the decay time, which is proportional to the capacity C and the resistance R by

$$\tau = R \cdot C \ . \tag{5.9}$$

The capacitance of the dielectric layers is directly proportional to the dielectric permittivity ϵ_r:

$$C = \epsilon_0 \epsilon_r \frac{A}{l} \ . \tag{5.10}$$

The resistance R of the dielectric layers can be described by its specific resistance ρ:

$$R = \frac{\rho \cdot l}{A} \ . \tag{5.11}$$

Here, A is the surface area of the electrodes covered with dielectric material and l is the thickness of the dielectric layers.
When inserting equations 5.10 and 5.11 in equation 5.9 leads to

$$\tau = \epsilon_0 \epsilon_r \cdot \rho \ . \tag{5.12}$$

Thus, if the relative permittivity ϵ_r increases and therefore the charge transfer within the gap, the decay time increases. In that case, the shape of the current would approach the shape of the voltage, which would mean that there is no dielectric barrier. But on the other hand, if the specific resistance increases and therefore suppresses the charge transfer, the decay time increases, too. So these two parameters, which both depend on the material composition and dimensions of the dielectric layer on the electrodes, compete each other.

To receive the development of the dielectric capacitor in dependence on the measuring time, the decay time τ of each current pulse must be determined.
Due to the influence of the power supply on the voltage pulse shape, the exponential decay of the current pulses must be reduced by the decay of the corresponding voltage pulses before determining the decay time τ. Therefore, each pair of pulses must be normalized and then the normalized voltage pulse must be subtracted from the corresponding normalized current pulse.
The exponential decay in the voltage pulse decays by $e^{-\frac{t}{\tau_1}}$ and the one in the current pulse by $e^{-\frac{t}{\tau_2}}$. So the difference between these both decays is $\Delta y(t) = e^{-\frac{t}{\tau_1}} - e^{-\frac{t}{\tau_2}}$. Normalizing the voltage and current pulses, the exponential decay describing the capacity of the dielectric layer also must start with the value 1. Therefore, the discharge function of the dielectric layer capacitor can be written by

$$y(t) = 1 - \Delta y(t) = 1 - \left(e^{-\frac{t}{\tau_1}} - e^{-\frac{t}{\tau_2}}\right) = e^{-\frac{t}{\tau}} \quad . \quad (5.13)$$

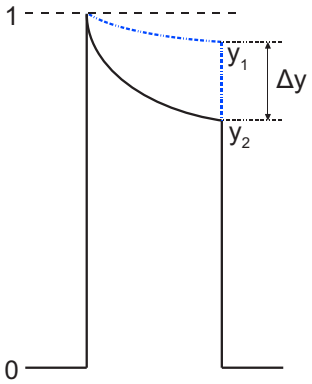

Figure 5-28: Normalized voltage (----) and current pulse (—)

To determine the decay time τ the calculated functions $\Delta y(t)$ were plotted for each pulse and approximated by an exponential decay function. The decay time of the approximated function then equals the decay which describes the behavior caused by the dielectric layer on the electrode surfaces. Figure 5-29 shows an example of the determination of τ.

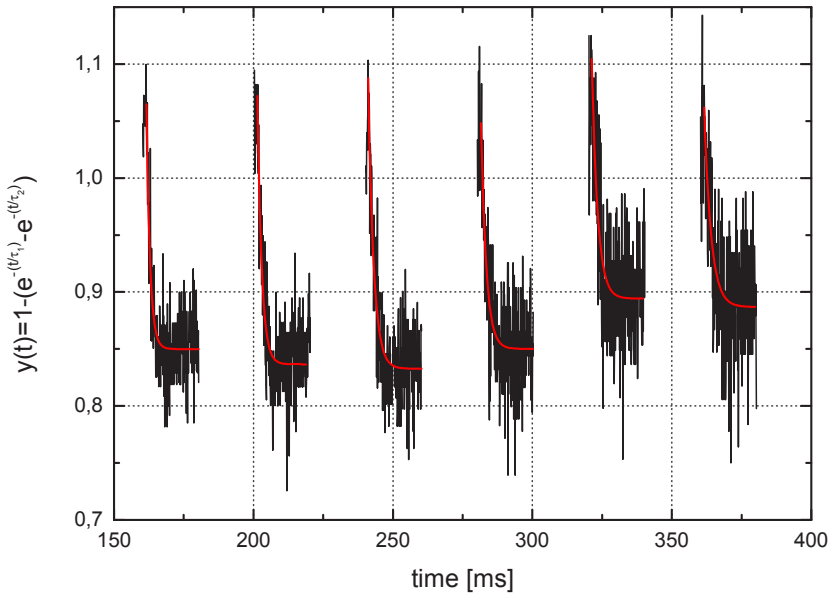

Figure 5-29: Example for the determination of the decay time τ for the data presented in figure 5-27 ($E = \pm 5.5\,\mathrm{kV/cm}$, $f = 25\,\mathrm{Hz}$, $n = 10$)

These working steps were done for each voltage-current-pulse pair of all measurements described in section 5.7.
The determined decay times τ are diagrammed in dependence on the measuring time in figure 5-30a and in dependence on the applied amount of charges in figure 5-30b.

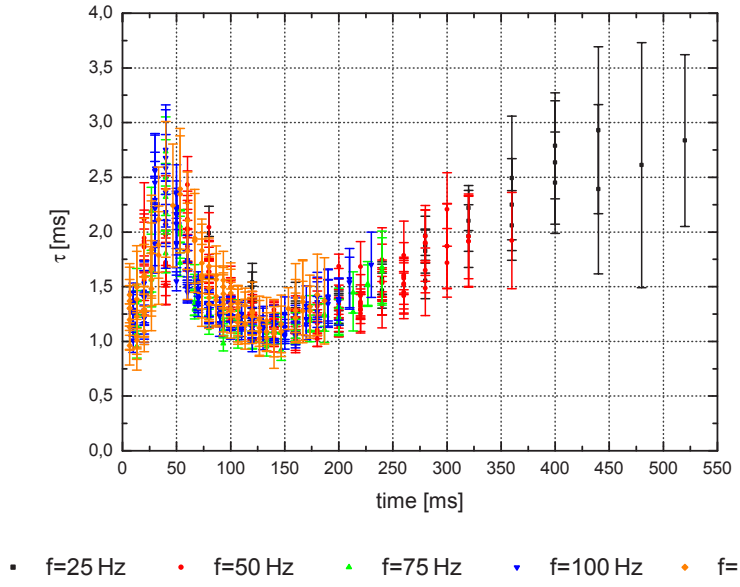

(a) Decay time τ of the current in dependence on the measuring time

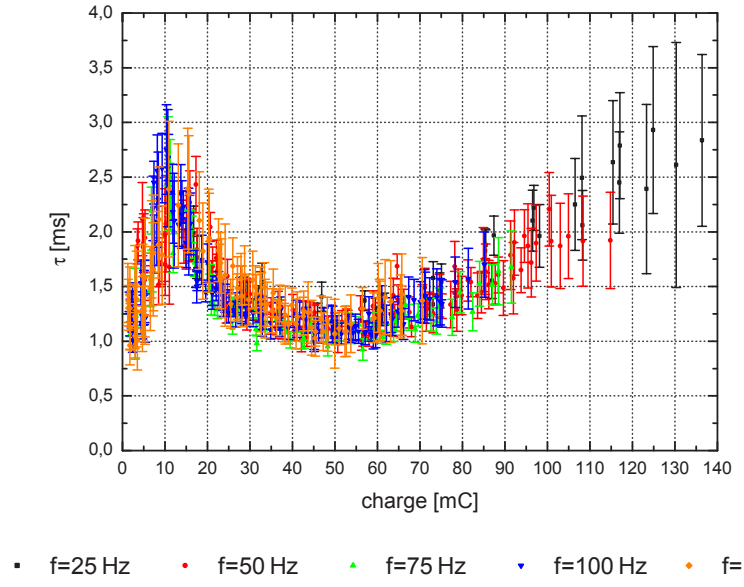

(b) Decay time τ of the current in dependence on the applied charge

Figure 5-30: Decay time τ of the current for several adjusted frequencies

At first τ increases, then decreases and then increases again. A possible explanation would be that there is some kind of dielectric layer on the electrode surfaces before the electroporation cuvettes are used for the first time. Due to the fact, that the electrodes are made of aluminum, it can be assumed, that there is an aluminum-oxide layer which is partly removed by electro-erosion. Afterwards, another dielectric layer establishes on the electrode surfaces (decreasing value for ϵ_r) which leads to the decrease of the exponential decay time τ (see equation 5.12). This dielectric layer may be due to a deposit of material from the bacteria suspension. Such a dielectric layer establishes due to material exchange which is parallel to the exchange of charge. The over-layer on the electrodes is growing layer by layer. There can be a development of a net layer on the surface by two-dimensional nucleation or a broadening of a growth step which arise from a screw dislocation and wind itself to a non-vanishing spiral. On an electrode, there normally are several screw dislocations which lead to a surface roughening. Such a roughening is advantaged in presence of low ionic concentration-solutions [HV05]. Due to the fact, that the *E.coli* C600 were washed twice with double-distilled water while making them electro-competent, the bacteria suspension can be assumed to be of low ionic concentration. Therefore, the surfaces of the electrodes within the electroporation cuvette may be roughened by non-vanishing spirals winding up on several areas on the electrodes, while there are still areas on the electrodes, where there is no deposit at all. This would be an explanation for the shape of the current pulses in figure 5-27. The current decreases exponentially in the first half of each half-cycle of a pulse to a certain level and then follows the development of the voltage pulse shape. Therefore, there must be a direct current at deposit-free areas at the electrodes combined with a displacement current through the "islands" of dielectric deposit on the electrode surfaces. An example for the growth of non-vanishing spirals arising from screw dislocations is shown in figure 2-9.

The anew increase of the decay time τ in figures 5-30a and 5-30b may be caused by another electro-erosion process.

As already shown in section 5.2, when using one and the same cuvette several times for electroporation by applying voltage pulses with an exponential decay, the measured conductivity decreased with each usage. As can be seen in figure 5-30b, the decay time τ, which is characteristic for the dielectric accumulation at the electrodes, depends on the amount of charges. Therefore, it should occur for all voltage pulse shapes. So the conductivity behavior reported in section 5.2 may be equal to the period whereat τ decreases.

Comparing figure 5-24a with figure 5-30a and figure 5-26 with figure 5-30b leads to the observation, that the transformation efficiency is maximal when the exponential decay τ on top of the current pulses is maximal. If the assumption is correct, that there is an aluminum-oxide layer on the electrode surfaces at the beginning which is partly removed, and that afterwards there is an accumulation of particles from the bacteria suspension, maximal transformation efficiencies occur when there is a minimum of a dielectric layer on the electrodes.

5.9 Influence of current flow direction on transformation rate

In the following experiment the correlation between transformation efficiency of *E.coli* C600 with pDsRed-Express plasmid DNA and the direction of electric current within the electroporation cuvette was determined.
Therefore, only single square wave pulses were applied to the bacteria suspension. The frequency and the amplitude of the electric field were kept constant at the values of $f = 75\,\mathrm{Hz}$ and $E = \pm 5.5\,\mathrm{kV/cm}$, while the duty-cycle was tuned in that way, that the ratio between the positive and the negative part of the pulse was changed in 10 %-steps.

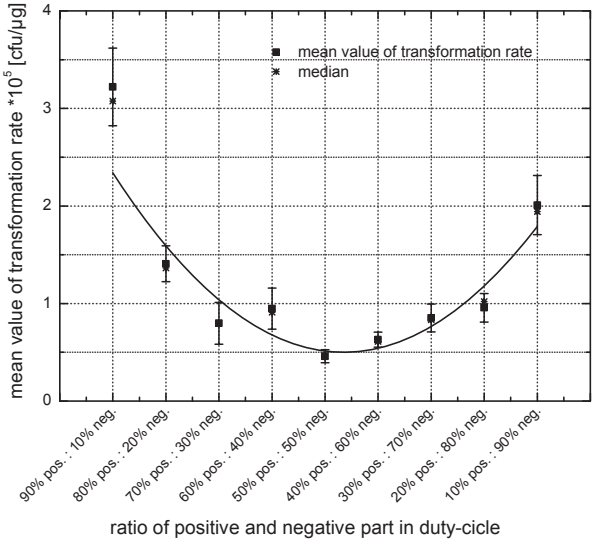

(a) Transformation efficiency

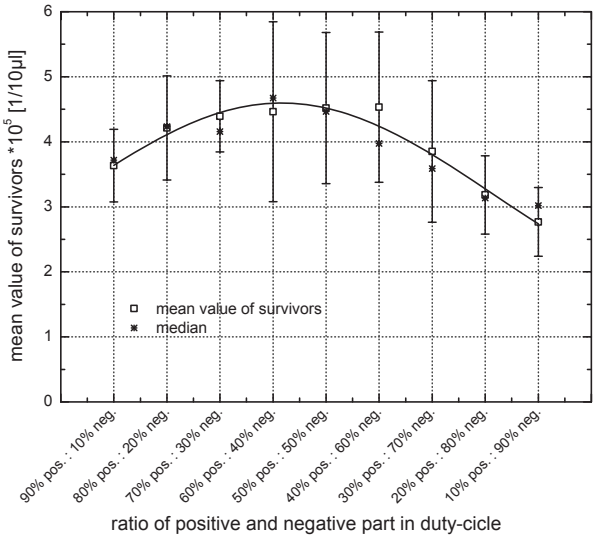

(b) Survivors

Figure 5-31: Transformation efficiency and survivors of electroporated *E.coli* C600 with pDsRed-Express plasmid DNA in dependence on the ratio between positive and negative part of the single voltage pulses ($n = 1$) with an applied electric field strength of $E = \pm 5.5\,\mathrm{kV/cm}$.

Figure 5-31 shows, that there are the most transformants, where there are the less survivors. The maximal transformation efficiencies were reached for a duty-cycle with a ratio of 90% : 10%, whereat it is not of relevance if the larger ratio is positive or negative. So for high transformation efficiencies, the current within the electroporation cuvette should flow only in one direction.
This phenomenon can be explained as the permeabilization of cell membranes caused by electroporation is due to a membrane polarization by ion movements and formation of dipoles along the electric field lines. In an AC field the voltage is changing rapidly. When applying such an electric field on a cell, fewer and fewer dipoles will be formed or reoriented in time which leads to dielectric dispersion and therefore to less permeabilization [Zim82].
On the other hand, TEKLE *et al.* reported in 1991, when compared transformation efficiency on NIH 3T3 cells with pSV2-neo plasmid DNA by applying a sequence of high-frequency unipolar or bipolar square waves or a single square pulse of the same duration, that transformation efficiency in dependence on the percent survival was best with bipolar square wave pulse [TAC91].
At least, all reports agree on the behavior of the number of survivors.

5.10 Transformation in dependence on charge

Due to the fact, that maximal transformation efficiency of *E.coli* C600 with pDsRed-Express plasmid DNA occurs when the current flows almost just in one direction, the square wave generator was modified. Now, the generator can only produce voltage pulses with a positive amplitude from zero up to 1.5 kV.
To detect the correlation between the transformation efficiency and the applied charge, *E.coli* C600 were treated with single voltage pulses of a constant electric field strength and frequency of $E = 8\,\mathrm{kV/cm}$ and $f = 50\,\mathrm{Hz}$, while the duty-cycle was tuned.
The transformation efficiency was determined and fitted in dependence on the duty-cycle (figure 5-32a), the current density (figure 5-32b) and the amount of charges (figure 5-32c).
It can be seen, that the transformation rate in dependence on the duty-cycle and on the amount of charge can be approximated with Gaussian distribution, while in dependence on the current density all data points form a cloud around the value $0.4\,\mathrm{A/cm^2}$.
Due to the fact that the electric field was kept constant at 8 kV/cm, the current density $j = I/A$ was also constant. But by changing the duty-cycle/pulse width, the duration t of the applied voltage pulses changed and therefore the amount of charge, which can be calculated by $q = I \cdot t$.
Here maximal transformation occurs at a duty-cycle of about 65 %. So with this configurations with a duty-cycle of 65 % the pulse width and therefore the duration of the current application led to optimal transformation conditions. The time integrated current corresponds to the applied amount of charges $\left(q = \int_0^t I(t)\right)$, which equals the area

below the function of the current. So with a pulse width, which results in a duty-cycle of 65 %, an ideal charge quantity must have passed through the bacteria suspension.
In 1989, SAUNDERS *et al.* compared transformation efficiencies of tobacco protoplasts with cucumber mosaic viral RNA, which were achieved by applying electric fields by exponential wave pulses or square wave pulses. They found, that the shape of the electroporation wave, the pulse amplitude and the pulse duration are all important for the formation of pores in the cell membrane [SSK89]. A similar behavior was detected by WOLF *et al.* when they determined the degree of permeabilization of Chinese hamster ovary cells in dependence on the applied electric field, the number of voltage pulses and their duration [W$^+$94]. These observations are conform with the previously described behavior of transformation efficiencies of *E.coli* C600 with pDsRed-Express.

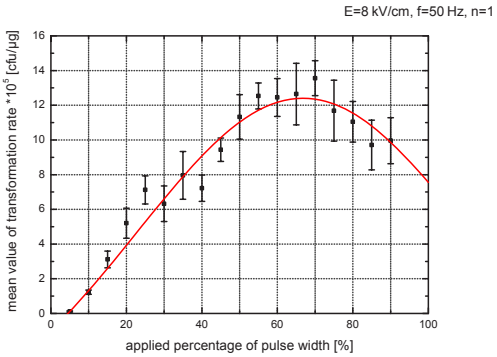

(a) Transformation rate in dependence on duty-cycle

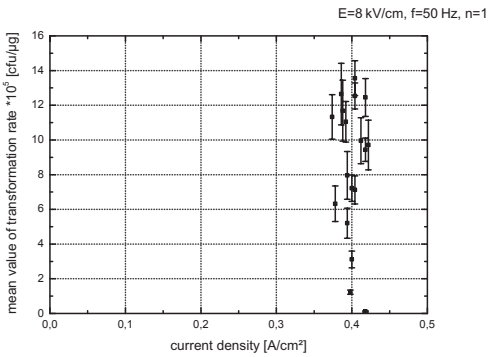

(b) Transformation rate in dependence on current density

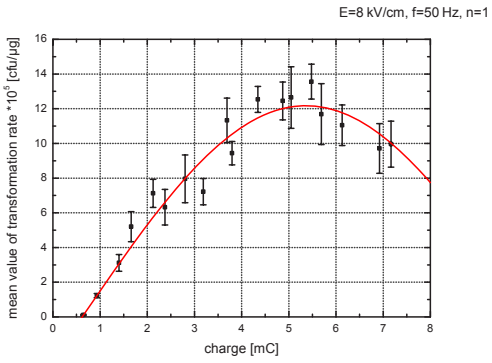

(c) Transformation rate in dependence on charge

Figure 5-32: Transformation efficiency of *E.coli* C600 with pDsRed-Express plasmid DNA treated by single voltage pulses of several duty-cycles with an applied electric field of $E = 8\,\mathrm{kV/cm}$.

A similar phenomenon was observed for the number of survivors. Here, a linear correlation was found between the number of survivors in dependence on the duty-cycle and the amount of charges, as can be seen in figures 5-33a and 5-33c.
Figure 5-33b shows the number of survivors in dependence on the current density. The data-points accumulate at a value of $0.4\,\mathrm{A/cm^2}$. This is conform to the observation made for the transformation efficiency in dependence on the current density.

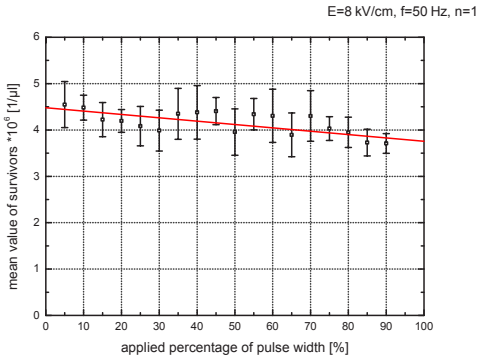

(a) Survivors in dependence on duty-cycle

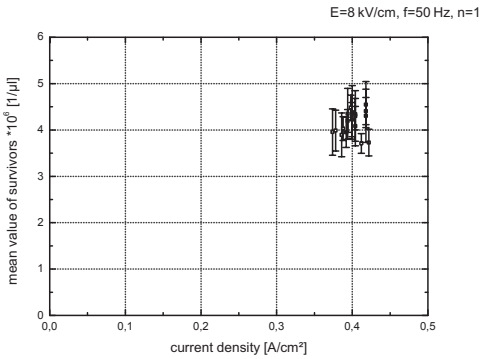

(b) Survivors in dependence on current density

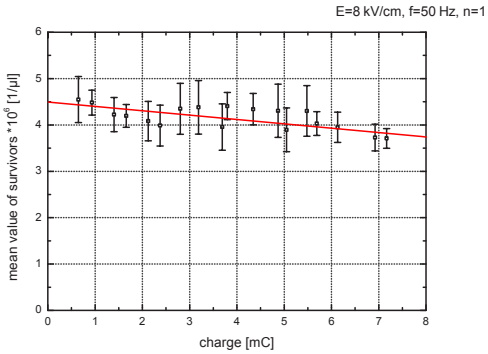

(c) Survivors in dependence on charge

Figure 5-33: Survivors of electroporated *E.coli* C600 with pDsRed-Express plasmid DNA treated by single voltage pulses of several duty-cycles with an applied electric field of $E = 8\,\mathrm{kV/cm}$.

In conclusion, it can be said, that the transformation efficiency as well as the number of survivors of electroporated *E.coli* C600 with pDsRed-Express plasmid DNA depends clearly on the applied amount of charges.

Summary

When exponential decaying voltage pulses with identical decay time τ are used for electroporation, the numbers of surviving and transformed *E.coli* C600 and *Bacillus subtilis* 168 depend on the conductivity of the bacteria suspension and the applied current density. With higher conductivities higher current densities are needed to reach the transformation maximum.
In spite of primary evidence, the concentration of present salts in the bacteria suspension have no effect on the magnitude of the transformation rate.
With the obtained experimental results out of the series of measurements whereat several concentrations of salts were added, a calibration graphic was developed to reach maximal transformation efficiencies for *E.coli* C600 with pDsRed-Express plasmid DNA when using a voltage generator with an exponential decay of a decay time of $\tau = 3\,\text{ms}$.
If the conductivity of the bacteria suspension is known, it is possible to predict the current density and at last the voltage, which has to be applied.
It has also been revealed, that a similar calculation could be done for *Bacillus subtilis* 168 with pBluescript KS II+ plasmid DNA. Maximal transformation rates were reached for *Bacillus subtilis* 168 with pBluescript KS II+ at current densities, which were about a factor 4 smaller than those for transformation maxima for *E.coli* C600 with pDsRed-Express. Both kinds of plasmid DNA, pBluescript KS II+ (2961 bp) and pDsRed-Express (3311 bp), are of nearly the same size. But *E.coli* are GRAM-negative and *Bacillus subtilis* are GRAM-positive bacteria. So the characters of the cell membrane and the cell wall seem to be important for the current density needed to reach maximal transformation efficiencies.
Due to the fact, that the transformation rates of *Bacillus subtilis* 168 with pBluescript KS II+ in dependence on the current density behave similar to those of *E.coli* C600 with pDsRed-Express, it can be assumed, that a calibration graphic can be developed for each kind of bacteria-DNA mixture. Possibly the dependence of the transformation efficiency on the current density is only a function of the species of bacteria and not correlated to the type of DNA because most plasmid DNA are supercoiled.
Treating the *E.coli* C600 with bipolar square wave pulses with a duty-cycle of 50% : 50% with a constant electric field but of several frequencies showed that for each frequency another number of applied voltage pulses is needed to reach maximal transformation efficiency. The transformation efficiencies in dependence on the measuring time showed

that for all frequencies the transformation maximum occurs after the same time duration. So there is no dependence on the applied frequency but on the duration of applied voltage/current.
Despite of the primary assumption, the magnitude of the transformation efficiency does not depend on the frequency as could be seen when regarding the corresponding number of survivors for the several frequencies.
It also could be observed that not only the transformation efficiencies but also the related conductivities of the bacteria suspension behave similar for all applied frequencies. For all measurements the conductivities followed the same course when plotting them in dependence on the measuring time. Diagramming the transformation efficiencies once again but in dependence on the applied amount of charges showed a clear correlation.
Measurements in which the duty-cycle of the bipolar square wave voltage pulses was tuned in 10 % steps, demonstrated that highest transformation rates of *E.coli* C600 with pDsRed-Express were reached at a duty-cycle of a ratio of 90 % : 10 %, while at a ratio of 50 % : 50 % the transformation efficiency was very low. The number of survivors behaved in quite the opposite way. This observation led to the guess, that the transformation efficiency depends on the amount of charges moving in one direction through the bacteria suspension. The assumption was proved true by a measurement with a square wave voltage generator, which produced pulses of only a positive amplitude (unipolar). In those measurements the current density was hold constant and the amount of charges was varied by changing the duty-cycle and therefore the pulse width. A correlation was not only shown for the transformation efficiencies but also for the number of survivors in dependence on the amount of charges.
In summary it can be said, that the key parameter for optimal transformation efficiencies is not the electric field or the current density, but for a given electric field the charge takes the major part.
A closer examination of the measured behavior of the voltage and current pulses showed that the shape of the current pulses does not completely equal the shape of the voltage pulses. There was an exponential decay on top of the first half of each half-cycle of current pulses, which implicates that there has to be a dielectric layer partly covering the electrode surfaces which leads to an establishment of a capacitor in between the cuvette electrodes. Due to the fact, that the exponential decay was only within the first half of each half-cycle of a current pulse and afterwards the current continued to follow the shape of the corresponding voltage pulse, it can be assumed, that there were only "islands" of deposit accumulating on the electrode surfaces, so there were still deposit-free areas of the electrode. At this deposit-free areas there is a direct current through the bacteria suspension. This direct current follows the shapes of the voltage pulses. The partial coverage of the electrodes leads to a combination of a direct current and a current initiated by a displacement current.
A determination of the decay time of each pulse for all adjusted frequencies showed that the behavior in dependence on the measuring time and in dependence on the ap-

plied amount of charges was the same for all cases. At first the decay time τ increased, then decreased and then increased again. This observation may be explained that there was a dielectric layer on the aluminum electrodes of the cuvette before its first usage. It can be assumed, that there is an aluminum-oxide layer on the electrodes which is partly removed by electroerosion after some time and that afterwards another dielectric layer of material of the bacteria suspension is deposited on the electrodes, decreasing the decay time. The anew increase of the decay time τ could be caused by another electroerosion process.
The optimal results for the transformation efficiency were reached when the exponential decay time of the dielectric discharge was maximal and the measuring time is short so there are many survivors.
If the assumption of the dielectric layer on the electrodes which vanishes, renews and vanishes again is correct, maximal transformation efficiencies occur when there is a minimum of a dielectric layer on the electrodes.
Due to the fact that the change in the decay time depends on the charge, a similar behavior should occur for all kinds of voltage pulse shapes applied to the electroporation cuvette.
The occurrence of the exponential decays on top of the current pulses and the change in the decay times suggest that the surface of the electrodes changes. Either the deposit on the electrodes increases or the electrodes get destroyed. This might be the reason why in general, a new cuvette should be used for each electroporation process.
The mechanism of electroporation could be simplified with a two-phase fluidic device, e. g. made out of glass. This device may consist of three reservoirs connected with a thin tube, whereat there are two reservoirs. One reservoir for the bacteria suspension and one for oil, at one end of the tube and one third reservoir at the other end of the tube.
The conductivity of the bacteria suspension containing DNA could be measured in the first reservoir by applying a voltage pulse of low magnitude through electrodes, which are inserted in the material enclosing the reservoir. With the measured conductivity, the electric field can be calculated, which is needed to achieve maximal transformation efficiencies. This electric field then can be applied on the electrodes, which are inserted in the tube connecting the reservoirs. The electroporated bacteria are then collected in the third reservoir.
The electric field applied at the electrodes in the tube could be hold constant, when oil drops are used to encapsulate the bacteria cells with DNA fragments into aqueous droplets. The duration and the intensity of the cell electroporation is given by the flow velocity and the dimensions of the oil droplets as well as the distance between the electrodes and the applied voltage[§]. In the third reservoir, where the electroporated bacteria are collected, the oil would separate itself from the aqueous droplets due to the

[§] A scheme of a possible droplet-based fluidic device to electroporate bacteria is shown in the appendix in figure 0-34a.

difference of density.
The electrodes inserted in the first reservoir and in the tube can be in direct contact with the bacteria suspension flowing through the tube, or they may be separated from the bacteria suspension by a dielectric material. In case of a direct contact between the electrodes and the bacteria suspension, the electrodes should be exchanged regularly[¶]. When a dielectric material separates the electrodes from the bacteria suspension, the device could easily be cleaned and disinfected and then used again without changing the electrodes. But it is not yet shown, if electroporation of bacteria is possible in a completely dielectric way. Therefore, further studies have to be done.
If such a fluidic device could be used to electroporate bacteria, the usage of electroporation cuvettes would not be necessary any more and a high trough put could be reached. Furthermore, in case of transformations with DNA which leads to a fluorescence, a cell-sorter can be used to distinguish between transformed and non-transformed cells and separate them. In that way, positive clones can be selected without using LB-Agar-plates.

Acknowledgements for the financial support

The financial support for the experiments done for this dissertation, given by the Ministerium für Innovation, Wissenschaft und Forschung des Landes Nordrhein-Westfalen, the Bundesministerium für Bildung und Forschung and the International Leibniz Graduate School "Systems Biology Lab-on-a-Chip" is gratefully acknowledged.

[¶] Figure 0-34b in the appendix shows a possible construction how electrodes, which should have direct contact with the bacteria suspension, could be inserted into the tube of the fluidic device.

Appendix

Figure 0-34 shows a possibility to construct a droplet-based fluidic device to electroporate bacteria and the corresponding mechanism for electrodes, which are in direct contact with the bacteria suspension flowing through the tube.

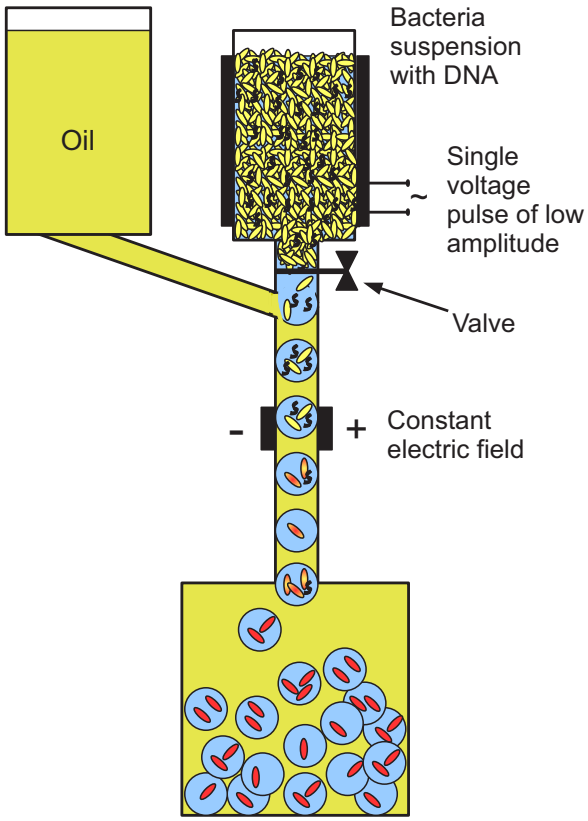

(a) Fluidic device for electroporation of bacteria

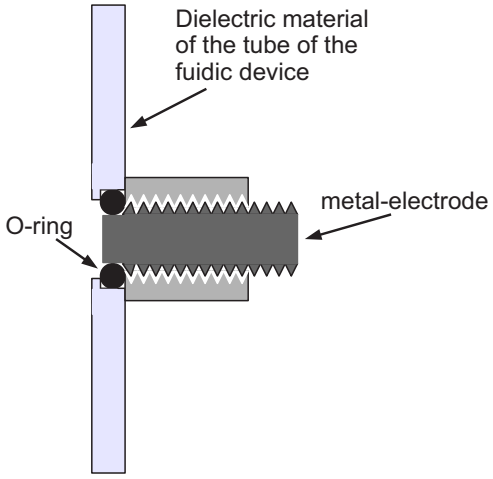

(b) Possible construction of an inserted electrode, which is in direct contact with the bacteria suspension.

Figure 0-34: Scheme of a possible fluidic device to electroporate bacteria without cuvettes.

Bibliography

[B+94] J. BELEHRADEK JR. et al., Biochim. Biophys. Acta **1190**, 155 (1994). [2]

[B+07] F. R. BLATTNER et al., United States Patent (2007). [48]

[BA65] M. E. BAYER and T. F. ANDERSON, Proc. Natl. Acad. Sci. USA **54** (1965). [8]

[Ber] J. BERNHARDT, *Bacillus subtilis*, Beschreibung und Charakterisierung, http://microbio1.biologie.uni-greifswald.de:8080/institute/85. [14, 15]

[BG04] J. N. BLATTMAN and P. D. GREENBERG, Science **305**, 200 (2004). [2]

[BMFK13] B. C. BRAMBACH, A. MICHELS, J. FRANZKE, and R. KETTLER, Progress in Biophysics and Molecular Biology **111**, 46 (2013). [3]

[BR70] M. E. BAYER and C. C. REMSEN, Journal of Bacteriology **101**, 304 (1970). [10]

[C+82] L. V. CHERNOMORDIK et al., Bioelectrochem. Bioenerget. **9**, 149 (1982). [37]

[C+86] G. CIPRANDI et al., Chemioterapia **5**, 404 (1986). [14]

[C+05] A. CRAIU et al., Blood **105**, 2235 (2005). [2]

[CCH72] S. N. COHEN, A. C. Y. CHANG, and L. HSU, Proc. Natl. Acad. Sci. USA. **69**, 2110 (1972). [36]

[CH88] N. M. CALVIN and P. C. HANAWALT, Journal of Bacteriology **170**, 2796 (1988). [70]

[CMF88] B. M. CHASSY, A. MERCENIER, and J. FLICKINGER, TIBTECH **6**, 303 (1988). [1]

[Coh72] F. COHN, Beitr. Biol. Pflanzen **1**, 127 (1872). [14]

[Cot08] R. COTTERILL, *Biophysik*, Wiley-VCH Verlag GmbH & Co. KGaA, Weinheim, 1st edition, 2008. [7, 8, 10]

[DE79] M. DAGERT and S. D. EHRLICH, Gene **6**, 23 (1979). [35, 36]

[DMR88] W. J. DOWER, J. F. MILLER, and C. W. RAGSDALE, Nucleic Acids Research **16**, 6127 (1988). [37, 41, 44, 59]

[Dow88] W. J. DOWER, United States Patent (1988). [47]

[Dow93] W. J. DOWER, United States Patent (1993). [36, 37, 47]

[Dru94] L. DRURY, *Transformation of bacteria by electroporation*, a. j. harwood, humana press inc., totowa, new jersey edition, 1994. [37]

[Ehr35] C. G. EHRENBERG, *Physikalische Abhandlungen der Königlichen Akademie der Wissenschaften zu Berlin aus den Jahren 1833-1835*, chapter Dritter Beitrag zur Erkenntnis großer Organisation in der Richtung des kleinsten Raumes, pp. 145–336, Druckerei der Königlichen Akademie der Wissenschaften, Berlin, 1835. [14]

[Fer10] Fermentas Life Sciences, *Molecular biology catalog & product application guide 2010-2011*, 2010. [50]

[FTW85] M. FROMM, L. P. TAYLOR, and V. WALBOT, Proc. Natl. Acad. Sci. USA **82**, 5824 (1985). [44, 61]

[FWW94] S. A. FREEMAN, M. A. WANG, and J. C. WEAVER, Biophys. Journal **67**, 42 (1994). [37]

[G+10] T. GENG et al., Journal of Controlled Release **144**, 91 (2010). [2]

[GLW86] D. GROSS, L. M. LOEW, and W. W. WEBB, Biophys. Journal **50**, 339 (1986). [40]

[GPG07] C. A. GERSBACH, J. E. PHILLIPS, and A. J. GARCÍA, Annu. Rev. Biomed. Eng. **9**, 87 (2007). [2]

[GT99] B. GABRIEL and J. TEISSIÉ, Biophys. Journal **76**, 2158 (1999). [43]

[H+91] M. HIBINO et al., Biophys. Journal **59**, 209 (1991). [37]

[Han83] D. HANAHAN, J. Mol. Biol. **166**, 557 (1983). [12, 44, 45]

[Har02] U. HARNACK, Laborjournal **10**, 40 (2002). [35]

[HS67] W. A. HAMILTON and A. J. H. SALE, Biochim. Biophys. Acta **148**, 789 (1967). [1, 37]

[HV05] C. H. HAMANN and W. VIELSTICH, *Elektrochemie*, Wiley-VCH Verlag GmbH & Co. KGaA, Weinheim, 4th edition, 2005. [15, 16, 17, 18, 19, 20, 21, 22, 23, 24, 25, 32, 33, 34, 56, 78, 81, 87]

[K+91] V. A. KLENCHIN et al., Biophys. Journal **60**, 804 (1991). [45]

[K+03] K. KOBAYASHI et al., PNAS **100**, 4678 (2003). [14]

[KCP08] S. KUMAR, D. CHANDA, and S. PONNAZHAGAN, Gene Therapy **15**, 711 (2008). [2]

[KMM08] K. KONTTURI, L. MURTOMÄKI, and J. A. MANZANARES, *Ionic Transport Processes*, Oxford University Press Inc., New York, 1st edition, 2008. [20, 21, 26, 27, 28, 29, 30, 31, 32]

[Kra] L. KRAMER, The *Bacillus subtilis* story, http://rense.com/general4/bac.htm. [14]

[KS86] D. E. KNIGHT and C. SCRUTTON, Biochem. J. **234**, 497 (1986). [35, 37, 40, 41, 42]

[KSN96] S. KAKORIN, S. P. STOYLOV, and E. NEUMANN, Biophys. Chem. **58**, 109 (1996). [40, 41]

[KT77] K. KINOSITA JR. and T. Y. TSONG, Proc. Natl. Sci. USA **74**, 1923 (1977). [60]

[KTSD05] M. H. KERSHAW, M. W. L. TENG, M. J. SMYTH, and P. K. DARCY, Nature Reviews | Immunology **5**, 928 (2005). [2]

[LCP99] Z. LIU, W. CHEN, and K. D. PAPADOPOULOS, Environmental Microbiology **1**, 99 (1999). [6, 12]

[LNR77] P. LINDNER, E. NEUMANN, and K. ROSENHECK, J. Membrane Biol. **32**, 231 (1977). [1, 37, 41]

[Man92] M. D. MANSON, Advances in Microbial Physiology **33**, 277 (1992). [6, 7, 12]

[MC88] A. MERCENIER and B. M. CHASSY, Biochimie **70**, 503 (1988). [1]

[MH70] M. MANDEL and A. HIGA, J. Mol. Biol. **53**, 159 (1970). [36]

[MMP03] M. T. MADIGAN, J. M. MARTINKO, and J. PARKER, *Brock Mikrobiologie*, Spektrum Akademischer Verlag GmbH, Heidelberg, Berlin, 2nd edition, 2003. [5, 6, 7, 8, 9, 10, 12, 14, 15]

[N+82] E. NEUMANN et al., EMBO Journal **1**, 841 (1982). [1, 2, 37, 40, 54, 59]

[N+98] E. NEUMANN et al., Biophys. Journal **74**, 98 (1998). [43]

[NRC99] L. K. NAKAMURA, M. S. ROBERTS, and F. M. COHAN, Int J Syst Bacteriol **49**, 1211 (1999). [49]

[NTA04] J. NEWMAN and K. E. THOMAS-ALYEA, *Electrochemical Systems*, John Wiley & Sons, Inc., Hoboken, New Jersey, 3rd edition, 2004. [16, 18, 19, 20, 21, 22, 23, 24, 25, 26, 27, 28, 29]

[O+98] M. R. OGGIONI et al., J. Clin. Microbiol. **36**, 325 (1998). [15]

[OM93] S. ORLOWSKI and L. M. MIR, Biochim. Biophys. Acta **1154**, 51 (1993). [1]

[Pie89] R. PIECHOCKI, *Das berühmteste Bakterium, 100 Jahre Escherichia-coli-Forschung*, Urania-Verlag Leipzig, Jena, Berlin, 1st edition, 1989. [5, 6, 7, 8, 12, 13, 14]

[Pos94] J. R. POSTGATE, *The outer reaches of life*, Cambrige University Press, 1st edition, 1994. [10, 11, 12, 13]

[Pot88] H. POTTER, Analytical Biochemistry **174**, 361 (1988). [1]

[PPM02] M. PAVLIN, N. PAVSELJ, and D. MIKLAVCIC, IEEE Trans. Biomed. Eng. **49**, 605 (2002). [40]

[R+98] M. P. ROLS et al., Nature Biotechnol. **16**, 168 (1998). [43]

[RMG94] A. M. RAJNICEK, C. D. MCCAIG, and N. A. R. GOW, Journal of Bacteriology **176**, 702 (1994). [11]

[Ros98] K. ROSENHECK, Biophys. Journal **75**, 1237 (1998). [1, 37, 40]

[RT98] M. P. ROLS and J. TEISSIÉ, Biophys. Journal **75**, 1415 (1998). [43]

[S+92a] H. SHIZUYA et al., Proc. Natl. Acad. Sci. USA **89**, 8794 (1992). [2]

[S+92b] S. I. SUKHAREV et al., Biophys. Journal **63**, 1320 (1992). [45]

[S+02] S. SATKAUSKAS et al., Molecular Therapy **5**, 133 (2002). [43]

[Sch57] H. P. SCHWAN, *Advances in Biological and Medical Physics*, volume 5, chapter Electrical properties of tissue and cell suspensions, pp. 147–209, Academic Press, New York, 1957. [2]

[SD88] K. SHIGEKAWA and W. J. DOWER, BioTechniques **6**, 742 (1988). [1, 2, 35, 37, 39, 40, 41, 42, 43, 44, 45, 50, 56, 59, 60]

[SH67] A. J. H. SALE and W. A. HAMILTON, Biochim. Biophys. Acta **148**, 781 (1967). [1, 60, 65]

[SH68] A. J. H. SALE and W. A. HAMILTON, Biochim. Biophys. Acta **168**, 37 (1968). [1, 2, 37, 40]

[SJ91] M. STEPHENSON and P. JARRETT, BioTechniques **5**, 9 (1991). [49]

[SLA93] W. SHI, M. J. LENTZ, and J. ADLER, Journal of Bacteriology **175**, 5785 (1993). [11]

[SR01] J. SAMBROOK and D. W. RUSSELL, *Molecular Cloning, A Laboratory Manual*, volume 1, Cold Spring Harbor Laboratory Press, Cold Spring Harbor, New York, 3rd edition, 2001. [50]

[SS10] W. SCHMICKLER and E. SANTOS, *Interfacial Electrochemistry*, Springer-Verlag, Berlin, Heidelberg, 2nd edition, 2010. [23, 32, 33, 34]

[SSA96] W. SHI, B. A. D. STOCKER, and J. ADLER, Journal of Bacteriology **178**, 1113 (1996). [12]

[SSK89] J. A. SAUNDERS, C. R. SMITH, and J. M. KAPER, BioTechniques **7**, 1124 (1989). [90]

[SSM98] R. SUSIL, D. SEMROV, and D. MIKLAVCIC, Electro. Magnetobiol. **17**, 391 (1998). [40]

[St8] R. STÄMPFLI, Anais da Academia Brasileira de Ciencias **30**, 57 (1958). [1]

[SYYS04] H. SUMI, Y. YANAGISAWA, C. YATAGAI, and J. SAITO, Food Sci. Technol. Res. **10**, 17 (2004). [15]

[T+04] T. E. TJELLE et al., Molecular Therapy **9**, 328 (2004). [2]

[TAC91] E. TEKLE, R. D. ASTUMIAN, and P. B. CHOOK, PNAS **88**, 4230 (1991). [89]

[TAC94] E. TEKLE, A. D. ASTUMIAN, and P. B. CHOCK, Proc. Natl. Acad. Sci. USA **91**, 11512 (1994). [43]

[TK02] U. K. TIRLAPUR and K. KÖNIG, Nature **418**, 290 (2002). [35]

[TP07] W. J. THIEMAN and M. A. PALLADINO, *Biotechnologie*, Pearson Education Deutschland GmbH, München, 2007. [36]

[TS11] S. TOPP and I. SCHNEIDER, Eppendorf Bio News , 7 (2011). [1, 37]

[TT81] J. TEISSIE and T. Y. TSONG, Biochemistry **20**, 1548 (1981). [1, 2, 37, 39, 40, 41, 42, 59]

[vHM05] R. VAN HOUDT and C. W. MICHIELS, Research in Microbiology **156**, 626 (2005). [12]

[W+94] H. WOLF et al., Biophys. Journal **66**, 524 (1994). [45, 90]

[Wea00] J. C. WEAVER, IEEE Transactions on plasma science **28**, 24 (2000). [37, 39]

[Y+00] M. YOSHIDA et al., Chem. Pharm. Bull. **48**, 1807 (2000). [37]

[Z+11] H. ZHANG et al., Journal of Microbiological Methods **84**, 114 (2011). [44]

[Zim82] U. ZIMMERMANN, Biochim. Biophys. Acta **694**, 224 (1982). [37, 38, 39, 89]

Danksagung

An dieser Stelle möchte ich mich bei allen Personen bedanken, die mir während meiner Promotionszeit mit Rat und Tat zur Seite standen.
Ein ganz besonders großes Dankeschön gilt meinem Ehemann Tobias. Er hat nicht nur mit Diskussionen über physikalische Themen, statistische Genauigkeit von Messwerten und Messmethoden zum guten Gelingen dieser Arbeit beigetragen und mich nach einem misslungenen Experiment wieder aufgebaut. Trotz einer arbeitsintensiven Zeit und langen, anstrengenden Tagen im Labor, hat er es unter anderem mit ausgefallenen, ganz besonders leckeren kulinarischen Besonderheiten immer wieder geschafft dafür zu sorgen, dass es mir an nichts fehlt und ich meine gute Laune nicht verliere. Wenn du für mich kochst, ist das wie Urlaub. Danke Tobi!
In den vergangenen drei Jahren, die meine Promotionszeit umfassten, wäre vieles ohne die Unterstützung meiner Familie nicht möglich gewesen.
Meine Eltern und meine Schwestern wurden nie müde mich zu unterstützen und in meiner Arbeit durch anregende Diskussionen weiter zu helfen.
Besonders möchte ich mich an dieser Stelle bei meiner Schwester Inge bedanken, die mir, wenn ich über meine Arbeit erzählt habe, immer zugehört hat und mich während langer Gespräche beim Frühstück oft auf neue Ideen gebracht hat. Ohne diese vielen konstruktiven Gespräche wären sicherlich viele der in dieser Dissertation präsentierten Experimente nicht zustande gekommen.
Auch möchte ich mich bei meiner Oma bedanken, die mit ihrer immer guten Laune mich immer wieder aufs Neue motiviert hat. Ihr immerwährendes Interesse an meinen Forschungsergebnissen haben mir geholfen meine Arbeit in einem anderen Blickwinkel zu sehen und letzt endlich den Inhalt meiner Dissertation in Worte zu fassen.
Diese Arbeit wurde aber noch von vielen anderen tollen Menschen zum Erfolg getragen, wie zum Beispiel von meinen Schwiegereltern. Auf alle vier meiner Schwiegereltern konnte ich stets zählen. Sie waren immer zur Stelle, wenn Not am Mann war. Dafür bin ich sehr dankbar. Auch meine Schwägerin ist nicht zu vergessen, die es verstand mich den Laboralltag auch mal vergessen zu lassen.
Dass ich während des Studiums und meiner Promotion immer Spaß und viel zu Lachen hatte, verdanke ich vor allem Christophe und Eva Cauet, Stefan Swientek und der kompletten Mannschaft des Lehrstuhls für Experimentelle Physik 5a der TU Dortmund. Die vielen Gespräche bei gemeinsam verbrachten Abenden haben an so mancher Stelle

bei der Erstellung dieser Promotionsarbeit weitergeholfen.
Ich bedanke mich für die sehr gute Betreuung von PD Dr. Joachim Franzke und Dr. Raffael Kettler, die sich stets Zeit für mich genommen haben, um fachliche Ungereimtheiten aus dem Weg zu räumen und mir außerdem ein gut ausgestattetes Labor und alle für diese Arbeit nötigen Materialien zur Verfügung gestellt haben.
Prof. Dr. Thomas Weis danke ich für seine großes Interesse an meiner Dissertation.
Auch danke ich für die tatkräftige Unterstützung der Mitarbeiter der Abteilung für Miniaturisierung um PD Dr. Joachim Franzke. Ganz besonders danke ich Antje Michels, die mir während stundenlanger Messungen bis in den späten Abend bei all meinen Experimenten zur Seite stand und mich tatkräftig unterstützt hat. Susanne Funken gilt ein ganz besonderer Dank dafür, dass sie nie müde wurde alle benötigten elektrokompetenten Bakterien zu präparieren und die LB-Agar-Platten zu gießen, die zur Detektion der transformierten Bakterien dienten. Günter Jestel möchte ich für den Bau der für die Experimente benutzten Spannungsgeneratoren danken und dafür, dass er auch sehr kurzfristig immer wieder alle Widerstände in den Generatoren ausgetauscht hat, wenn wir mitten in der Messreihe ausversehen einen Kurzschluss verursacht hatten. Auch möchte ich Sarah Waide, Saskia Müller und Heike Hardelauf für ihr Interesse an meiner Arbeit und die hilfreichen Ideen danken.
Mein Dank gilt auch allen anderen, die bisher noch nicht genannt wurden, die mich durch die letzten Jahre an der Technischen Universität Dortmund und am Leibniz-Institut für Analytische Wissenschaften - ISAS - e. V. begleitet haben oder mir einfach nur zugehört haben.